UNIVERSITAT DE
BARCELONA

Mathematical work on the foundation of Jones-Mueller formalism and its application to nano optics
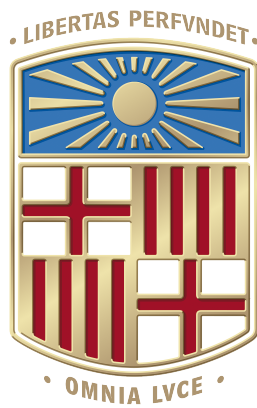
Ertan Kuntman

Mathematical work on the foundations of Jones-Mueller formalism and its application to nano optics

Ertan Kuntman

Departament de Física Aplicada

Universitat de Barcelona

Supervisors: Dr. Oriol Arteaga Barriel and Dr. Adolf Canillas Biosca

This dissertation is submitted for the degree of

Doctor of Philosophy in Physics

October 2019

Table of contents

Acknowledgment

Resumen en Español

La matriz de Jones y la matriz de Mueller-Jones (es decir la matriz de Mueller no despolarizante) son los elementos matemáticos centrales del cálculo de óptica de polarización. En esta tesis discutimos otras formas que pueden usarse para representar las propiedades de polarización de los sistemas deterministas. Investigamos cuatro formas diferentes que interpretamos como los estados de los sistemas ópticos deterministas. El estado vectorial $|h\rangle$ es el elemento central de nuestro formalismo. La combinación paralela coherente de sistemas ópticos deterministas puede expresarse, más convenientemente, como una combinación lineal de estados vectoriales. En otras palabras, cualquier sistema óptico no despolarizante puede considerarse como una combinación coherente de otros sistemas deterministas que sirven como sistemas basé. Sin embargo, los estados vectoriales no son adecuados para representar la combinación en serie de sistemas ópticos, porque los vectores $|h\rangle$ no se pueden multiplicar como $|h_1\rangle|h_2\rangle|h_3\rangle$. Observamos que existe un estado de matriz complejo $\mathbf{Z}$ que imita todas las propiedades de las matrices de Jones, incluida la propiedad de multiplicación de estados. Las matrices $\mathbf{Z}$ también son similares a las matrices de Mueller no despolarizantes por la relación $\mathbf{M} = \mathbf{ZZ}^*$. Mostramos que las matrices $\mathbf{Z}$ transforman la matriz de Stokes $\mathbf{S}$ en otra matriz de Stokes $\mathbf{S}'$ de acuerdo con la relación $\mathbf{S}' = \mathbf{ZSZ}^\dagger$, donde la matriz $\mathbf{S}$ corresponde al vector Stokes $|s\rangle$ y $\mathbf{S}'$ corresponde al vector Stokes transformado $|s'\rangle$ ($|s'\rangle = \mathbf{M}|s\rangle$).

Las matrices $\mathbf{Z}$ también transforman los vectores de Stokes, $|s\rangle$, en vectores complejos $|\tilde{s}\rangle$ según $|\tilde{s}\rangle = \mathbf{Z}|s\rangle$. Se puede demostrar que, a diferencia de un vector $|s\rangle$, un vector $|\tilde{s}\rangle$ contiene la fase introducida por el sistema óptico. Además observamos que los vectores $|h\rangle$ y las matrices $\mathbf{Z}$ son representaciones diferentes de estados cuaternión, $\boldsymbol{h}$. Los estados de cuaternión se pueden agregar o multiplicar para producir nuevos estados de cuaternión, por lo tanto, son adecuados para representar cualquier combinación coherente de sistemas ópticos deterministas. Los resultados muestran que los estados de cuaternión transforman cuaternion de Stokes, $\boldsymbol{s}$, en un cuaternión de Stokes, $\boldsymbol{s}'$, de acuerdo con el esquema $\boldsymbol{s}' = \boldsymbol{hsh}^\dagger$. Las formulaciones de matriz $\mathbf{Z}$ y cuaternión son especialmente útiles para describir la aparición de efectos de despolarización. El enfoque de matriz de densidad es más conveniente cuando queremos encontrar los componentes originales de una matriz de Mueller despolarizante.

Las matrices de densidad asociadas con los sistemas ópticos deterministas (puros) se definen en términos de vectores $|h\rangle$ como $\mathbf{H} = |h\rangle\langle h|$. Una matriz de Mueller despolarizante puede escribirse como una suma convexa de matrices de Mueller no despolarizantes. La matriz $\mathbf{H}$ asociada (matriz de densidad de la mezcla) también se puede escribir como una suma convexa de matrices de densidad correspondientes a los sistemas de componentes puros. Se puede demostrar que si existe algún conocimiento sobre las propiedades de anisotropía de los sistemas de componentes, es posible encontrar las matrices de Mueller no despolarizantes de los componentes originales únicamente mediante las condiciones de clasificación de las matrices $\mathbf{H}$. Aplicamos nuestro formalismo a varios fenómenos, en particular estudiamos por ejemplo los efectos de interferencia en un experimento de doble rendija de Young con métodos polarimétricos completos. También demostramos que nuestro formalismo puede ser útil para la formulación analítica de sistemas dipolo interactivos. Finalmente, aplicamos el método de descomposición del estado vectorial para analizar la hibridación de plasmones, resonancias de Fano y efectos circulares en geometrías quirales y aquirales.

Summary

The Jones matrix and the nondepolarizing Mueller matrix are the basic mathematical objects of polarization optics calculus. In this thesis we discus other forms that can be used to represent optical properties of deterministic systems. We investigate four different forms that we interpret as the states of deterministic optical systems. Vector state $|h\rangle$ is the central element of our formalism. Coherent parallel combination of deterministic optical systems can be most conveniently expressed as a linear combination of vector states. In other words, any nondepolarizing optical system can be considered as a a coherent combination of other deterministic systems that serve as basis systems. Nevertheless, vector states are not suitable for representing serial combination of optical systems, because $|h\rangle$ vectors cannot be multiplied as $|h_1\rangle|h_2\rangle|h_3\rangle$. We observe that there exists a complex matrix state $\mathbf{Z}$ that mimics all properties of Jones matrices, including the multiplication of states property. $\mathbf{Z}$ matrices are also akin to the nondepolarizing Mueller matrices by the relation $\mathbf{M} = \mathbf{Z}\mathbf{Z}^*$. We show that $\mathbf{Z}$ matrices transform the Stokes matrix $\mathbf{S}$ into another Stokes matrix $\mathbf{S}'$ according to the relation $\mathbf{S}' = \mathbf{Z}\mathbf{S}\mathbf{Z}^\dagger$, where $\mathbf{S}$ corresponds to the Stokes vector $|s\rangle$ and $\mathbf{S}'$ corresponds to the transformed Stokes vector $|s'\rangle$ ($|s'\rangle = \mathbf{M}|s\rangle$).

$\mathbf{Z}$ matrices also transform Stokes vectors, $|s\rangle$ into complex vectors $|\tilde{s}\rangle$, according to $|\tilde{s}\rangle = \mathbf{Z}|s\rangle$. It can be shown that $|\tilde{s}\rangle$ vectors bears the phase introduced by the optical system. We observe that $|h\rangle$ vectors and $\mathbf{Z}$ matrices are different representations of quaternion states, $\boldsymbol{h}$. Quaternion states can be added or multiplied to yield new quaternion states, therefore they are suitable for representing any coherent combination of deterministic optical systems. It can be shown that quaternion states transform the Stokes quaternion, $\boldsymbol{s}$, into a Stokes quaternion, $\boldsymbol{s}'$, according to the scheme $\boldsymbol{s}' = \boldsymbol{h}\boldsymbol{s}\boldsymbol{h}^\dagger$. The $\mathbf{Z}$ matrix and the quaternion formulations are especially useful for describing the emergence of depolarization effects. The density matrices that associated with deterministic (pure) optical systems are defined in terms of $|h\rangle$ vectors as $\mathbf{H} = |h\rangle\langle h|$. However, since a depolarizing Mueller matrix can be written as a convex sum of nondepolarizing Mueller matrices, the associated $\mathbf{H}$ matrix (density matrix of the mixture) can also be written as a convex sum of density matrices corresponding to the pure component systems. It can be shown that if there exists some knowledge about the anisotropy

properties of component systems it is possible to find the nondepolarizing Mueller matrices of original constituents uniquely by means of the rank conditions of **H** matrices. We apply our formalism to several phenomena, for example we study the interference effects in a Young's double slit experiment with complete polarimetric methods. Moreover, we show that our formalism can be useful for the analytic formulation of interacting dipole systems. Finally, we apply the vector state decomposition method to analyze plasmon hybridization, Fano resonances and circular effects in chiral and achiral geometries.

Preface

In this thesis we propose an alternative point of view to the Jones-Mueller formalism that is based on vector/matrix states or, alternatively, on quaternion states. Our new formalism is ultimately equivalent to the combination of Jones and Mueller formalisms and it is possible to shift from one formalism to another. Nevertheless, our method is not redundant, we think that it is a step towards the unification of the formalism and it permits a better understanding of some aspects of the optical phenomena. In particular, we will present its applications to the description of coherent, partially coherent and incoherent combinations of optical systems, decomposition of depolarizing Mueller matrices, interactions between nanoparticles that lead to interesting phenomena such as hybridization of energies, Fano resonances and circular effects in achiral and chiral configurations. We believe that every mathematical tool brings new potential perspectives of its own. There are many examples in the history of science that a new point of view introduces new perspectives. The Lagrangian formulation of classical mechanics is basically equivalent to the Newtonian formulation, but it has provided a new point of view for the universal stationary action (least action) formulation of physical laws. The Hamiltonian formalism is still another form of the Lagrangian formalism with the Poisson brackets (prototypes of quantum mechanical commutators), and constitutes the backbone of quantum mechanics and quantum field theories. Similarly, the vector/matrix and quaternion states formalism of polarization optics may suggest new perspectives that allow new conception of optical phenomena.

In classical mechanics the state of the physical system is represented by a point in the phase space. In quantum mechanics the state of the system is a vector, or, strictly speaking, a ray in the Hilbert space. Quantum mechanical state vector contains all information that can be retrieved about the physical system. Jones formalism is about the interaction of light with the optical medium. In polarization optics, Jones matrix is considered as a mathematical tool that represents the scattering properties of a deterministic optical system. Jones matrix can be formulated in terms of the basic spectroscopic parameters that characterize the effect of the optical system on the state of light. Accordingly, the Jones matrix transforms the polarization state of incoming light into a new polarization state, but, the Jones matrix itself

is not considered as a *state* of the optical system. In this thesis we suggest that the Jones matrices, and all other alternative forms, can be considered as the state of the optical system. System state contains all the information about the optical system besides its scattering properties. Significance of the state representation approach becomes more apparent when the system state is represented by a vector state.

This thesis consists of four main chapters. The first chapter includes the history and the background material for the foundations of Jones-Stokes-Mueller formalism. The second chapter presents the original work that has been studied in seven sections with the references to the published papers. First three sections are about the vector and matrix states of optical media and their coherent linear combinations. The fourth section attempts to unify several alternative state representations by means of the quaternion state concept. Next section is about the outer product of vector states and the density matrix formalism of polarization optics, in a very similar way to the formalism of quantum mechanics of mixtures. Applications of the vector/matrix state formalism to various phenomena, such as dipole-dipole interaction between nano particles, plasmon hybridization, Fano resonances, circular effects in chiral and achiral configurations, and depolarization effects due to the incoherent combination of deterministic optical systems are investigated in the last two sections. The published papers are presented in the third chapter in a chronological order and last chapter contains a short discussion and conclusions of the thesis, followed by an appendix and the bibliography.

Chapter 1

Background

Polarimetry is the technique that works on the measurement and interpretation of the polarization of transverse waves [1]. The instruments used are called polarimeters. Polarimetry itself is a very broad field and it includes many other more specific techniques or methods. Thus, the application as a technique to extract information about the physical properties of thin films or bulk materials from the changes in the polarization of light is usually known as ellipsometry. In a similar way, the polarimeter that is used to determine the concentration of sugar in a solution is called saccharimeter, etc.

Generally speaking, we can distinguish two basic forms of polarimetry: when the goal is to characterize the polarization of light detected, Stokes polarimeters are used, for example, we can highlight the wide application of these insturments in astronomy [2]. On the other hand, when the goal is to measure optical properties of a material medium one uses polarimeter that generate and detect polarized light and that, in their most general form, are called Mueller matrix polarimeters (or Mueller matrix ellipsometers) [3, 4]. This thesis is focused on this second form of polarimetry.

A quasi-monochromatic beam of light is said to be polarized when both, the relative amplitudes and the relative phase between the different components of the electromagnetic field remain related to each other in a deterministic and predictable way. If for some reason for example the phase relation is perturbed, light will become partially polarized. Besides its polarization properties light is an electromagnetic wave in the usual sense which is described by Maxwell's equations [5].

A plane wave is a constant frequency wave whose wavefronts are infinite planes perpendicular to the propagation axis. For a plane wave propagating along the z-axis, the electric field vector can be written as

$$\mathbf{E} = (E_{x0}e^{i\delta_x}\hat{\mathbf{x}} + E_{y0}e^{i\delta_y}\hat{\mathbf{y}})e^{i(\omega t - kz)}, \tag{1.1}$$

where E_{x0}, E_{y0} and δ_x, δ_y are the amplitudes and phases along the x and y directions.

Within this assumption, the polarization state of light is given by the relations between the relative magnitudes and phases of the x and y components of the electric field vector **E**. For a quasi-monochromatic light $\frac{E_{0x}}{E_{0y}}$ and δ_x - δ_y are constants, hence **E** is completely polarized and it can be described by a Jones vector which contains all the information about the polarization of the wave. The Jones vector can be written as a column vector [1]:

$$|E\rangle = \begin{pmatrix} E_{0x}e^{i(\omega t - kz + \delta_x)} \\ E_{0y}e^{i(\omega t - kz + \delta_y)} \end{pmatrix} = e^{i(\omega t - kz)} \begin{pmatrix} E_{0x}e^{i\delta_x} \\ E_{0y}e^{i\delta_y} \end{pmatrix}. \tag{1.2}$$

In some parts of this Thesis we will use Dirac's Bra-Ket notation [6], as you can see in Eq. (1.2) . This notation is not very extended in polarization optics, but it will be adopted for convenience because it eases some of the calculations.

The intensity of light can be obtained by multiplying the Jones vector $|E\rangle$ by its Hermitian adjoint,

$$I = \langle E|E\rangle = E_{0x}^* E_{0x} + E_{0y}^* E_{0y}, \tag{1.3}$$

The effect that a deterministic optical element has on the polarized light is described by a 2×2 complex Jones matrix **J** [8, 9]

$$\begin{pmatrix} E_{0x}^{out} \\ E_{0y}^{out} \end{pmatrix} = \begin{pmatrix} J_{00} & J_{01} \\ J_{10} & J_{11} \end{pmatrix} \begin{pmatrix} E_{0x}^{in} \\ E_{0y}^{in} \end{pmatrix}. \tag{1.4}$$

The Jones matrix describing the net effect of a series of optical elements is obtained by the matrix product of Jones matrices of the optical elements. The total effect of N optical elements is described by

$$\mathbf{J} = \mathbf{J}_N \mathbf{J}_{N-1} \cdots \mathbf{J}_2 \mathbf{J}_1. \tag{1.5}$$

In this scheme the incident Jones vector interacts with the optical element $\mathbf{J}_1$ first, then with element $\mathbf{J}_2$, etc.

Jones matrices are described in terms of the basis of a particular coordinate system. If we want to use a rotated coordinated system, the Jones matrix expressed in the new coordinate system can be obtained as follows:

$$\mathbf{J}' = \mathbf{R}(\alpha)\mathbf{J}\mathbf{R}(-\alpha), \quad \text{with} \quad \mathbf{R}(\alpha) = \begin{pmatrix} \cos(\alpha) & \sin(\alpha) \\ -\sin(\alpha) & \cos(\alpha) \end{pmatrix}. \tag{1.6}$$

where α is the orientation of the axis of the new coordinate system with respect to old coordinate system and $\mathbf{J}'$ is the Jones matrix expressed in terms of the new coordinate system.

The Jones vector is an efficient way of describing completely polarized light. But unpolarized or partially polarized light can not be expressed by a Jones vector. In order to describe a general polarization state, a Stokes vector, $|s\rangle$, is introduced in terms of the Stokes parameters s_0, s_1, s_2 and s_3 [10]:

$$|s\rangle = \begin{pmatrix} s_0 \\ s_1 \\ s_2 \\ s_3 \end{pmatrix} = \begin{pmatrix} \langle E_{0x}^* E_{0x} + E_{0y}^* E_{0y} \rangle \\ \langle E_{0x}^* E_{0x} - E_{0y}^* E_{0y} \rangle \\ \langle E_{0y}^* E_{0x} + E_{0x}^* E_{0y} \rangle \\ \langle i(E_{0y}^* E_{0x} - E_{0x}^* E_{0y}) \rangle \end{pmatrix}, \tag{1.7}$$

which includes unpolarized states as well as completely polarized states. The expressions in the brackets denote time averages in order to account for the variations in the amplitude and phase. The Stokes parameters satisfy the following inequality:

$$s_0^2 \geq s_1^2 + s_2^2 + s_3^2. \tag{1.8}$$

The equality is only satisfied in case of completely polarized light. The equation, $s_0^2 = s_1^2 + s_2^2 + s_3^2$, represents a sphere of three dimensions s_1, s_2, s_3 with a radius s_0, which is called the Poincare sphere. For an unpolarized or partially polarized light equality is not satisfied. In this case, the degree of polarization p is defined in terms of the Stokes parameters,

$$p = \frac{\sqrt{s_1^2 + s_2^2 + s_3^2}}{s_0}. \tag{1.9}$$

For completely polarized light $p = 1$, for unpolarized light $p = 0$, and for partially polarized light $0 < p < 1$. Partially polarized light can be written as a sum of two components: an unpolarized component and a completely polarized component,

The matrix method which manipulates Stokes vectors was developed and popularized by Hans Mueller [11] after the pioneering contributions of Paul Soleillet and Francis Perrin [12–14]. The Mueller formalism has a direct connection with experiment, because it works with real and measurable intensities instead of complex amplitudes. Therefore, Stokes vector and Mueller matrices are much convenient for experimental work in polarimetry. The effect of an optical element on the polarization state of incident light is described by a 4×4 Mueller matrix. A Mueller matrix $\mathbf{M}$ consists of 16 real elements and connects the input and output Stokes vectors:

$$|s'\rangle = \mathbf{M}|s\rangle, \tag{1.10}$$

where

$$\mathbf{M} = \begin{pmatrix} M_{00} & M_{01} & M_{02} & M_{03} \\ M_{10} & M_{11} & M_{12} & M_{13} \\ M_{20} & M_{21} & M_{22} & M_{23} \\ M_{30} & M_{31} & M_{32} & M_{33} \end{pmatrix}. \tag{1.11}$$

For every Jones matrix there exists a corresponding Mueller-Jones matrix (also known as nondepolarizing Mueller matrix or pure Mueller matrix) which can be found by means of the following relation:

$$\mathbf{M} = \mathbf{A}(\mathbf{J} \otimes \mathbf{J}^*)\mathbf{A}^{-1}, \tag{1.12}$$

where $\otimes$ is the the Kronecker product and $\mathbf{A}$ is a unitary matrix,

$$\mathbf{A} = \begin{pmatrix} 1 & 0 & 0 & 1 \\ 1 & 0 & 0 & -1 \\ 0 & 1 & 1 & 0 \\ 0 & i & -i & 0 \end{pmatrix}, \quad \mathbf{A}^{-1} = \frac{1}{2}\mathbf{A}^\dagger = \frac{1}{2}\begin{pmatrix} 1 & 1 & 0 & 0 \\ 0 & 0 & 1 & -i \\ 0 & 0 & 1 & i \\ 1 & -1 & 0 & 0 \end{pmatrix}, \tag{1.13}$$

the superscript † indicates conjugate transpose.

A beam of light is said to be polarized when the relative phase between the different components of the electromagnetic field remain related to each other in a definite way. If for some reason the phase relation is perturbed, light will become partially polarized. In practice as the light passes through a medium, phase correlations may be destroyed or the relative amplitudes of the electric field vector may be affected due to selective absorption of polarization states. Hence, polarized light becomes partially depolarized, i.e., the degree of polarization is reduced. In polarimetry experiments the depolarization usually can be due to incoherent scattering introduced by the sample or the incoherent superposition of the light interacting with different materials. Another source of depolarization is the limited spectral resolution of the instruments. In general, optical elements are not perfectly monochromatic; they integrate over a range of wavelengths and can cause depolarization. Isotropic depolarizing samples depolarize all input polarization states equally; on the other hand, anisotropic depolarizing samples depolarize particular polarization states but may not depolarize other polarization states. To quantify the depolarization effect of a medium, the depolarization index (DI) of a Mueller matrix was introduced by Gil and Bernabeu [15, 16]. The DI is defined as the Euclidian distance of the normalized Mueller matrix from the ideal depolarizer:

$$\mathrm{DI} = \frac{\sqrt{(\sum_{ij} M_{ij}^2) - M_{00}^2}}{\sqrt{3}M_{00}}. \tag{1.14}$$

DI varies from zero to the unity. For an ideal depolarizer DI= 1, for a non-depolarizing medium DI= 0, and intermediate values correspond to partial depolarization.

We can associate a complex 4×4 covariance (coherency) matrix, $\mathbf{H}$, to any Mueller matrix [18, 17],

$$\mathbf{H} = \frac{1}{4} \sum_{i,j=0}^{3} M_{ij} \mathbf{A}(\boldsymbol{\sigma}_i \otimes \boldsymbol{\sigma}_j^*) \mathbf{A}^{-1}, \tag{1.15}$$

$\boldsymbol{\sigma}_i$ are the Pauli matrices with the 2×2 identity in the following order:

$$\begin{aligned}
\boldsymbol{\sigma}_0 &= \begin{pmatrix} 1 & 0 \\ 0 & 1 \end{pmatrix}, \quad \boldsymbol{\sigma}_1 = \begin{pmatrix} 1 & 0 \\ 0 & -1 \end{pmatrix}, \\
\boldsymbol{\sigma}_2 &= \begin{pmatrix} 0 & 1 \\ 1 & 0 \end{pmatrix}, \quad \boldsymbol{\sigma}_3 = \begin{pmatrix} 0 & -i \\ i & 0 \end{pmatrix}.
\end{aligned} \tag{1.16}$$

The matrix $\mathbf{H}$ given in Eq.(1.15) is named in many works as *coherency matrix* and identified with the letter $\mathbf{C}$, as it was given by Cloude [19]. This is done to distinguish it from a different definition of $\mathbf{H}$ that does not include the matrix $\mathbf{A}$ (note that as $\mathbf{A}$ is only a unitary matrix, it does not add or remove any polarimetric information). However, in all the published works associated with this thesis we always denote $\mathbf{H}$ as the *covariance matrix* and it must be understood according to the definition given in Eq.(1.15).

$\mathbf{H}$ matrix is very useful for eigenanalysis. Most importantly, for a physical Mueller matrix (either depolarizing or nondepolarizing) the eigenvalues of $\mathbf{H}$ must be non-negative (i.e. $\mathbf{H}$ must be a positive semidefinite Hermitian matrix). The rank of $\mathbf{H}$ is also informative about the depolarization. If the Mueller matrix of a system is non-depolarizing (alternatively, pure or deterministic), then the rank of the associated covarience matrix is one. In practice, due to the unavoidable noise, one finds that experimental Mueller matrices are never strictly non-depolarizing.

Chapter 2

Introduction

The Jones and Mueller formalisms that we have introduced in the previous section may not be regarded as two competing formalisms but, instead, as two complementary formalisms. For example, addition of Stokes vectors represents an incoherent combination (intensity superposition) of beams while addition of Jones vectors represents a coherent superposition (amplitude superposition). Therefore, with the combination of both formalisms, something we will generally refer as Jones-Mueller formalism, one can get a complete and consistent framework for the phenomenological study of interaction of light with optical material media [4].

As stated by Parke [7] scattering properties of a coherent parallel combination of optical systems can be expressed as a linear combination of Jones matrices of individual systems,

$$\mathbf{J} = \mathbf{J}_1 + \mathbf{J}_2 + \mathbf{J}_3 + \cdots \tag{2.1}$$

Jones matrices are complex 2×2 matrices. It will be shown that it is also possible to define complex 4×4 matrices ($\mathbf{Z}$ matrices) which are equivalent to Jones matrices, and the coherent linear combination of states can be written in terms of $\mathbf{Z}$ matrices [20–24]:

$$\mathbf{Z} = c_1\mathbf{Z}_1 + c_2\mathbf{Z}_2 + c_3\mathbf{Z}_3 + \cdots \tag{2.2}$$

where $\mathbf{Z}$ is the matrix associated with the coherently combined system, $\mathbf{Z}_i$ denote the matrices associated with subsystems and c_i are complex coefficients. We also argue that the Jones and $\mathbf{Z}$ matrices are more than scattering matrices, they can be considered as *matrix states* that define all optical properties of deterministic optical systems. This coherent linear combination of states principle brings the formalism of polarization optics more closer to the formalism of quantum mechanics. But, when expressed in terms of Jones or $\mathbf{Z}$ matrices the power of the

coherent linear combination principle may not be fully appreciated. There exists one more mathematical object that may be used for representing the state of a deterministic optical systems. The vector state $|h\rangle$ is more suitable for representing linear combination of states,

$$|h\rangle = c_1|h\rangle_1 + c_2|h\rangle_2 + c_3|h\rangle_3 + \cdots \tag{2.3}$$

where $|h\rangle$ and $|h\rangle_i$ are vector states associated with the combined system and subsystems, respectively, and each vector state can be represented by a four component complex vector. In Eq.(2.3) c_i play the role of probability amplitudes of quantum mechanics, but for macroscopic optical systems, including systems at the nano scale, such as nanoantennas, c_i cannot be interpreted as probability amplitudes. Nevertheless, the analogy with the quantum mechanical state superposition is more clear in terms of vector states.

To our knowledge, $\mathbf{Z}$ was first introduced by Chipman [26]. But, the significance of the $\mathbf{Z}$ matrix becomes more apparent when we make the connection with the nondepolarizing Mueller matrix. We observe that every nondepolarizing Mueller matrix, $\mathbf{M}$, can be written as $\mathbf{M} = \mathbf{Z}^*\mathbf{Z} = \mathbf{Z}\mathbf{Z}^*$. This observation allows us to interpret $\mathbf{Z}$ matrix (or $|h\rangle$ vector) as the *state* of an optical system analogous to the state vector of quantum mechanics, $|\psi\rangle$. At first sight, it may be plausible to interpret $\mathbf{M} = \mathbf{Z}^*\mathbf{Z} = \mathbf{Z}\mathbf{Z}^*$ as an analogue of the expression for quantum mechanical probability in terms of probability amplitudes: *probability* $= \psi^*\psi = \psi\psi^*$. But unfortunately, this analogy cannot be pursued too far [27–29].

2.1 Representations of deterministic optical media states and their properties

We write the Jones matrix in terms of the parameters τ, α, β and γ:

$$\mathbf{J} = \begin{pmatrix} \tau + \alpha & \beta - i\gamma \\ \beta + i\gamma & \tau - \alpha \end{pmatrix}. \tag{2.4}$$

The corresponding nondepolarizing Mueller matrices can be obtained from the Jones matrices by a transformation, $\mathbf{M} = \mathbf{A}(\mathbf{J} \otimes \mathbf{J}^*)\mathbf{A}^\dagger$, where $\mathbf{A}$ is a unitary matrix given by Eq.(1.13).

We introduce, $\mathbf{Z}$ matrix, written in terms of τ, α, β and γ as follows:

$$\mathbf{Z} = \begin{pmatrix} \tau & \alpha & \beta & \gamma \\ \alpha & \tau & -i\gamma & i\beta \\ \beta & i\gamma & \tau & -i\alpha \\ \gamma & -i\beta & i\alpha & \tau \end{pmatrix}, \tag{2.5}$$

where τ, α, β and γ are complex numbers, and they are closely related with the real valued anisotropy coefficients defined by Arteaga et al. [30]. α is related with linear horizontal anisotropy, β is related with linear $45°$ anisotropy and γ is related with circular anisotropy. [20]. τ can always be chosen as real and positive if the overall phase is not taken into account. In terms of spectroscopic parameters [31] isotropic phase retardation (η), isotropic amplitude absorption (κ), circular dichroism (CD), circular birefringence (CB), horizontal and $45°$ linear dichorism (LD and LD'), horizontal and $45°$ linear birefringence (LB and LB'), τ, α, β and γ can be written as:

$$
\begin{aligned}
\tau &= e^{-\frac{i\chi}{2}} \cos\left(\frac{T}{2}\right), \\
\alpha &= -e^{-\frac{i\chi}{2}} \frac{iL}{T} \sin\left(\frac{T}{2}\right), \\
\beta &= -e^{-\frac{i\chi}{2}} \frac{iL'}{T} \sin\left(\frac{T}{2}\right), \\
\gamma &= e^{-\frac{i\chi}{2}} \frac{iC}{T} \sin\left(\frac{T}{2}\right)
\end{aligned}
\tag{2.6}
$$

where $\chi = \eta - i\kappa$, $L = LB - iLD$, $L' = LB' - iLD'$, $C = CB - iCD$, $T = \sqrt{L^2 + L'^2 + C^2}$ [20, 32, 33].

In all respects, the **Z** matrix is equivalent to the Jones matrix, and the **Z** matrix transforms the Stokes vector representing complete polarization state of light, $|s\rangle = (s_0, s_1, s_2, s_3)^T$, into a complex vector, $|\tilde{s}\rangle = (\tilde{s}_0, \tilde{s}_1, \tilde{s}_2, \tilde{s}_3)^T$:

$$
\mathbf{Z}|s\rangle = |\tilde{s}\rangle.
\tag{2.7}
$$

It can be shown that $|\tilde{s}\rangle$ bears the relevant phase introduced by the optical system,

$$
\langle s|\mathbf{Z}|s\rangle = 2\langle E|\mathbf{J}|E\rangle = 2\langle E|E'\rangle,
\tag{2.8}
$$

where $|E\rangle$ and $|E'\rangle$ are input and output Jones vectors. **Z** matrix also transforms the Stokes matrix, **S** [34], into a complex matrix, $\tilde{\mathbf{S}}$, which is the matrix analogue of $|\tilde{s}\rangle$,

$$
\mathbf{ZS} = \tilde{\mathbf{S}},
\tag{2.9}
$$

where $\mathbf{S}$ is defined as

$$\mathbf{S} = \begin{pmatrix} s_0 & s_1 & s_2 & s_3 \\ s_1 & s_0 & -is_3 & is_2 \\ s_2 & is_3 & s_0 & -is_1 \\ s_3 & -is_2 & is_1 & s_0 \end{pmatrix}. \tag{2.10}$$

The vector state $|h\rangle$ can be written as a column vector,

$$|h\rangle = \begin{pmatrix} \tau \\ \alpha \\ \beta \\ \gamma \end{pmatrix}. \tag{2.11}$$

$|h\rangle$ vectors are generators of nondepolarizing Mueller matrices. It is possible to define and classify the Mueller matrix symmetries according to nonzero components of $|h\rangle$ vectors [20].

The appendix contains a tabulated list of $|h\rangle$ vector states, $\mathbf{Z}$ matrix states and their corresponding Mueller matrix $\mathbf{M}$ for the most common optical components used in polarimetry.

2.2   Coherent linear combination of states

The representation of an optical system with a vector state becomes more prominent when we want to study coherently combined optical systems. When analyzed in terms of vector/matrix states, analytic formulas become very similar to the quantum mechanical formulas [35]. But, it is worth noting that linear combination of two or more vector/matrix states should not be understood in the sense of quantum superposition. The vector/matrix states are mathematical objects that describe properties of optical systems (including nano systems). We never suggest a superposition of states belonging to the same optical system. Linear combination of states of optical systems means that associated deterministic physical systems are combined in parallel coherently so that they are illuminated by the same coherent wave front simultaneously. The combined system's state, in general, can be associated with a single new optical system endowed with optical properties that may be different from the optical properties of its constituents. Conversely, we may consider any deterministic optical system as a coherent parallel combination of two or more deterministic optical systems in the physical sense described above. For example, physically, a quarter-wave plate can be considered as a coherent parallel combination of two orthogonal linear polarizers and, mathematically, the state of the combined system (QWP) can be written as a linear combination of orthogonal

linear polarizer states:

$$|h_{QWP}\rangle = \frac{1+i}{2}|h_{HP}\rangle + \frac{1-i}{2}|h_{VP}\rangle, \tag{2.12}$$

where $|h_{HP}\rangle$ is a linear horizontal polarizer state vector with $\tau = \frac{1}{\sqrt{2}}, \alpha = \frac{1}{\sqrt{2}}, \beta = \gamma = 0$, $|h_{VP}\rangle$ is a linear vertical polarizer state vector with $\tau = \frac{1}{\sqrt{2}}, \alpha = -\frac{1}{\sqrt{2}}, \beta = \gamma = 0$ and $|h_{QWP}\rangle$ is a quarter-wave plate state vector with $\tau = \frac{1}{\sqrt{2}}, \alpha = \frac{i}{\sqrt{2}}, \beta = \gamma = 0$. Here, $|h_{HP}\rangle$ and $|h_{VP}\rangle$ are the basis states that span the relevant vector space. Complex coefficients $c_1 = (1+i)/2$ and $c_2 = (1-i)/2$ can be calculated in terms of scalar products of $|h\rangle$ vectors,

$$c_1 = \langle h_{HP}|h_{QWP}\rangle, \quad c_2 = \langle h_{VP}|h_{QWP}\rangle. \tag{2.13}$$

In this example basis vectors are orthogonal. In general, they could be nonorthogonal states as well, provided that they satisfy the completeness relation defined for nonorthogonal basis system for a given vector space.

2.3 Coherent combinations of states in a Young's double slit experiment

In a separate paper [22] we investigate interference effects and Pancharatnam phase [36] for several coherent combinations of $\mathbf{Z}$ matrices. We describe an experiment in which coherent light is sent through a calcite crystal that separates the photons by their polarization (due to its double refracting effect), which is an analog of Young's double slit experiment with polarizers [37, 38]. Calcite crystal can be considered as a coherent linear combination of two orthogonal linear polarizer states [25],

$$\mathbf{Z} = \frac{1}{\sqrt{2}}(\mathbf{Z_H} + e^{i\phi}\mathbf{Z_V}), \tag{2.14}$$

where $c_1 = \frac{1}{\sqrt{2}}, c_2 = \frac{e^{i\phi}}{\sqrt{2}}$ and $\mathbf{Z_H}$ and $\mathbf{Z_V}$ are matrix states corresponding to horizontal and vertical linear polarizers, respectively. Separated beams are then let to superpose, and the recombined beam is used to measure the Mueller matrix of the system, which is also calculated by the relation $\mathbf{M} = \mathbf{ZZ}^*$. The results are interpreted according to $\mathbf{Z}$ matrix formulation of coherent linear combination. When ϕ is zero or it is a multiple of 2π the result is an identity Mueller matrix, while for other values, $\mathbf{M}$ progressively evolves between a horizontal quarter-wave plate ($\phi = -\pi/2$), a vertical quarter-wave plate ($\phi = \pi/2$), and a half-wave plate ($\phi = \pi$) Mueller matrices. This work can be considered as the first experimental implementation of a Young's experiment with complete polarimetry, which

demonstrates that our method can be used for the experimental synthesis of optical devices with on demand optical properties.

2.4 Quaternion formulation of optical media states

When the light interacts with two or more optical systems ($\mathbf{J_1}, \mathbf{J_2}, \mathbf{J_3} \cdots \mathbf{J_N}$) sequentially, Jones matrix of the overall process can be written as a product of Jones matrices,

$$\mathbf{J} = \mathbf{J_N J_{N-1}} \cdots \mathbf{J_3 J_2 J_1}. \tag{2.15}$$

A similar algebra is also possible with $\mathbf{Z}$ matrices,

$$\mathbf{Z} = \mathbf{Z_N Z_{N-1}} \cdots \mathbf{Z_3 Z_2 Z_1}. \tag{2.16}$$

But, it is not possible to define multiplication of $|h\rangle$ vectors that give a similar expression. Nevertheless, $|h\rangle$ vectors are the representatives of nondepolarizing states and in the paper entitled, "Quaternion algebra for Stokes Mueller formalism" [39] we show that calculus of polarization optics can be reformulated in terms of quaternion states so that the vector and matrix states are different forms of the same quaternion state, $\boldsymbol{h}$.

The quaternion state, $\boldsymbol{h}$, is also defined in terms of τ, α, β and γ,

$$\boldsymbol{h} = \tau \mathbf{1} + i\alpha \mathbf{i} + i\beta \mathbf{j} + i\gamma \mathbf{k}, \tag{2.17}$$

where $\mathbf{1}, \mathbf{i}, \mathbf{j}$ and $\mathbf{k}$ are the quaternion basis [40]. In this work, we study the properties of $\boldsymbol{h}$ quaternion and its applications to polarization optics. Quaternion multiplication of $\boldsymbol{h}_i$ states that results in a new quaternion state $\boldsymbol{h}$ is feasible:

$$\boldsymbol{h} = \boldsymbol{h}_N \boldsymbol{h}_{N-1} \cdots \boldsymbol{h_3 h_2 h_1}. \tag{2.18}$$

Quaternion states can also be linearly combined to yield a new quaternion state, hence, coherent parallel combinations of nondepolarizing optical systems can be reformulated in terms of quaternion states. It is also shown that quaternion state, $\boldsymbol{h}$, turns out to be the rotator of the Stokes quaternion:

$$\boldsymbol{s}' = \boldsymbol{h s h}^{\dagger}, \tag{2.19}$$

where $\boldsymbol{s}$ is the quaternion form of Stokes vector ($\boldsymbol{s} = s_0 \mathbf{1} + i s_1 \mathbf{i} + i s_2 \mathbf{j} + i s_3 \mathbf{k}$), $\boldsymbol{h}^{\dagger}$ is the Hermitian conjugate of $\boldsymbol{h}$ and $\boldsymbol{s}'$ is the transformed (rotated) Stokes quaternion that corresponds

to the output Stokes vector $|s'\rangle$ of Stokes-Mueller formalism,

$$|s'\rangle = \mathbf{M}|s\rangle, \qquad (2.20)$$

where $|s\rangle$ is the usual Stokes vector.

In this thesis it is shown that $\mathbf{Z}$ matrix can be written in an exponential form, so as the quaternion state $\boldsymbol{h}$,

$$\boldsymbol{h} = e^{\hbar},$$

$$\hbar = -\frac{i}{2}(\chi\mathbf{1} + iL\mathbf{i} + iL'\mathbf{j} - iC\mathbf{k}). \qquad (2.21)$$

When we differentiate $\boldsymbol{h}$ with respect to ℓ (distance along the direction of propagation of light) we get

$$\frac{d\boldsymbol{h}}{d\ell} = \frac{d\hbar}{d\ell}\boldsymbol{h} = \frac{\hbar}{\ell}\boldsymbol{h}. \qquad (2.22)$$

This equation is a reformulation of the Stokes–Mueller differential formalism, and it can be compared with the well-known quaternion differentiation formula:

$$\dot{\boldsymbol{q}} = \frac{1}{2}\omega\boldsymbol{q}, \qquad (2.23)$$

where ω is the angular velocity. Hence, $2\hbar/\ell$ can be interpreted as the angular velocity of rotation by an angle $\theta(=T/2)$ of the quaternion state through the medium, where $\hbar$ describes the changing rate of $\boldsymbol{h}$ along the pathlength. Since, the vector state $|h\rangle$ and matrix state concepts (Jones and $\mathbf{Z}$ matrices) are different forms of the same quaternion state, $\boldsymbol{h}$, quaternion state may serve as a key element for the unification of all formalisms developed thus far at different stages by many contributors. [4, 5, 7–13, 15, 16, 18, 26, 32, 36, 38, 41–44]

2.5   Outer product of vector states and the density matrix

Linear combination and multiplication of Jones matrices, $\mathbf{Z}$ matrices and $\boldsymbol{h}$ quaternions are feasible and these forms are suitable to represent parallel and serial combinations of optical systems. Multiplication of $|h\rangle$ vectors in the form $|h\rangle|h\rangle|h\rangle\cdots$ is not defined, therefore they are not suitable to represent serial combinations. But, inner product and cross product (and even tensor product) of $|h\rangle$ vectors can be defined and vector states are suitable for all familiar vector operations. $|h\rangle$ vectors have one more advantage over the other state representations:

outer product of $|h\rangle$ vectors can also be defined [34, 46]:

$$\mathbf{H} = |h_i\rangle\langle h_j|. \tag{2.24}$$

If $i = j$, $\mathbf{H}$ is a 4×4 Hermitian matrix. In this case, $\mathbf{H}$ has a special meaning and it is called covariance matrix (also known as coherency matrix or $\mathbf{C}$ matrix) in polarization optics. But, we have a tendency to interpret $\mathbf{H}$ as a density matrix, similarly with the density matrix of quantum mechanics. In fact, $\mathbf{H}$ matrix can be considered as another form of optical media states. If there is only one deterministic system $\mathbf{H}$ matrix represents a pure system. When two or more optical systems are combined incoherently $\mathbf{H}$ matrix of the combined system will be a mixed state. $\mathbf{H}$ matrix becomes more important in case of depolarization. $\mathbf{H}$ matrix and the associated Mueller matrix can be converted into each other by a one-to-one transformation [20], and $\mathbf{H}$ matrix is very useful for analyzing depolarizing Mueller matrices.

2.6 Applications of the formalism: Interacting optical systems at the nano scale

In a coherent linear combination given by Eq.(2.3) we assume that the subsystems do not interact with each other. Coherent linear combination of interacting optical systems is another issue that we have analyzed in detail [21, 45]. In case of interaction, the combined state is no more a simple linear combination of the original constituents, now it contains a new ingredient: the interaction state contribution, $|h\rangle_{interaction}$,

$$|h\rangle = c_1|h\rangle_1 + c_2|h\rangle_2 + c_{int}|h\rangle_{interaction}. \tag{2.25}$$

Advantages of vector/matrix state formalism becomes more prominent in describing optical behaviour of interacting nanoparticles (nanoantennas) that scatter light [47, 50]. Scattering characteristics of rod shaped nanoparticles can be modelled as linear polarizer states. A rod shaped particle can be viewed as an oriented dipole endowed with a Lorentzian polarizability. When we consider two or more nanoparticles we have to take into account two basic processes: coherent parallel combination and coherent serial combination. In a coherent parallel combination wavefront of an incident plane wave interacts with the nanoparticles simultaneously, whereas, in a serial combination several successive coherent interaction stages are applied. In general, due to the mutual dipole-dipole interactions between the nanoparticles the system responds to the incident light as a whole, and the state of the combined system can be described by a single vector/matrix state. From the holistic point

of view it would be rather complicated to analyze the phenomenological behaviour of the coupled system. However, applying the state decomposition procedure could be of considerable help. It can be shown that the state of the coupled system can be written as a linear combination of several states: state vectors of individual (noninteracting) subsystems and mutual interaction states. We call this procedure "decomposition of state of interacting systems" and we apply it to several configurations of coupled nanoantenna systems. The first stage of the decomposition procedure can be carried out in terms of Jones matrices. In fact, Jones matrices are more appropriate for this purpose, because dipole-dipole interactions can be more conveniently worked out by means of the dyadic Green functions [47]. However, when we try to analyze the measured or simulated scattering matrix (Jones matrix or Mueller matrix) of the coupled system it is much more easier to work with vector states in order to exploit conventional methods of vector algebra.

Our first example is a coherent combination of two interacting coplanar nanoantennas. It is shown that the state of the coupled system can be written as a linear combination of three states: states for individual (noninteracting) nanoantennas and a state for the mutual interaction,

$$\mathbf{J} = g[\alpha_1 \mathbf{J_1} + \alpha_2 \mathbf{J_2} + (\alpha_1 \alpha_2 \Delta)\mathbf{J_{int}}], \tag{2.26}$$

where α_1 and α_2 are the Lorentzian polarizabilities of particles, Δ is the interaction coefficient, g is the overall factor which is also a function of α_1, α_2 and Δ, $\mathbf{J}$ is the Jones matrix of the coupled system, $\mathbf{J_1}$ and $\mathbf{J_2}$ are Jones matrices of noninteracting individual systems and $\mathbf{J_{int}}$ is the Jones matrix of the interaction contribution. The isolation of the interaction part from other states is very important for the analytical investigation of various phenomena such as plasmon hybridization, Fano resonances and circular effects.

Plasmon hybridization is well known in nano optics [48]. When two systems interact with each other via an interaction potential the individual resonance energy levels get shifted. These hybridized energy levels depend on in-phase and out-of-phase vibrational modes and they are very sensitive to the geometry. Even for the simplest geometries, the problem of plasmon hybridization cannot be easily tackled without an analytic approach based on the proposed decomposition of the coupled state into more basic states.

We study the case of two coupled nanoantennas [45, 49]. One antenna is oriented with an angle of $45°$ with respect to the other one. It is possible to isolate the effect of interaction mathematically as a separate state, and the contribution of this state to the whole process can be figured out by an interaction coefficient which can be calculated from the observed or simulated scattering matrices. We work on simulated scattering matrices[50]. Our first observation is that the interaction coefficient depends on the wavelength (energy) of the incident light and it diminishes by increasing distance between the particles. We also show

that the state of the coupled system has an overall coefficient, g, that also depends on energy, interaction coefficient Δ and the Lorentzian polarizabilities:

$$g \propto \frac{1}{1 - \alpha_1 \alpha_2 \Delta^2}. \tag{2.27}$$

Hybridized energies, $\omega^{\pm}$, can be calculated from the harmonic oscillator model for the coupled system,

$$\omega^{\pm} = \sqrt{\frac{\omega_1^2 + \omega_2^2 \pm \sqrt{(\omega_1^2 - \omega_2^2)^2 + 4\omega_1^2 \omega_2^2 \eta_1 \eta_2 \Delta^2}}{2}}, \tag{2.28}$$

where ω is the frequency of the incoming radiation (driving force), ω_i are the individual resonance frequencies of particles, η_i are the corresponding amplitudes of oscillations that depend on the size of the particles. Eq.(2.28) reduces to a simple equation for identical particles ($\alpha_1 = \alpha_2, \eta_1 = \eta_2, \omega_1 = \omega_2 = \omega_0$),

$$\omega^{\pm} = \omega_0 \sqrt{1 \pm \eta \Delta}. \tag{2.29}$$

The overall coefficient, g, is in general a complex number. From the roots of the denominator of g it is possible to calculate the peaks of the spectra that correspond to hybridized energies, $\omega^{\pm}$. Derivation of the hybridized energies from the vector/matrix state formalism of interacting particles shows how powerful can be the proposed analytic approach when applied to a complicated problem of coupled nanoparticles. Vector form is more flexible than the other forms when we want to play with the basis states. We first write Eq. (2.26) in terms of vector states:

$$|h\rangle = g_1 |h\rangle_1 + g_2 |h\rangle_2 + g_{int} |h\rangle_{int}, \tag{2.30}$$

where $g_1 = g\alpha_1, g_2 = g\alpha_2$, and $g_{int} = g\alpha_1 \alpha_2 \Delta$ are complex coefficients that can be determined algebraically from the results of the measurement [45]. It can be shown that the state of the coupled system can be written in an alternative way by applying the following change of basis:

$$|h^{\pm}\rangle = \frac{g_1 |h\rangle_1 + g_2 |h\rangle_2}{2\sqrt{g_1 g_2}} \pm \frac{|h\rangle_{int}}{2}. \tag{2.31}$$

We may call $|h^{\pm}\rangle$ as hybrid basis, and in terms of hybrid basis, $|h\rangle$ can be written as a linear combination of two hybrid modes, so that it is no longer necessary to make an explicit reference to the interaction term. In terms of hybrid basis Eq.(2.30) can be written as

$$|h\rangle = v^+ |h^+\rangle + v^- |h^-\rangle, \tag{2.32}$$

where $v^{\pm} = \sqrt{g_1 g_2} \pm g_{int}$. The maxima of g (i.e., the resonant conditions for the hybridized modes) occur when either $v^+ = 0$ or $v^- = 0$. In general g_1 and g_2 may vary with energy, and hybrid basis are energy dependent. If $g_1 = g_2$ hybrid basis become merely geometrical and energy independent:

$$|h^{\pm}\rangle = \frac{|h\rangle_1 + |h\rangle_2}{2} \pm \frac{|h\rangle_{int}}{2}. \qquad (2.33)$$

Resolution of the hybridized energies by the proposed analytic method becomes important when the hybridized peaks cannot be clearly identified in the scattering spectra. Strength of the interaction between the nano systems mainly depends on the orientations of the particles and the separation between the particles. If the interaction between the particles is weak the hybridized energy peaks cannot be clearly distinguished and they manifest themselves only as peak-broadening. As the interaction gets weaker peak broadening diminishes, but, with the proposed analytic method it is still possible to resolve the hybridized energy contributions.

Another interesting phenomena that our decomposition scheme can provide a clear explanation is the Fano resonances [51, 52]. In certain conditions coupled oscillators show interesting characteristics due to the interference effects between the hybrid modes. In order to observe interference effects at least two overlapping states are needed. Since the interference effects between hybrid modes stem from the linear combination of states, without the decomposition theorem Fano resonances in coupled systems cannot be analyzed. Our formulation is also in accordance with the coupled oscillator model for Fano resonances and experimental observations.

Besides all other interesting phenomena, circular polarization effects may emerge from the interaction between nano systems [53]. We have taken nanoantennas as basic constituents of more complex nanosystems and macrosystems, and we modelled the optical response of nanoantennas as oriented dipoles that behave as linear polarizers. Hence, we assume that the state of a nanoantenna oriented in a certain direction in space can be represented by a linear polarizer state. To be more specific, a linear polarizer state is characterized by a vector with real valued τ, α and β with $\gamma = 0$. Parameter γ is associated with the circular response of the system. Without accounting the interaction effects it is not possible to obtain a linearly combined system state of noninteracting linear polarizers with a nonzero γ parameter. Mathematically this means that any linear combination of linear polarizer states in the form of $|h\rangle = \alpha_1 |h\rangle_1 + \alpha_2 |h\rangle_2 + \cdots$ cannot yield circular effects without an interaction term that couples the individual states. Therefore, when we consider parallelly combined two or more nanoantennas circular effects could only emerge if there are mutual dipole-dipole interactions and there are path differences to the observation point. In fact results show that, even for interacting coplanar nanoantennas, circular effects are mostly observed at the near field where phase differences between the component nanoantennas are more prominent. In

a serial coherent combination of dipoles, it can be shown that decomposition of the state of the combined system yields two more terms that account for the circular effects due to the phase and sequential field transactions [54].

2.7 Depolarization effects and decomposition of depolarizing Mueller matrices

Up to now, we have encountered various forms of deterministic optical media states ($\mathbf{M}$, $\mathbf{J}$, $\mathbf{Z}$, $|h\rangle$, $\boldsymbol{h}$). Some of them have advantages over the other forms in some cases. But, $\mathbf{Z}$ matrix formulation is still has a distinguished property that $\mathbf{M} = \mathbf{Z}\mathbf{Z}^* = \mathbf{Z}^*\mathbf{Z}$. In other words, $\mathbf{Z}$ matrix is very akin to the nondepolarizing Mueller matrix, $\mathbf{M}$. This property becomes important when we begin to study depolarization effects.

Let us consider the simplest case and let $\mathbf{Z_1}$ and $\mathbf{Z_2}$ be two matrix states that combined coherently with complex coefficients c_1 and c_2 with the normalization condition, $c_1 c_1^* + c_2 c_2^* = 1$,

$$\mathbf{Z} = c_1 \mathbf{Z_1} + c_2 \mathbf{Z_2}. \tag{2.34}$$

Corresponding nondepolarizing Mueller matrix can be written as

$$\mathbf{M} = \mathbf{Z}\mathbf{Z}^* = c_1 c_1^* \mathbf{Z_1}\mathbf{Z_1^*} + c_2 c_2^* \mathbf{Z_2}\mathbf{Z_2^*} + c_1 c_2^* \mathbf{Z_1}\mathbf{Z_2^*} + c_2 c_1^* \mathbf{Z_2}\mathbf{Z_1^*}. \tag{2.35}$$

First two terms correspond to nondepolarizing Mueller matrices, $\mathbf{M_1}$ and $\mathbf{M_2}$,

$$\mathbf{M} = \mathbf{Z}\mathbf{Z}^* = c_1 c_1^* \mathbf{M_1} + c_2 c_2^* \mathbf{M_2} + c_1 c_2^* \mathbf{Z_1}\mathbf{Z_2^*} + c_2 c_1^* \mathbf{Z_2}\mathbf{Z_1^*}. \tag{2.36}$$

Last two terms in the expansion are not Mueller matrices, and if the optical systems are combined incoherently these coherency terms vanish,

$$\mathbf{M}_{dep} = w_1 \mathbf{M_1} + w_2 \mathbf{M_2}, \tag{2.37}$$

where $w_1 = c_1 c_1^*$, $w_2 = c_2 c_2^*$ and $\mathbf{M}_{dep}$ is a depolarizing Mueller matrix. In general, any depolarizing Mueller matrix can always be written as a convex sum of at most four nondepolarizing Mueller matrices [18].

If the Mueller matrix of a depolarizing optical system is given it can be decomposed into its arbitrary nondepolarizing constituents; but, arbitrary decompositions will not be unique,

in general, there will be infinitely many equivalent decompositions,

$$\mathbf{M}_{dep} = w_1\mathbf{M_1} + w_2\mathbf{M_2} = w_1'\mathbf{M_1'} + w_2'\mathbf{M_2'} = w_1''\mathbf{M_1''} + w_2''\mathbf{M_2''} = \cdots \qquad (2.38)$$

In the paper entitled, "Decomposition of a depolarizing Mueller matrix into its nondepolarizing components by using symmetry conditions", [1][56] we show that, in case of a two-term combination, depolarizing Mueller matrix of the combined system can be decomposed into its *original* nondepolarizing components *uniquely* if one of the component systems has a symmetry, i.e., if one of the parameters $(\tau, \alpha, \beta, \gamma)$ of one component system is zero, and if the symmetries of two component systems do not overlap completely. Decomposition procedure makes use of outer products of $|h\rangle$ vectors. Each nondepolarizing component of a depolarizing Mueller matrix can also be expressed as an outer product of $|h_i\rangle$ vectors;

$$\mathbf{H}_i = |h_i\rangle\langle h_i|, \qquad (2.39)$$

where $\mathbf{H}_i$ is the complex-Hermitian matrix (density matrix) associated with the nondepolarizing Mueller matrix, $\mathbf{M}_i$. Since, all $\mathbf{M}$ and $\mathbf{H}$ are linked with each other by a one-to-one transformation, Eq.(2.37) can be written in terms of $\mathbf{H}$ matrices also:

$$\mathbf{H}_{dep} = w_1\mathbf{H}_1 + w_2\mathbf{H}_2, \qquad (2.40)$$

where $\mathbf{H}_i$ are *rank* $= 1$ density matrices (pure states) and in case of a two-term combination $\mathbf{H}_{dep}$ is a *rank* $= 2$ density matrix (mixed state). Hence, original component Mueller matrices and their weights w_1 and w_2 can be solved uniquely from the rank conditions [55–57].

To conclude, in this thesis we investigate different forms of optical system states and we try to introduce a complete mathematical framework. We apply our formalism to several phenomena such as coherent linear combination and decomposition of deterministic optical systems, plasmon hybridization, Fano resonances and circular effects observed in different configurations of interacting nanoantennas, depolarization effects and resolution of a mixed state into its pure components by the density matrix approach.

---

[1]Note that this paper does not make use of vector and matrix states formalism that is used in the other publications discussed this thesis. At the time this paper was published (chronologically it was the first) the formalism was not yet developed.

Chapter 3

List of Publications

The main results of this thesis are included in the following original articles published in international journals:

- **Decomposition of a depolarizing Mueller matrix into its nondepolarizing components by using symmetry conditions**
  E. Kuntman and O. Arteaga, "Decomposition of a depolarizing Mueller matrix into its nondepolarizing components by using symmetry conditions," Appl. Opt. 55, 2543-2550 (2016).
  DOI: 10.1364/AO.55.002543

- **Vector and matrix states for Mueller matrices of nondepolarizing optical media**
  E. Kuntman, M. Ali Kuntman, and O. Arteaga, "Vector and matrix states for Mueller matrices of nondepolarizing optical media," J. Opt. Soc. Am. A 34, 80-86 (2017).
  DOI: 10.1364/JOSAA.34.000080

- **Formalism of optical coherence and polarization based on material media states**
  E. Kuntman, M. Ali Kuntman, J. Sancho-Parramon, and O. Arteaga, "Formalism of optical coherence and polarization based on material media states," Phys. Rev. A 95, 063819 (2017).
  DOI: 10.1103/PhysRevA.95.063819

- **Mueller matrix polarimetry on a Young's double-slit experiment analog**
  O. Arteaga, R. Ossikovski, E. Kuntman, M Ali. Kuntman, A. Canillas, and E. Garcia-Caurel, "Mueller matrix polarimetry on a Young's double-slit experiment analog," Opt. Lett. 42, 3900-3903 (2017).
  DOI: 10.1364/OL.42.003900

- **Light scattering by coupled oriented dipoles: Decomposition of the scattering matrix**

  M. Ali Kuntman, E. Kuntman, J. Sancho-Parramon, and O. Arteaga, "Light scattering by coupled oriented dipoles: Decomposition of the scattering matrix," Phys. Rev. B 98, 045410 (2018).

  DOI: 10.1103/PhysRevB.98.045410

- **Quaternion algebra for Stokes–Mueller formalism**

  Ertan Kuntman, M. Ali Kuntman, A. Canillas, and O. Arteaga, "Quaternion algebra for Stokes–Mueller formalism," J. Opt. Soc. Am. A 36, 492-497 (2019).

  DOI: 10.1364/JOSAA.36.000492

These articles are reproduced in this chapter in the published format.

applied optics

Decomposition of a depolarizing Mueller matrix into its nondepolarizing components by using symmetry conditions

ERTAN KUNTMAN AND ORIOL ARTEAGA*

Departamento de Física Aplicada i Òptica, Institute of Nanoscience and Nanotechnology IN2UB, C/Marí i Franquès, Universitat de Barcelona, 08028 Barcelona, Catalonia, Spain
*Corresponding author: oarteaga@ub.edu

A procedure for the parallel decomposition of a depolarizing Mueller matrix with an associated rank 2 covariance matrix into its two nondepolarizing components is presented. We show that, if one of the components agrees with certain symmetry conditions, the arbitrary decomposition becomes unique, and its calculation is straightforward. Solutions for six different symmetries, which are relevant for the physical interpretation of polarimetric measurements, are provided. With this procedure, a single polarimetric measurement is sufficient to fully disclose the complete polarimetric response of two different systems and evaluate their weights in the overall response. The decomposition method we propose is illustrated by obtaining the ellipsometric responses of a silicon wafer and a holographic grating from a single measurement in which the light spot illuminates sectors of both materials. In a second example, we use the decomposition to analyze an optical system in which a polarizing film is partially covered by another misaligned film.   © 2016 Optical Society of America

OCIS codes: (260.2130) Ellipsometry and polarimetry; (260.5430) Polarization; (290.5855) Scattering, polarization.

http://dx.doi.org/10.1364/AO.55.002543

1. INTRODUCTION

Many polarimetric measurements lead to depolarizing Mueller matrices. The analysis and interpretation of a depolarizing Mueller matrix tends to be more difficult than the nondepolarizing case because it is not possible to directly identify the basic polarimetric properties (different forms of diattenuation and retardance) characteristic to the material sample or remote sensing target. From an experimental point of view, it is of great interest to identify and calculate, if possible, the nondepolarizing (pure) components included in a depolarizing polarimetric measurement.

In general a depolarizing Mueller matrix can be considered as a parallel combination (convex sum) of two or more nondepolarizing Mueller (or Mueller–Jones) matrices [1,2]. The minimum number of pure components to describe a Mueller matrix depends on the rank of its covariance matrix, **H**. The rank of **H** ranges between 1 (for a nondepolarizing system) and 4. Therefore, at most four nondepolarizing components are sufficient to describe any depolarizing Mueller matrix. This work deals with the case in which the covariance matrix **H** has rank 2, and the depolarizing Mueller matrix arises from the parallel combination of two pure components:

$$\mathbf{M} = \alpha_1 \mathbf{M}_1 + \alpha_2 \mathbf{M}_2, \tag{1}$$

where the weights satisfy $\alpha_1 + \alpha_2 = 1$ and $\mathbf{M}_1$ and $\mathbf{M}_2$ are nondepolarizing Mueller matrices.

From an experimental perspective, this two-term parallel decomposition is quite relevant because it corresponds to the case in which the light beam interacts with two different types of optical media and then the emerging beams recombine incoherently at the detector. This often happens in finite spot size measurements when the light spot impinges on two spatially distributed areas of the sample with distinct optical properties. The objective of this work is to determine the individual optical response of these two areas (i.e., $\mathbf{M}_1$ and $\mathbf{M}_2$) and their weights from a single measurement of **M**. The only additional *a priori* knowledge required is that one, and only one, of the component matrices has a certain symmetry.

In a recent publication [3], Ossikovski *et al.* provided a method for such decomposition and applied it to finite spot size measurements when one of the two Mueller matrices has block-diagonal symmetry. This work offers an alternative solution to calculate the pure components and generalizes the result to six different types of symmetries of a nondepolarizing state. Even if the optical properties of a material, optical

system, or target are not known in detail, it is often possible to anticipate the Mueller matrix symmetry of at least one of the constituents because it is tightly related to its crystallographic, mesoscopic or macroscopic structure [4].

The manuscript is organized as follows: in Section 2, we review the Cloude (spectral) and arbitrary decompositions. Section 3 introduces the three fundamental symmetries in **M** and **H** for basic nondepolarizing states. The analytic equations of our two-term decomposition for each fundamental symmetry are given in Section 4. In Section 5, we study three additional symmetry cases and provide their decomposition. The decomposition procedure is illustrated with numerical and experimental examples in Sections 6 and 7, respectively.

2. CLOUDE DECOMPOSITION AND THE ARBITRARY DECOMPOSITION

Every physically acceptable Mueller matrix **M** with elements m_{ij} is associated to a positive semi-definite Hermitian matrix, **H**:

$$\mathbf{H} = \frac{1}{4} \sum_{i,j=0}^{3} m_{ij}(\sigma_i \otimes \sigma_j), \tag{2}$$

which is known as the covariance matrix. σ_k are the set composed by the Pauli matrices and the 2×2 identity matrix. $\otimes$ stands for the Kronecker product. All over this work, we assume that Mueller matrices are normalized to their element m_{00}. This brings also the condition $\operatorname{tr} \mathbf{H_1} = \operatorname{tr} \mathbf{H_2} = \operatorname{tr} \mathbf{H} = m_{00} = 1$. The elements m_{ij} of **M** can be calculated from **H** by

$$m_{ij} = \operatorname{tr}[(\sigma_i \otimes \sigma_j)\mathbf{H}]. \tag{3}$$

The Cloude decomposition [5] (also known as the spectral decomposition) shows that any **H** matrix can be considered as a combination of up to four nondepolarizing components:

$$\mathbf{H} = \sum_{i=0}^{3} \lambda_i \mathbf{u}_i \otimes \mathbf{u}_i^{\dagger} = \sum_{i=0}^{3} \lambda_i \mathbf{H}_i, \tag{4}$$

in which the weights λ_i are the non-negative eigenvalues of **H** and $\mathbf{u}_i$ are the normalized eigenvectors. The superscript $\dagger$ indicates the conjugate transpose. $\mathbf{H}_i$ are rank 1 covariance matrices. Due to the equivalency between **H** and **M**, this can also be expressed as

$$\mathbf{M} = \sum_{i=0}^{3} \lambda_i \mathbf{M}_i. \tag{5}$$

The Cloude decomposition is, in fact, a particular case among many different possible parallel combinations of a depolarizing system into pure components that are, in general, referred as the *arbitrary decomposition* of a Mueller matrix [1–3]. The arbitrary decomposition of **M** into a linear combination of pure states can be expressed as convex sum of Mueller–ones matrices:

$$\mathbf{M} = \sum_{i=0}^{3} p_i \mathbf{M}_i; \qquad \sum_{i=0}^{3} p_i = 1; \qquad p_i > 0. \tag{6}$$

In this work, we will deal with a particular case of the arbitrary decomposition in which **M** has a rank 2 covariance matrix, and the decomposition has only two terms.

3. SYMMETRIES OF THE THREE FUNDAMENTAL PURE STATES

The identification of the three distinct forms of anisotropy of a Mueller matrix leads to the definition of three possible fundamental pure states [6]. Each one of them is characterized by a simple symmetry. We organize them as follows.

A. Type 1

$$\mathbf{M}_L = \begin{bmatrix} 1 & m_{01} & 0 & 0 \\ m_{01} & 1 & 0 & 0 \\ 0 & 0 & m_{22} & m_{23} \\ 0 & 0 & -m_{23} & m_{22} \end{bmatrix}, \tag{7}$$

with $m_{01}^2 + m_{22}^2 + m_{23}^2 = 1$. Type 1 symmetry leads to a block diagonal Mueller matrix. In this case, the retardation and/or diattenuation anisotropies of the optical wave coincide with the two orthogonal axes that define the laboratory plane of reference. This symmetry is, for example, typical of ellipsometry measurements at a certain angle of incidence on isotropic materials.

B. Type 2

$$\mathbf{M}_{L'} = \begin{bmatrix} 1 & 0 & m_{02} & 0 \\ 0 & m_{11} & 0 & m_{13} \\ m_{02} & 0 & 1 & 0 \\ 0 & -m_{13} & 0 & m_{11} \end{bmatrix}, \tag{8}$$

with $m_{02}^2 + m_{11}^2 + m_{13}^2 = 1$. Type 2 symmetry corresponds to a situation in which the directions of retardation and/or diattenuation of the optical wave are aligned with the bisectors of the coordinate axes. This is a nonreciprocal symmetry.

C. Type 3

$$\mathbf{M}_C = \begin{bmatrix} 1 & 0 & 0 & m_{03} \\ 0 & m_{11} & m_{12} & 0 \\ 0 & -m_{12} & m_{11} & 0 \\ m_{03} & 0 & 0 & 1 \end{bmatrix}, \tag{9}$$

with $m_{03}^2 + m_{11}^2 + m_{12}^2 = 1$. Type 3 symmetry corresponds to a system in which the anisotropy occurs between left- and right-handed circular polarization states. In this case, there is rotational symmetry.

All these three types of nondepolarizing Mueller matrices contain only two independent parameters. The covariance matrices **H** associated to these highly symmetric pure states also exhibit some characteristic symmetries. They are presented in Table 1 together with equations that add constraints between the different **H** matrix elements. Note that each one of the three covariance matrices shown contains only two independent parameters, as $\mathbf{M}_L$, $\mathbf{M}_{L'}$ and $\mathbf{M}_C$.

4. CALCULATION OF THE TWO-TERM DECOMPOSITION

This section shows how to calculate the two nondepolarizing terms of the decomposition $\mathbf{M} = \alpha_1 \mathbf{M}_1 + \alpha_2 \mathbf{M}_2$. Due to the equivalence between **M** and **H**, this factorization can be also written as $\mathbf{H} = \alpha_1 \mathbf{H}_1 + \alpha_2 \mathbf{H}_2$. Now it has to be assumed that $\mathbf{H}_1$ has one of the symmetries shown in Table 1, while $\mathbf{H}_2$ has a

Table 1. Three Fundamental Pure States Expressed in Terms of M and H

Case	Mueller Matrix M	Covariance Matrix H[a]
Type 1	$\begin{bmatrix} 1 & m_{01} & 0 & 0 \\ m_{01} & 1 & 0 & 0 \\ 0 & 0 & m_{22} & m_{23} \\ 0 & 0 & -m_{23} & m_{22} \end{bmatrix}$	$\begin{bmatrix} P & 0 & 0 & W \\ 0 & 0 & 0 & 0 \\ 0 & 0 & 0 & 0 \\ W^* & 0 & 0 & \overline{P} \end{bmatrix}$ $\begin{array}{l} P = (1 + m_{01})/2 \\ W = (m_{22} + im_{23})/2 \\ \overline{P} = 1 - P \\ P\overline{P} = W^*W \end{array}$
Type 2	$\begin{bmatrix} 1 & 0 & m_{02} & 0 \\ 0 & m_{11} & 0 & m_{13} \\ m_{02} & 0 & 1 & 0 \\ 0 & -m_{13} & 0 & m_{11} \end{bmatrix}$	$\begin{bmatrix} K & N & N & K \\ N^* & \overline{K} & \overline{K} & N^* \\ N^* & \overline{K} & \overline{K} & N^* \\ K & N & N & K \end{bmatrix}$ $\begin{array}{l} K = (1 + m_{11})/4 \\ N = (m_{02} + im_{13})/4 \\ \overline{K} = 0.5 - K \\ K\overline{K} = N^*N \end{array}$
Type 3	$\begin{bmatrix} 1 & 0 & 0 & m_{03} \\ 0 & m_{11} & m_{12} & 0 \\ 0 & -m_{12} & m_{11} & 0 \\ m_{03} & 0 & 0 & 1 \end{bmatrix}$	$\begin{bmatrix} E & V & -V & E \\ V^* & \overline{E} & -\overline{E} & V^* \\ -V^* & -\overline{E} & \overline{E} & -V^* \\ E & V & -V & E \end{bmatrix}$ $\begin{array}{l} E = (1 + m_{11})/4 \\ V = (m_{12} + im_{03})/4 \\ \overline{E} = 0.5 - E \\ E\overline{E} = V^*V \end{array}$

[a]denotes the complex conjugate.

different symmetry or no specific symmetry. The symmetric $\mathbf{H}_1$ will be indicated as $\mathbf{H}_{1S}$.

The pure component $\alpha_2\mathbf{H}_2$ can be written:

$$\alpha_2\mathbf{H}_2 = \mathbf{H} - \alpha_1\mathbf{H}_{1S}, \qquad (10)$$

then, if $\mathbf{H}_{1S}$ is a type 1 matrix:

$$\alpha_2\mathbf{H}_2 = \begin{bmatrix} h_{00} - \alpha_1 P & h_{01} & h_{02} & h_{03} - \alpha_1 W \\ h_{10} & h_{11} & h_{12} & h_{13} \\ h_{20} & h_{21} & h_{22} & h_{23} \\ h_{30} - \alpha_1 W^* & h_{31} & h_{32} & h_{33} - \alpha_1 \overline{P} \end{bmatrix}, \qquad (11)$$

where h_{ij} are the elements of $\mathbf{H}$. As $\mathbf{H}_2$ is nondepolarizing, this matrix should be of rank 1. For a rank 1 matrix, the determinant of any 2 × 2 submatrix must be zero; otherwise, the matrix would have rank 2 or higher.

Let us consider the following determinants:

$$\begin{vmatrix} h_{00} - \alpha_1 P & h_{01} \\ h_{10} & h_{11} \end{vmatrix} = 0, \quad \begin{vmatrix} h_{00} - \alpha_1 P & h_{03} - \alpha_1 W \\ h_{10} & h_{13} \end{vmatrix} = 0. \qquad (12)$$

From these two equations, it is possible to calculate $\alpha_1 P$ and $\alpha_1 W$. $\alpha_1\overline{P}$ is calculated from the additional condition $\overline{P} = W^*W/P$ that warrants that the calculated $\mathbf{H}_{1S}$ will also be a rank 1 matrix. Finally, α_1 can be determined from the trace of $\alpha_1\mathbf{H}_{1S}$ [$\alpha_1 = \mathrm{tr}(\alpha_1\mathbf{H}_{1S})$].

Note that A, B, and C are always real parameters while G, H, M, and Y can be complex. ∗ denotes the complex conjugate.

The determinants in Eq. (12) are not the only possible alternatives to calculate the unknown parameters; in fact, there are many options. For example, P and W can also be calculated from the following determinants:

$$\begin{vmatrix} h_{00} - \alpha_1 P & h_{02} \\ h_{20} & h_{22} \end{vmatrix} = 0, \quad \begin{vmatrix} h_{00} - \alpha_1 P & h_{03} - \alpha_1 W \\ h_{20} & h_{23} \end{vmatrix} = 0. \qquad (13)$$

Interestingly, the unknown parameters cannot be calculated when central 2 × 2 submatrix of $\mathbf{H}$ (i.e., the elements h_{11}, h_{12}, h_{21}, and h_{22}) vanishes. This clearly occurs when $\mathbf{H}_2$ has the same symmetry as $\mathbf{H}_{1S}$, i.e., when it has type 1 symmetry, too. Such an overlap makes the decomposition impossible. In all the other situations, i.e., when $\mathbf{H}_2$ is of type 2 or 3, or a combination between different types, will lead to a nonvanishing 2 × 2 central submatrix.

A calculation similar to Eq. (11)–(13) can be repeated when $\mathbf{H}_{1S}$ is assumed to have type 2 or type 3 symmetry. Table 2 summarizes the solutions for all three types. The equations presented there can be directly used to calculate $\mathbf{H}_{1S}$ from $\mathbf{H}$ for a given symmetry in $\mathbf{H}_{1S}$.

In Table 2, the symmetries 2 and 3 are split in two different cases (a and b). Cases labeled as *a* offer a solution based on the most outer determinant, i.e.:

$$\mathrm{Det}\,\mathbf{A} = \begin{vmatrix} h_{00} & h_{03} \\ h_{30} & h_{33} \end{vmatrix}, \qquad (14)$$

Table 2. Equations That Solve the Two-Term Parallel Decomposition for H$_{1S}$ Having Type 1, 2, or 3 Symmetry

Symmetry	Equations
Type 1	$\alpha_1 P = (h_{11}h_{00} - h_{10}h_{01})/h_{11}$ $\alpha_1 W = [h_{10}h_{03} - h_{13}(h_{00} - \alpha_1 P)]/h_{10}$ $\alpha_1 \overline{P} = \alpha_1 W W^*/P$ alternatively, $\alpha_1 P = (h_{22}h_{00} - h_{20}h_{02})/h_{22}$ $\alpha_1 W = [h_{20}h_{03} - h_{23}(h_{00} - \alpha_1 P)]/h_{20}$
Type 2a	$\alpha_1 K = \frac{h_{30}h_{03} - h_{00}h_{33}}{h_{30} + h_{03} - h_{33} - h_{00}}$ $\alpha_1 N = \frac{h_{30}h_{01} - h_{00}h_{31} + \alpha_1 K(h_{31} - h_{01})}{h_{30} - h_{00}}$ $\alpha_1 \overline{K} = \alpha_1 NN^*/K$
Type 2b	$\alpha_1 \overline{K} = \frac{h_{21}h_{12} - h_{11}h_{22}}{h_{21} + h_{12} - h_{22} - h_{11}}$ $\alpha_1 N = \frac{h_{11}h_{02} - h_{12}h_{01} + \alpha_1 \overline{K}(h_{01} - h_{02})}{h_{11} - h_{12}}$ $\alpha_1 K = \alpha_1 NN^*/\overline{K}$
Type 3a	$\alpha_1 E = \frac{h_{30}h_{03} - h_{00}h_{33}}{h_{30} + h_{03} - h_{33} - h_{00}}$ $\alpha_1 V^* = \frac{h_{10}h_{03} - h_{00}h_{13} + \alpha_1 E(h_{13} - h_{10})}{h_{03} - h_{00}}$ $\alpha_1 \overline{E} = \alpha_1 V V^*/E$
Type 3b	$\alpha_1 \overline{E} = \frac{h_{11}h_{22} - h_{21}h_{12}}{h_{21} + h_{12} - h_{22} + h_{11}}$ $\alpha_1 V = \frac{h_{01}h_{12} - h_{11}h_{02} + \alpha_1 \overline{E}(h_{01} + h_{02})}{h_{11} + h_{12}}$ $\alpha_1 E = \alpha_1 V V^*/\overline{E}$
In all cases α_1 is determined from $\alpha_1 = \mathrm{tr}(\alpha_1\mathbf{H}_{1S})$	

while cases labeled as b offer a solution based on the central determinant,

$$\text{Det } \mathbf{B} = \begin{vmatrix} h_{11} & h_{12} \\ h_{21} & h_{22} \end{vmatrix}. \tag{15}$$

When dealing with experimental data and to avoid numerically ill conditions, it is advisable to calculate the unknowns using determinants that do not lead to divisions by small numbers. Therefore, we should choose the solution based on the determinant that contains elements with larger values because it is numerically more stable and noise robust. Moreover, in some particular situations, only one of the two sets of solutions may be applicable. For example, if $\mathbf{H}$ is a combination between type 1 and type 2, Det $\mathbf{B}$ will vanish, and only solutions based on Det $\mathbf{A}$ will work. Likewise, if $\mathbf{H}$ is a combination between types 2 and 3, then solutions based on Det $\mathbf{A}$ need to be avoided.

Instead of using different sets of solutions, one for every matrix type, it is also possible to use a unique set if columns and rows permutations are used to transform the symmetry type. For example, a Mueller matrix with type 2 symmetry can be reduced to a type 1 by permuting the second and third rows and columns, and one with type 3 symmetry can be reduced to a type 1 by cyclically permuting the second, third, and fourth rows and columns. This operation is geometrically equivalent to relabeling the axes of the Poincaré sphere. Thus, after applying these permutations, the equations corresponding to type 1 symmetry could be used to study all three matrix types. If this approach is used to calculate the decomposition, it is then necessary to undo the permutations to recover the original symmetry type.

5. OTHER SYMMETRIC PURE STATES

The three fundamental symmetries defined in the previous section are not the only cases in which a pure state exhibits symmetries in its Mueller matrix. The anisotropies corresponding to symmetry types 1, 2, and 3 can appear combined one with another, thus generating pure states that are less simple than those given in Table 1 but still highly symmetric. We identify these symmetries as types 1-2, 1-3, and 2-3. The type 1-2

symmetry has no circular anisotropy, the type 1-3 symmetry has no linear anisotropy along the bisectors of the coordinate frame and the type 2-3 has no linear anisotropy aligned with the axes of the reference frame.

Table 3 shows the parameterization of the Mueller matrices and their equivalent covariance matrices for these three additional symmetry cases. The two-term parallel decomposition given in Eq. (1) also has a solution when one of the components has symmetry type 1-2, 1-3, or 2-3. The only additional requirement is that the other component of the factorization must include some anisotropy of the missing type. For example, if one of the components has a known symmetry type 1-2, the decomposition is solvable as long as the other term has some circular anisotropy (i.e., of type 3).

The procedure to calculate the terms of decomposition is analog to the one in the previous section. The elements of the covariance matrix can be calculated from zeroing the determinant of every 2×2 submatrix of the matrix given by Eq. (10). The analytic equations that permit the decomposition for these symmetry cases are summarized in Table 4. All covariance matrix elements not listed in this table can be directly calculated using the additional relations between parameters given in the last column of Table 3.

6. NUMERICAL EXAMPLE

Consider the two pure states given by the Mueller matrices:

$$\mathbf{M}_1 = \begin{bmatrix} 1 & 0 & 0 & 0.1489 \\ 0 & 0.9108 & 0.3851 & 0 \\ 0 & -0.3851 & 0.9108 & 0 \\ 0.1489 & 0 & 0 & 1 \end{bmatrix}, \tag{16a}$$

$$\mathbf{M}_2 = \begin{bmatrix} 1 & 0.0544 & 0.6124 & 0.2719 \\ 0.2502 & 0.7064 & 0.2447 & 0.2273 \\ 0.6124 & -0.2146 & 0.8118 & 0.4669 \\ -0.1196 & -0.0768 & -0.4519 & 0.5935 \end{bmatrix}. \tag{16b}$$

$\mathbf{M}_1$ has type 3 symmetry, while $\mathbf{M}_2$ contains all types of anisotropy and offers no evident symmetry. For this example,

Table 3.   Three Additional Symmetry Cases for Pure States

Case	Mueller Matrix M	Covariance Matrix H[a]
Type 1-2	$\begin{bmatrix} 1 & m_{01} & m_{02} & m_{03} \\ m_{01} & m_{11} & m_{12} & m_{13} \\ m_{02} & m_{12} & m_{22} & m_{23} \\ -m_{03} & -m_{13} & -m_{23} & m_{33} \end{bmatrix}$	$\begin{bmatrix} A & G & G & M \\ G^* & B & B & H^* \\ G^* & B & B & H^* \\ M^* & H & H & C \end{bmatrix} \begin{array}{l} AB = GG^* \\ GH^* = MB \\ BC = HH^* \end{array}$
Type 1-3	$\begin{bmatrix} 1 & m_{01} & m_{02} & m_{03} \\ m_{01} & m_{11} & m_{12} & m_{13} \\ -m_{02} & -m_{12} & m_{22} & m_{23} \\ m_{03} & m_{13} & -m_{23} & m_{33} \end{bmatrix}$	$\begin{bmatrix} A & G & -G & M \\ G^* & B & -B & H^* \\ G^* & -B & B & -H^* \\ M^* & H & -H & C \end{bmatrix} \begin{array}{l} AB = GG^* \\ GH^* = MB \\ BC = HH^* \end{array}$
Type 2-3	$\begin{bmatrix} 1 & m_{01} & m_{02} & m_{03} \\ -m_{01} & m_{11} & m_{12} & m_{13} \\ m_{02} & -m_{12} & m_{22} & m_{23} \\ m_{03} & -m_{13} & m_{23} & m_{33} \end{bmatrix}$	$\begin{bmatrix} A & G & H & A \\ G^* & B & Y & G^* \\ H^* & Y^* & C & H^* \\ A & G & H & A \end{bmatrix} \begin{array}{l} AB = GG^* \\ HG^* = AY \\ AC = HH^* \end{array}$

[a]Note that A, B and C are always real parameters while G, H, M and Y can be complex. * denotes the complex conjugate.
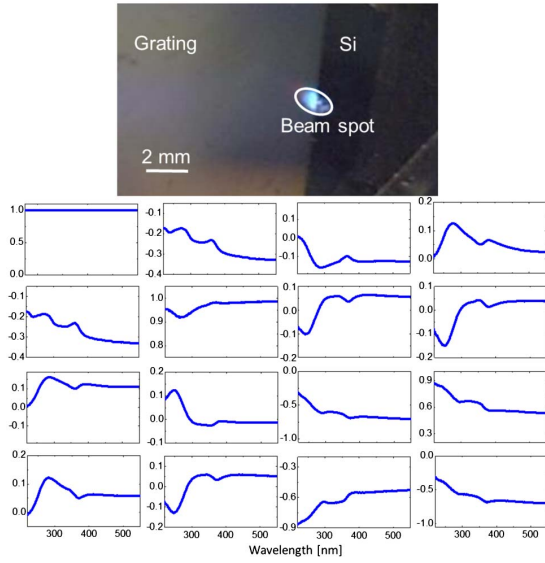
Fig. 1. Spectroscopic ellipsometry measurement in the boundary between a Si wafer and a holographic grating. The light spot was carefully placed so that it impinged simultaneously on both materials, as is shown in the top photo. The angle of incidence was 60°.

Table 4. Equations That Solve the Two-Term Parallel Decomposition for Types 1-2, 1-3, and 2-3

Symmetry	Equations
Type 1-2	$\alpha_1 B = \frac{h_{21}h_{12}-h_{11}h_{22}}{h_{21}+h_{12}-h_{22}-h_{11}}$ $\alpha_1 G = \frac{h_{02}h_{11}-h_{01}h_{12}+\alpha_1 B(h_{01}-h_{02})}{h_{11}-h_{12}}$ $\alpha_1 H = \frac{h_{31}h_{22}-h_{21}h_{32}-\alpha_1 B(h_{31}-h_{32})}{h_{22}-h_{21}}$
Type 1-3	$\alpha_1 B = \frac{h_{11}h_{22}-h_{21}h_{12}}{h_{11}+h_{22}+h_{21}+h_{12}}$ $\alpha_1 G = \frac{h_{01}h_{12}-h_{11}h_{02}+\alpha_1 B(h_{01}+h_{02})}{h_{11}+h_{12}}$ $\alpha_1 H = \frac{h_{31}h_{22}-h_{21}h_{32}-\alpha_1 B(h_{31}+h_{32})}{h_{22}+h_{21}}$
Type 2-3	$\alpha_1 A = \frac{h_{30}h_{03}-h_{00}h_{33}}{h_{30}+h_{03}-h_{33}-h_{00}}$ $\alpha_1 G^* = \frac{h_{10}h_{03}-h_{00}h_{13}-\alpha_1 A(h_{10}-h_{13})}{h_{03}-h_{00}}$ $\alpha_1 H^* = \frac{h_{20}h_{03}-h_{00}h_{23}-\alpha_1 A(h_{20}-h_{23})}{h_{03}-h_{00}}$

In all cases α_1 is determined from $\alpha_1 = \mathrm{tr}(\alpha_1 \mathbf{H}_{1S})$

we take the weights $\alpha_1 = 0.3$ and $\alpha_2 = 0.7$ to generate a combined state given by $\mathbf{M} = \alpha_1 \mathbf{M}_1 + \alpha_2 \mathbf{M}_2$. The covariance matrix associated with this combined Mueller matrix is

$$\mathbf{H} = \begin{bmatrix} 0.4952 & 0.1789+0.0985i & 0.0407+0.0232i & 0.3892+0.0161i \\ 0.1789-0.0985i & 0.0923 & 0.0315-0.0026i & 0.1736-0.0037i \\ 0.0407-0.0232i & 0.0315+0.0026i & 0.0238 & 0.0355+0.0190i \\ 0.3892-0.0161i & 0.1736+0.0037i & 0.0355-0.0190i & 0.3886 \end{bmatrix}. \quad (17)$$

In this example, Det $\mathbf{A}$ clearly involves larger values than Det $\mathbf{B}$; thus, it is advisable to chose *type 3a* equations of Table 2 to solve this particular case. However, there is enough numerical precision in this example to use any of the two sets of equations (3a or 3b) to obtain $\alpha_1 \mathbf{H}_{1S}$ successfully.

In the given numerical example, the parameters are found as follows:

$$E\alpha_1 = 0.1433, \quad (18)$$

$$V\alpha_1 = 0.0289 + 0.0112i, \quad (19)$$

$$\overline{E}\alpha_1 = 0.0067, \quad (20)$$

and α_1 is calculated as $\alpha_1 = \mathrm{tr}(\alpha_1 \mathbf{H}_{1S}) = 2(E\alpha_1 + \overline{E}\alpha_1) = 0.3$. Finally, we obtain the following covariance matrix:

$$\mathbf{H}_1 = \begin{bmatrix} 0.4777 & 0.0962+0.0372i & -0.0962-0.0372i & 0.4777 \\ 0.0962-0.0372i & 0.0223 & -0.0223 & 0.0962-0.0037i \\ -0.0962+0.0372i & -0.0223 & 0.0223 & -0.0962+0.0372i \\ 0.4777 & 0.0962+0.0372i & -0.0962-0.0372i & 0.4777 \end{bmatrix}, \quad (21)$$

and $\mathbf{H}_2$ will be trivially recovered from $\alpha_2 \mathbf{H}_2 = \mathbf{H} - \alpha_1 \mathbf{H}_1$.

In summary, only with the information given by Eq. (17) and the *a priori* knowledge about type 3 symmetry, we have recovered the two covariance matrices of the original pure states.

7. EXPERIMENTAL EXAMPLES

To demonstrate the applicability of the decomposition with a real experiment, we have considered two different examples.
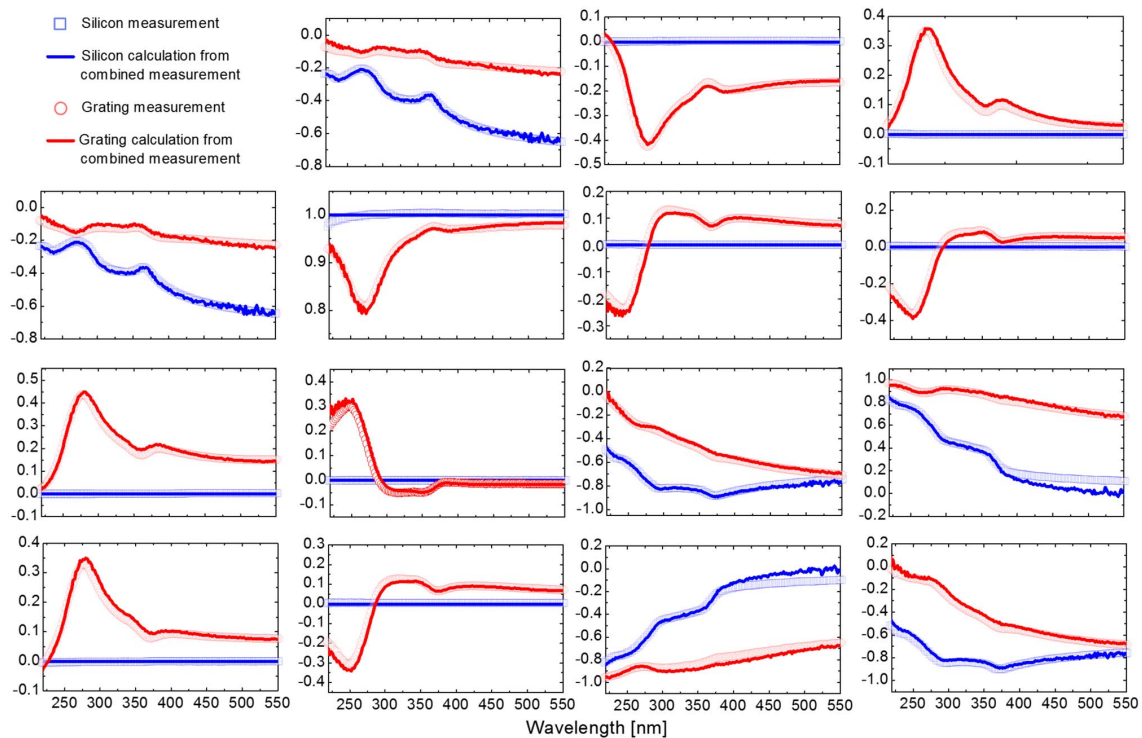
Fig. 2. Solid lines show the calculated ellipsometric response for the silicon wafer (blue) and the grating (red) from the "mixed" Si-grating measurement. The experimental spectroscopic Mueller matrix measured for Si (circles) and the grating (squares) are also shown for comparison.

A. Combined Measurement of a Silicon Wafer and a Holographic Grating

Here, we used a holographic reflection grating (1800 lines/mm) and studied its ellipsometric specular reflection (zeroth order diffraction) at an angle of incidence of 60°. A silicon wafer was placed on top of the grating so that the light spot (of around 2 mm in diameter) impinged simultaneously on the two different media: silicon and grating. Spectroscopic measurements were created with the homemade Mueller matrix ellipsometer based on four photoelastic modulators described in [7]. Figure 1 shows the Mueller matrix measurement of the combined Si + grating system as the light beam illuminates a region that includes both materials.

Silicon has a cubic crystal structure, and measurement on a Si wafer leads to a type 1 Mueller matrix that is typical of ellipsometry measurements. With this *a priori* knowledge, and by using the decomposition procedure we have described, we will be able to obtain the polarimetric responses of Si and the grating from the "mixed" measurement given in Fig. 1. In principle, this decomposition will be possible if the grating does not exhibit a Mueller matrix symmetry that coincides with the one of Si. The diffraction grating is sensitive to the polarization of the incoming radiation, and it is well-known that, when the direction of the grooves is not parallel or perpendicular to the plane of incidence, the characteristic Mueller matrix of the grating differs considerably from type 1 symmetry. The accuracy and validity of the decomposed data (i.e., the retrieved

Mueller matrices of Si and the grating) is going to be checked with independent measurements made on silicon and on the grating at the same orientations that were used for the combined measurement.

The covariance matrices **H** associated to the experimental depolarizing Mueller matrices of Fig. 1 should have rank 2, as we know that the studied optical system consists of two spatially distributed nondepolarizing components. However, in practice, due to the unavoidable noise and other experimental nonidealities, it is possible that the other two eigenvalues of **H** are small but not strictly zero. To amend this, we imposed the
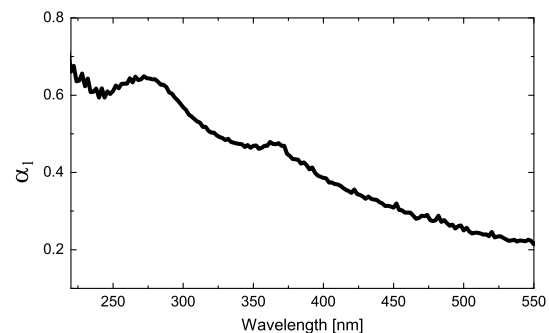
Fig. 3. Calculated weight of Si (α_1) for the combined Si-grating measurement.
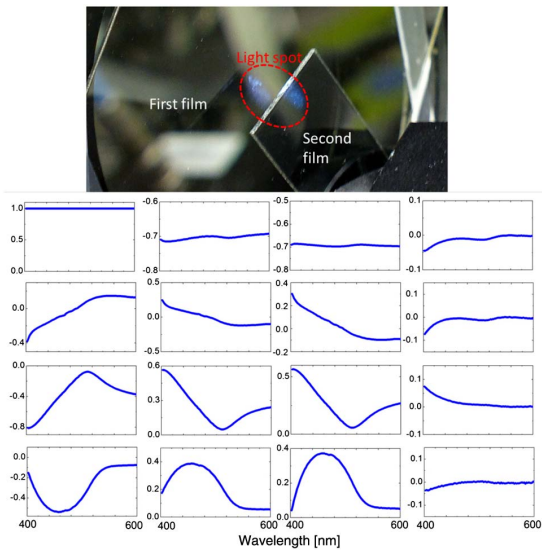
Fig. 4. Spectroscopic transmission measurement in which a portion of the beam goes through two superposed polarizing films; the other portion only goes through one.

rank 2 condition by Cloude-decomposing the experimental data and truncating the summation in Eq. (4) to only two terms, those associated to the two largest eigenvalues. Once the rank 2 condition is warranted, the equations shown in the first entry of Table 2 can be used to decompose $\mathbf{H}$ into the two nondepolarizing components corresponding to Si ($\mathbf{H}_{1S}$) and the grating ($\mathbf{H}_2$).

Figure 2 shows the resulting Mueller matrices for the Si wafer and the grating. This figure compares the data calculated from the combined measurement with the independent measurements made on both materials. The agreement with the experimental data shows that the decomposition is physically meaningful because it recovers the true optical response of the two components. In addition to the data included in Fig. 2, the decomposition also provides the weights. Figure 3 shows the spectroscopically determined α_1. In the UV region of the spectra, α_1 takes larger values because silicon has a higher reflectivity than the grating. In fact, it is possible to distinguish two peaks at around 275 and 360 nm, which are characteristic of the reflectance spectra of silicon. However, above 500 nm, the contribution of the grating is clearly dominant ($\alpha_1 < 0.3$), and, because of its smaller weight, there is slightly more uncertainty in the determination of the polarimetric response of silicon.
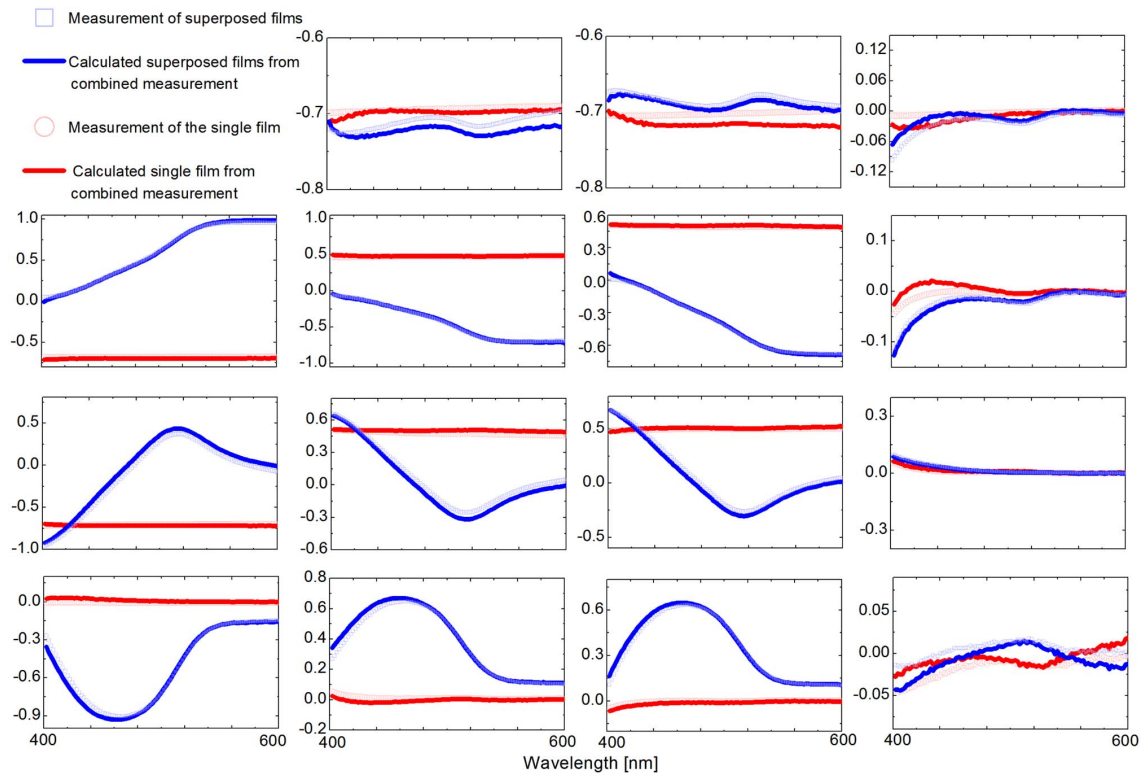
Fig. 5. Solid lines show the calculated transmission Mueller matrix for the single polarizing film (red) and the superposed films (blue) from the "mixed" measurement. The experimental Mueller matrices measured for single film (circles) and the superposed films (squares) are also shown for comparison.

B. Measurement of a Polarizer Film Partially Covered by Another Misaligned Polarizing Film

In this example, we studied a randomly oriented polarizing film that was partially covered by another misaligned polarizing film, as is shown in the photo in Fig. 4. This second polarizing film had nonideal characteristics and exhibited some remarkable retardance below 500 nm. The light spot was placed so that a portion of the beam transmitted only through the first polarizing film, while the other portion of the beam transmitted through the two superposed films. This combined system was measured in transmission, and we obtained the Mueller matrix spectra, as shown in Fig. 4.

The effect of a randomly oriented polarizing film is described by a type 1-2 Mueller matrix because it has no circular anisotropy (the change in polarization is the same effect for left- and right-circular polarization states). The region with the two superposed and misaligned films does not have any particular symmetry in the Mueller matrix because it contains all three types of anisotropy.

The same approach as in the previous example was used: we independently measured the Mueller matrix of every component of system and compared these values with the data extracted from the combined measurement after imposing the rank 2 condition using the Cloude decomposition. Experimental and calculated results from the combined measurement in the spectral range from 400 to 600 nm are presented together in Fig. 5. The agreement between both sets of data shows, here, too, that the decomposition is capable of calculating the optical response of the two components from a single Mueller matrix measurement.

8. CONCLUSION

We have shown that, for depolarizing polarimetric experiments, which are a combination of two nondepolarizing states, it is possible to analytically retrieve the individual polarimetric response of each component. The decomposition of the combined state into its pure constituents is possible if one of them agrees to a certain symmetry pattern; no other specific knowledge about the individual responses is required. We have reviewed the three basic fundamental symmetries of a nondepolarizing system plus three additional symmetry cases that arise when different types of anisotropy are combined. The analytic equations that solve the decomposition for each one of these six cases have been provided so that the Mueller matrices of the two pure components and their respective weight can be directly calculated.

We believe that this two-term parallel decomposition can be useful for the experimentalist dealing with depolarizing systems because it offers insights about the depolarization mechanisms and permits obtaining physical information about the constituents of complex optical media without any modeling effort.

REFERENCES

1. J. J. Gil, "Review on Mueller matrix algebra for the analysis of polarimetric measurements," J. Appl. Remote Sens. **8**, 081599 (2014).
2. J. J. Gil, "Polarimetric characterization of light and media," Eur. Phys. J. Appl. Phys. **40**, 1–47 (2007).
3. R. Ossikovski, E. Garcia-Caurel, M. Foldyna, and J. J. Gil, "Application of the arbitrary decomposition to finite spot size Mueller matrix measurements," Appl. Opt. **53**, 6030–6036 (2014).
4. O. Arteaga, "Useful Mueller matrix symmetries for ellipsometry," Thin Solid Films **571**, 584–588 (2014).
5. S. R. Cloude, "Conditions for physical realizability of matrix operators in polarimetry," Proc. SPIE **1166**, 177–187 (1990).
6. O. Arteaga, E. Garcia-Caurel, and R. Ossikovski, "Anisotropy coefficients of a Mueller matrix," J. Opt. Soc. Am. A **28**, 548–553 (2011).
7. O. Arteaga, J. Freudenthal, B. Wang, and B. Kahr, "Mueller matrix polarimetry with four photoelastic modulators: theory and calibration," Appl. Opt. **51**, 6805–6817 (2012).

Journal of the
Optical Society
of America
A

OPTICS, IMAGE SCIENCE, AND VISION

Vector and matrix states for Mueller matrices of nondepolarizing optical media

Ertan Kuntman,[1] **M. Ali Kuntman,**[2] **and Oriol Arteaga**[1,*]

[1]*Dep. Física Aplicada, Feman Group, IN2UB, Universitat de Barcelona, Barcelona, Spain*
[2]*Independent Scholar, Ankara, Turkey*
Corresponding author: oarteaga@ub.edu

Nondepolarizing Mueller matrices contain up to seven independent parameters. However, these seven parameters typically do not appear explicitly among the measured 16 parameters of a Mueller matrix, so that they are not directly accessible for physical interpretation. This work shows that all the information contained in a nondepolarizing Mueller matrix can be conveniently expressed in terms of a four component covariance vector state or a generating 4 × 4 matrix, which can be understood as a matrix state. The generating matrix, besides being directly related to the nondepolarizing Mueller matrix, mimics all properties of the Jones matrix and provides a powerful mathematical tool for formulating all properties of nondepolarizing systems, including the Mueller symmetries and the anisotropy coefficients.   © 2016 Optical Society of America

OCIS codes: (260.2130) Ellipsometry and polarimetry; (260.5430) Polarization; (290.5855) Scattering, polarization.

https://doi.org/10.1364/JOSAA.34.000080

1. INTRODUCTION

The 16 real elements of a Mueller matrix describe the transformation of the polarization of a beam when interacting with an optical material or system. In absence of depolarization the Mueller matrix contains only seven independent parameters [1].

To study the properties of a Mueller matrix $\mathbf{M}$ (nondepolarizing or depolarizing), it is useful to transform $\mathbf{M}$ into a Hermitian matrix $\mathbf{H}$. This Hermitian matrix is sometimes called the covariance matrix of $\mathbf{M}$ and is defined as

$$\mathbf{H} = \frac{1}{4}\sum_{i,j=0}^{3} M_{ij}(\boldsymbol{\sigma}_i \otimes \boldsymbol{\sigma}_j^*), \tag{1}$$

where M_{ij} are the elements of $\mathbf{M}$, the superscript * indicates conjugate, $\otimes$ is the Kronecker product, and $\boldsymbol{\sigma}_i$ are the Pauli matrices with the 2 × 2 identity in the following order:

$$\boldsymbol{\sigma}_0 = \begin{pmatrix} 1 & 0 \\ 0 & 1 \end{pmatrix}, \qquad \boldsymbol{\sigma}_1 = \begin{pmatrix} 1 & 0 \\ 0 & -1 \end{pmatrix}, \tag{2}$$

$$\boldsymbol{\sigma}_2 = \begin{pmatrix} 0 & 1 \\ 1 & 0 \end{pmatrix}, \qquad \boldsymbol{\sigma}_3 = \begin{pmatrix} 0 & -i \\ i & 0 \end{pmatrix}. \tag{3}$$

Here 4 × 4 matrices $\boldsymbol{\sigma}_i \otimes \boldsymbol{\sigma}_j^*$ form a complete basis for a given $\mathbf{M}$ to $\mathbf{H}$ transformation. However, the *representation* of $\mathbf{H}$ is not unique. Instead of the basis $\boldsymbol{\sigma}_i \otimes \boldsymbol{\sigma}_j^*$, we can use

the transformed basis $\mathbf{U}(\boldsymbol{\sigma}_i \otimes \boldsymbol{\sigma}_j^*)\mathbf{U}^{-1}$, where $\mathbf{U}$ is any suitable unitary transformation.

In this work we will let $\mathbf{U} = \mathbf{A}$, and we will use the following transformed basis:

$$\Pi_{ij} = \mathbf{A}(\boldsymbol{\sigma}_i \otimes \boldsymbol{\sigma}_j^*)\mathbf{A}^{-1}, \tag{4}$$

where

$$\mathbf{A} = \begin{pmatrix} 1 & 0 & 0 & 1 \\ 1 & 0 & 0 & -1 \\ 0 & 1 & 1 & 0 \\ 0 & i & -i & 0 \end{pmatrix},$$

$$\mathbf{A}^{-1} = \frac{1}{2}\mathbf{A}^\dagger = \frac{1}{2}\begin{pmatrix} 1 & 1 & 0 & 0 \\ 0 & 0 & 1 & -i \\ 0 & 0 & 1 & i \\ 1 & -1 & 0 & 0 \end{pmatrix}, \tag{5}$$

where the superscript † indicates the conjugate transpose. In terms of the new basis Π_{ij}, the covariance matrix $\mathbf{H}$ becomes

$$\mathbf{H} = \frac{1}{4}\sum_{i,j=0}^{3} M_{ij}\Pi_{ij}. \tag{6}$$

In an explicit matrix form,

$$\mathbf{H} = \frac{1}{4}\begin{pmatrix} \begin{matrix} M_{00} + M_{11} \\ M_{22} + M_{33} \end{matrix} & \begin{matrix} M_{01} + M_{10} \\ -i(M_{23} - M_{32}) \end{matrix} & \begin{matrix} M_{02} + M_{20} \\ +i(M_{13} - M_{31}) \end{matrix} & \begin{matrix} M_{03} + M_{30} \\ -i(M_{12} - M_{21}) \end{matrix} \\ \begin{matrix} M_{01} + M_{10} \\ +i(M_{23} - M_{32}) \end{matrix} & \begin{matrix} M_{00} + M_{11} \\ -M_{22} - M_{33} \end{matrix} & \begin{matrix} M_{12} + M_{21} \\ +i(M_{03} - M_{30}) \end{matrix} & \begin{matrix} M_{13} + M_{31} \\ -i(M_{02} - M_{20}) \end{matrix} \\ \begin{matrix} M_{02} + M_{20} \\ -i(M_{13} - M_{31}) \end{matrix} & \begin{matrix} M_{12} + M_{21} \\ -i(M_{03} - M_{30}) \end{matrix} & \begin{matrix} M_{00} - M_{11} \\ +M_{22} - M_{33} \end{matrix} & \begin{matrix} M_{23} + M_{32} \\ +i(M_{01} - M_{10}) \end{matrix} \\ \begin{matrix} M_{03} + M_{30} \\ +i(M_{12} - M_{21}) \end{matrix} & \begin{matrix} M_{13} + M_{31} \\ +i(M_{02} - M_{20}) \end{matrix} & \begin{matrix} M_{23} + M_{32} \\ -i(M_{01} - M_{10}) \end{matrix} & \begin{matrix} M_{00} - M_{11} \\ -M_{22} + M_{33} \end{matrix} \end{pmatrix}. \tag{7}$$

This form of **H** was given by Cloude in 1986 [2]; he referred to this matrix as the "coherency" matrix, and, while the matrix in Eq. (1) seems to be more popular in the literature, he reserved the name "covariance" matrix. However, posterior authors have not necessarily kept the same naming distinction. Here, to avoid confusion, we will refer to any representation of **H** as a covariance matrix.

The inverse transformation from **H** to **M** is given by

$$M_{ij} = \text{tr}(\Pi_{ij}\mathbf{H}) \qquad \text{or} \qquad \mathbf{M} = \sum_{i,j=0}^{3} H_{ij}\Pi_{ij}, \tag{8}$$

where H_{ij} are the elements of the matrix **H**.

2. COVARIANCE VECTOR OF A NONDEPOLARIZING MUELLER MATRIX

If and only if the Mueller matrix of the system is nondepolarizing, the associated covariance matrix **H** will be of rank 1. In this case it is always possible to define a covariance vector $|h\rangle$ such that

$$\mathbf{H} = |h\rangle\langle h|, \tag{9}$$

where the vector $|h\rangle$ is the eigenvector of **H** corresponding to the single non-zero eigenvalue of **H** [3–5]. If $M_{00} = 1$, $\lambda_0 = \text{tr}(\mathbf{H}) = 1$, and all other eigenvalues being equal to zero, $\langle h|h\rangle = 1$. In general, if rank $(\mathbf{H}) = 1$, $\lambda_0 = \text{tr}(\mathbf{H}) = M_{00}$, $\lambda_1 = \lambda_2 = \lambda_3 = 0$; hence, if $M_{00} > 0$, **H** is positive semidefinite.

In our preferred basis Π_{ij}, we will parametrize the dimensionless components of $|h\rangle$ as τ, α, β, and γ and write

$$|h\rangle = \begin{pmatrix} \tau \\ \alpha \\ \beta \\ \gamma \end{pmatrix}. \tag{10}$$

If determined from a Mueller matrix, α, β, and γ will generally be complex parameters, while τ can always be chosen as real and positive because the Mueller matrix does not contain information about the global phase.

In terms of the parameters τ, α, β, γ the covariance matrix **H** takes its simplest form:

$$\mathbf{H} = |h\rangle\langle h| = \begin{pmatrix} \tau\tau^* & \tau\alpha^* & \tau\beta^* & \tau\gamma^* \\ \alpha\tau^* & \alpha\alpha^* & \alpha\beta^* & \alpha\gamma^* \\ \beta\tau^* & \beta\alpha^* & \beta\beta^* & \beta\gamma^* \\ \gamma\tau^* & \gamma\alpha^* & \gamma\beta^* & \gamma\gamma^* \end{pmatrix}. \tag{11}$$

Any nondepolarizing Mueller matrix can thus be written in terms of τ, α, β, and γ as

$$\mathbf{M} = \begin{pmatrix} \begin{matrix} \tau\tau^* + \alpha\alpha^* \\ \beta\beta^* + \gamma\gamma^* \end{matrix} & \begin{matrix} \tau\alpha^* + \alpha\tau^* \\ +i(\gamma\beta^* - \beta\gamma^*) \end{matrix} & \begin{matrix} \tau\beta^* + \beta\tau^* \\ +i(\alpha\gamma^* - \gamma\alpha^*) \end{matrix} & \begin{matrix} \tau\gamma^* + \gamma\tau^* \\ +i(\beta\alpha^* - \alpha\beta^*) \end{matrix} \\ \begin{matrix} \tau\alpha^* + \alpha\tau^* \\ -i(\gamma\beta^* - \beta\gamma^*) \end{matrix} & \begin{matrix} \tau\tau^* + \alpha\alpha^* \\ -\beta\beta^* - \gamma\gamma^* \end{matrix} & \begin{matrix} \alpha\beta^* + \beta\alpha^* \\ +i(\tau\gamma^* - \gamma\tau^*) \end{matrix} & \begin{matrix} \alpha\gamma^* + \gamma\alpha^* \\ +i(\beta\tau^* - \tau\beta^*) \end{matrix} \\ \begin{matrix} \tau\beta^* + \beta\tau^* \\ -i(\alpha\gamma^* - \gamma\alpha^*) \end{matrix} & \begin{matrix} \alpha\beta^* + \beta\alpha^* \\ -i(\tau\gamma^* - \gamma\tau^*) \end{matrix} & \begin{matrix} \tau\tau^* - \alpha\alpha^* \\ +\beta\beta^* - \gamma\gamma^* \end{matrix} & \begin{matrix} \beta\gamma^* + \gamma\beta^* \\ +i(\tau\alpha^* - \alpha\tau^*) \end{matrix} \\ \begin{matrix} \tau\gamma^* + \gamma\tau^* \\ -i(\beta\alpha^* - \alpha\beta^*) \end{matrix} & \begin{matrix} \alpha\gamma^* + \gamma\alpha^* \\ -i(\beta\tau^* - \tau\beta^*) \end{matrix} & \begin{matrix} \beta\gamma^* + \gamma\beta^* \\ -i(\tau\alpha^* - \alpha\tau^*) \end{matrix} & \begin{matrix} \tau\tau^* - \alpha\alpha^* \\ -\beta\beta^* + \gamma\gamma^* \end{matrix} \end{pmatrix}. \tag{12}$$

From the diagonal elements of Eqs. (7) and (11), we can write

$$\tau\tau^* = \frac{1}{4}[M_{00} + M_{11} + M_{22} + M_{33}] \geq 0, \tag{13}$$

$$\alpha\alpha^* = \frac{1}{4}[M_{00} + M_{11} - M_{22} - M_{33}] \geq 0, \tag{14}$$

$$\beta\beta^* = \frac{1}{4}[M_{00} - M_{11} + M_{22} - M_{33}] \geq 0, \qquad (15)$$

$$\gamma\gamma^* = \frac{1}{4}[M_{00} - M_{11} - M_{22} + M_{33}] \geq 0. \qquad (16)$$

And we can directly read from these expressions the trace of $\mathbf{H}$:

$$\mathrm{tr}(\mathbf{H}) = \tau\tau^* + \alpha\alpha^* + \beta\beta^* + \gamma\gamma^* = M_{00}. \qquad (17)$$

We note that, although the values of the parameters τ, α, β, and γ depend on the system of basis used in the definition of the covariance matrix $\mathbf{H}$, the quantities $\tau\tau^*$, $\alpha\alpha^*$, $\beta\beta^*$, and $\gamma\gamma^*$ are independent of any representation, i.e., they are *invariants* of the formalism.

It is also worth noting that the above inequalities are also true for depolarizing Mueller matrices, which can be written as a convex sum of nondepolarizing Mueller matrices. Therefore, these conditions are *necessary* for a real matrix to be considered as a Mueller matrix.

Similarly, a Jones matrix also can be parameterized as

$$\mathbf{J} = \tau\boldsymbol{\sigma}_0 + \alpha\boldsymbol{\sigma}_1 + \beta\boldsymbol{\sigma}_2 + \gamma\boldsymbol{\sigma}_3, \qquad (18)$$

so that

$$\mathbf{J} = \begin{pmatrix} \tau + \alpha & \beta - i\gamma \\ \beta + i\gamma & \tau - \alpha \end{pmatrix}. \qquad (19)$$

In this parameterization τ also can be a complex parameter because the Jones matrix can contain the global phase.

A. Relation to the Anisotropy Coefficients

One particular advantage of the preferred basis defined in Eq. (4) is that τ, α, β, γ can be closely related to the anisotropy coefficients defined by Arteaga *et al.* [6]. It is also possible to define and classify the Mueller symmetries in terms of the components of the covariance vector $|h\rangle$ in a very concise form.

In [6] three anisotropy coefficients were defined:

$$\alpha_A = \sqrt{\frac{1}{\Sigma}[(M_{01} + M_{10})^2 + (M_{23} - M_{32})^2]}, \qquad (20)$$

$$\beta_A = \sqrt{\frac{1}{\Sigma}[(M_{02} + M_{20})^2 + (M_{13} - M_{31})^2]}, \qquad (21)$$

$$\gamma_A = \sqrt{\frac{1}{\Sigma}[(M_{03} + M_{30})^2 + (M_{12} - M_{21})^2]}, \qquad (22)$$

where only the positive signs of the roots are considered and Σ is given as

$$\Sigma = 3M_{00}^2 - (M_{11}^2 + M_{22}^2 + M_{33}^2)$$
$$+ 2(M_{01}M_{10} + M_{02}M_{20} + M_{03}M_{30})$$
$$- 2(M_{23}M_{32} + M_{13}M_{31} + M_{12}M_{21}). \qquad (23)$$

The anisotropy coefficients satisfy the inequality

$$\alpha_A^2 + \beta_A^2 + \gamma_A^2 \leq 1. \qquad (24)$$

Equality is satisfied only if the Mueller matrix is nondepolarizing.

If the factor Σ becomes zero, the coefficients α_A, β_A, and γ_A are undefined, and then they cannot be applied to the Mueller matrices of the form $\mathrm{diag}(1, e_1, e_2, e_1 e_2)$, $e_1^2 = e_2^2 = 1$.

The different types of anisotropies defined in [6] lead to three basic types of symmetry for nondepolarizing systems.

Type 1 symmetry: Linear horizontal anisotropy ($\alpha_A = 1$, $\beta_A = 0$, $\gamma_A = 0$):

$$\mathbf{M}_L = \begin{pmatrix} 1 & M_{01} & 0 & 0 \\ M_{10} & 1 & 0 & 0 \\ 0 & 0 & M_{22} & M_{23} \\ 0 & 0 & M_{32} & M_{33} \end{pmatrix}, \qquad (25)$$

where $M_{01} = M_{10}, M_{22} = M_{33}, M_{23} = -M_{32}$, and $M_{01}^2 + M_{22}^2 + M_{23}^2 = 1$.

Type 2 symmetry: Linear 45° anisotropy ($\alpha_A = 0$, $\beta_A = 1$, $\gamma_A = 0$):

$$\mathbf{M}_{L'} = \begin{pmatrix} 1 & 0 & M_{02} & 0 \\ 0 & M_{11} & 0 & M_{13} \\ M_{20} & 0 & 1 & 0 \\ 0 & M_{31} & 0 & M_{33} \end{pmatrix}, \qquad (26)$$

where $M_{02} = M_{20}, M_{11} = M_{33}, M_{13} = -M_{31}$, and $M_{02}^2 + M_{11}^2 + M_{13}^2 = 1$.

Type 3 symmetry: Circular anisotropy ($\alpha_A = 0$, $\beta_A = 0$, $\gamma_A = 1$):

$$\mathbf{M}_C = \begin{pmatrix} 1 & 0 & 0 & M_{03} \\ 0 & M_{11} & M_{12} & 0 \\ 0 & M_{21} & M_{22} & 0 \\ M_{30} & 0 & 0 & 1 \end{pmatrix}, \qquad (27)$$

where $M_{03} = M_{30}, M_{11} = M_{22}, M_{12} = -M_{21}$, and $M_{03}^2 + M_{11}^2 + M_{12}^2 = 1$.

For a nondepolarizing Mueller matrix, we can define the anisotropy parameters α_A, β_A, and γ_A in terms of the components of the covariance vector. In order to do this, we first write Σ in terms of τ, α, β, and γ:

$$\Sigma = 16|\tau|^2[|\alpha|^2 + |\beta|^2 + |\gamma|^2]. \qquad (28)$$

With this definition of Σ, it can be shown that the anisotropy parameters can be written as follows:

$$\alpha_A = \sqrt{\frac{|\alpha|^2}{|\alpha|^2 + |\beta|^2 + |\gamma|^2}}, \qquad (29a)$$

$$\beta_A = \sqrt{\frac{|\beta|^2}{|\alpha|^2 + |\beta|^2 + |\gamma|^2}}, \qquad (29b)$$

$$\gamma_A = \sqrt{\frac{|\gamma|^2}{|\alpha|^2 + |\beta|^2 + |\gamma|^2}}. \qquad (29c)$$

For depolarizing Mueller matrices, it is not possible to define the anisotropy parameters in terms of the components of the covariance vector in a simple way like this. But, for depolarizing Mueller matrices, α_A, β_A, and γ_A still are, respectively, proportional to the weighted average of the absolute values of α, β, and γ associated with the covariance vectors that represent a depolarizing system.

B. Covariance Vector and Mueller Matrix Symmetries

Different forms of the covariance vector translate in different symmetries of the Mueller matrix. There are four main situations or classes that depend on the number of vanishing component(s) of the covariance vector.

Class 1. Only one of the parameters τ, α, β, γ is non-zero. There are four possibilities in this class. For a normalized Mueller matrix, the vector generators are as follows:

$$
\begin{aligned}
\text{generator}_\tau \quad |h\rangle &= (1, 0, 0, 0)^T, \\
\text{generator}_\alpha \quad |h\rangle &= (0, 1, 0, 0)^T, \\
\text{generator}_\beta \quad |h\rangle &= (0, 0, 1, 0)^T, \\
\text{generator}_\gamma \quad |h\rangle &= (0, 0, 0, 1)^T.
\end{aligned}
\tag{30}
$$

These covariance vectors generate a Mueller symmetry that corresponds to a diagonal matrix of the form $\mathrm{diag}(1, e_1, e_2, e_1 e_2)$, where $e_1^2 = e_2^2 = 1$, i.e., all the possible diagonal nondepolarizing Mueller matrices. This includes the cases of a half-wave plate, a mirror reflection, and the identity.

Class 2. Only two of the parameters τ, α, β, γ are non-zero. There are six different possibilities in this class, which are given by the following vector generators:

$$
\begin{aligned}
\text{generator}_{\tau\alpha} \quad |h\rangle &= (\tau, \alpha, 0, 0)^T, \\
\text{generator}_{\tau\beta} \quad |h\rangle &= (\tau, 0, \beta, 0)^T, \\
\text{generator}_{\tau\gamma} \quad |h\rangle &= (\tau, 0, 0, \gamma)^T, \\
\text{generator}_{\alpha\beta} \quad |h\rangle &= (0, \alpha, \beta, 0)^T, \\
\text{generator}_{\alpha\gamma} \quad |h\rangle &= (0, \alpha, 0, \gamma)^T, \\
\text{generator}_{\beta\gamma} \quad |h\rangle &= (0, 0, \beta, \gamma)^T.
\end{aligned}
\tag{31}
$$

The generating vectors labeled as $\text{generator}_{\tau\alpha}$, $\text{generator}_{\tau\beta}$, and $\text{generator}_{\tau\gamma}$ lead to the symmetries labeled type-1, type-2, and type-3 in [7], respectively. The vectors $\text{generator}_{\alpha\beta}$, $\text{generator}_{\alpha\gamma}$, and $\text{generator}_{\beta\gamma}$ correspond, respectively, to a type-3 matrix multiplied by $\mathrm{diag}(1, 1, -1, -1)$, a type-2 matrix multiplied by $\mathrm{diag}(1, -1, -1, 1)$, and a type-1 matrix multiplied by $\mathrm{diag}(1, -1, 1, -1)$.

Class 3. One of the parameters τ, α, β, γ is zero. There are four possible generators in this class:

$$
\begin{aligned}
\text{generator}_{\alpha\beta\gamma} \quad |h\rangle &= (0, \alpha, \beta, \gamma)^T, \\
\text{generator}_{\tau\beta\gamma} \quad |h\rangle &= (\tau, 0, \beta, \gamma)^T, \\
\text{generator}_{\tau\alpha\gamma} \quad |h\rangle &= (\tau, \alpha, 0, \gamma)^T, \\
\text{generator}_{\tau\alpha\beta} \quad |h\rangle &= (\tau, \alpha, \beta, 0)^T,
\end{aligned}
\tag{32}
$$

where $\text{generator}_{\tau\beta\gamma}$, $\text{generator}_{\tau\alpha\gamma}$, and $\text{generator}_{\tau\alpha\beta}$ are, respectively, generating the symmetries labeled type-23, type-13, and type-12 in [7], while $\text{generator}_{\alpha\beta\gamma}$ generates either a type-23 symmetry multiplied by $\mathrm{diag}(1, 1, -1, -1)$ or a type-12 symmetry multiplied by $\mathrm{diag}(1, -1, -1, 1)$ or a type-13 symmetry multiplied by $\mathrm{diag}(1, -1, 1, -1)$.

Class 4. None of the parameters τ, α, β, or γ vanish. This class does not generate any particular symmetry in the Mueller matrix.

The covariance vectors listed above can be alternatively classified according to the parameter τ: symmetries with $\tau = 0$, and the symmetries with $\tau \neq 0$. When $\tau = 0$ the resulting nondepolarizing matrices have some particular properties, as, for example, these matrices do not have a real logarithm, and they

cannot be decomposed with the differential decomposition [8], although they can be still correctly treated with the analytic method [9].

3. GENERATING MATRIX FOR NONDEPOLARIZING OPTICAL MEDIA

A nondepolarizing optical media can either be described by a covariance vector or by a Jones matrix. Here we introduce one more mathematical object ($\mathbf{Z}$) in matrix form, which is closely related to the Mueller matrix:

$$
\mathbf{Z} = \begin{pmatrix}
\tau & \alpha & \beta & \gamma \\
\alpha & \tau & -i\gamma & i\beta \\
\beta & i\gamma & \tau & -i\alpha \\
\gamma & -i\beta & i\alpha & \tau
\end{pmatrix}.
\tag{33}
$$

By direct matrix multiplication, it can be shown that the Mueller matrix of any nondepolarizing optical media can be written as

$$
\mathbf{M} = \mathbf{Z}\mathbf{Z}^* = \mathbf{Z}^*\mathbf{Z}.
\tag{34}
$$

Formally, $\mathbf{Z}$ and $\mathbf{Z}^*$ can be defined in terms of the Jones matrix:

$$
\mathbf{Z} = \mathbf{A}(\mathbf{J} \otimes \mathbf{I})\mathbf{A}^{-1}, \qquad \mathbf{Z}^* = \mathbf{A}(\mathbf{I} \otimes \mathbf{J}^*)\mathbf{A}^{-1},
\tag{35}
$$

where $\mathbf{I}$ is the 2×2 identity. With these definitions it is straightforward to prove Eq. (34). It is also possible to show that $\mathbf{Z}$ matrices mimic all properties of Jones matrices. For example, if we consider a sequential product of Jones matrices

$$
\mathbf{J} = \mathbf{J}_N \cdot \mathbf{J}_{N-1} \ldots \mathbf{J}_2 \cdot \mathbf{J}_1,
\tag{36}
$$

then the definition of $\mathbf{Z}$ in terms of $\mathbf{J}$, Eq. (35), leads to the following sequential combination:

$$
\mathbf{Z} = \mathbf{Z}_N \cdot \mathbf{Z}_{N-1} \ldots \mathbf{Z}_2 \cdot \mathbf{Z}_1.
\tag{37}
$$

By direct matrix multiplication it can be shown that all $\mathbf{Z}_i$ and $\mathbf{Z}_j^*$ matrices commute; then it is a simple exercise to find the associated expression for the sequential product of nondepolarizing Mueller matrices:

$$
\begin{aligned}
\mathbf{M} &= (\mathbf{Z}_N \mathbf{Z}_{N-1} \ldots \mathbf{Z}_2 \mathbf{Z}_1)(\mathbf{Z}_N^* \mathbf{Z}_{N-1}^* \ldots \mathbf{Z}_2^* \mathbf{Z}_1^*) \\
&= (\mathbf{Z}_N \mathbf{Z}_N^*)(\mathbf{Z}_{N-1} \mathbf{Z}_{N-1}^*) \ldots (\mathbf{Z}_2 \mathbf{Z}_2^*)(\mathbf{Z}_1 \mathbf{Z}_1^*) \\
&= \mathbf{M}_N \cdot \mathbf{M}_{N-1} \ldots \mathbf{M}_2 \cdot \mathbf{M}_1.
\end{aligned}
\tag{38}
$$

A. Differential Treatment: Z Matrix as a Matrix Exponential

The differential analysis of the $\mathbf{Z}$ matrix can be treated analogously to the Jones matrix [10] or to the Mueller matrix. The equation

$$
\frac{d\mathbf{Z}}{dl} = \mathbf{z}\mathbf{Z}
\tag{39}
$$

introduces the differential matrix $\mathbf{z}$, which relates the $\mathbf{Z}$ matrix of a homogeneous anisotropic medium to its spatial derivative along the direction of propagation of light (l).

This differential equation has a solution of the form $\mathbf{Z} = e^{\mathbf{z}}$ and, as $\mathbf{Z} = \mathbf{A}(\mathbf{J} \otimes \mathbf{I})\mathbf{A}^{-1}$, we can rely on the Jones matrix exponential [11] to find the differential $\mathbf{Z}$ matrix:

$$
\mathbf{Z} = \mathbf{A}(\mathbf{J} \otimes \mathbf{I})\mathbf{A}^{-1}, = \mathbf{A}(e^{\mathbf{N}l} \otimes \mathbf{I})\mathbf{A}^{-1} = e^{(\mathbf{A}(\mathbf{N} \otimes \mathbf{I})\mathbf{A}^{-1})l},
\tag{40}
$$

where N is the differential Jones matrix, which is given by [12]

$$\mathbf{N} = -\frac{i}{2l}\begin{pmatrix} \chi + L & L' + iC \\ L' - iC & \chi - L \end{pmatrix}, \tag{41}$$

where $\chi = \eta - i\kappa$, $L = \mathrm{LB} - i\mathrm{LD}$, $L' = \mathrm{LB}' - i\mathrm{LD}'$, $C = \mathrm{CB} - i\mathrm{CD}$. Here we have introduced the spectroscopic parameters [12], which are defined as follows: isotropic phase retardation (η), isotropic amplitude absorption (κ), circular dichroism (CD), circular birefringence (CB), horizontal and 45° linear dichorism (LD and LD'), and horizontal and 45° linear birefringence (LB and LB'). Their relationship with τ, α, β, and γ is

$$\tau = e^{-\frac{i\chi}{2}}\cos\left(\frac{T}{2}\right) \qquad \alpha = -e^{-\frac{i\chi}{2}}\frac{iL}{T}\sin\left(\frac{T}{2}\right), \tag{42}$$

$$\beta = -e^{-\frac{i\chi}{2}}\frac{iL'}{T}\sin\left(\frac{T}{2}\right) \qquad \gamma = e^{-\frac{i\chi}{2}}\frac{iC}{T}\sin\left(\frac{T}{2}\right), \tag{43}$$

where $T = \sqrt{L^2 + L'^2 + C^2}$.

As

$$\mathbf{z} = (\mathbf{A}(\mathbf{N}\otimes\mathbf{I})\mathbf{A}^{-1})l, \tag{44}$$

this differential $\mathbf{Z}$ can be written as

$$\mathbf{z} = \frac{-i}{2}\begin{pmatrix} \chi & L & L' & -C \\ L & \chi & iC & iL' \\ L' & -iC & \chi & -iL \\ -C & -iL' & iL & \chi \end{pmatrix}. \tag{45}$$

Because $\mathbf{z}$ commutes with the complex conjugate of itself ($\mathbf{z}^*$), the exponential form of $\mathbf{Z}$ leads immediately to the exponential form of a nondepolarizing Mueller matrix:

$$\mathbf{M} = \mathbf{Z}\mathbf{Z}^* = \mathbf{Z}^*\mathbf{Z} = e^{\mathbf{z}}e^{\mathbf{z}^*} = e^{(\mathbf{z}+\mathbf{z}^*)} = e^{\mathbf{L}}, \tag{46}$$

where

$$\mathbf{L} = \mathbf{z} + \mathbf{z}^* = \begin{pmatrix} -\kappa & -\mathrm{LD} & -\mathrm{LD}' & \mathrm{CD} \\ -\mathrm{LD} & -\kappa & \mathrm{CB} & \mathrm{LB}' \\ -\mathrm{LD}' & -\mathrm{CB} & -\kappa & -\mathrm{LB} \\ \mathrm{CD} & -\mathrm{LB}' & \mathrm{LB} & -\kappa \end{pmatrix}. \tag{47}$$

One advantageous aspect of $\mathbf{z}$ and $\mathbf{Z}$ matrices is that, similarly to Jones matrices, they can include the global phase (represented by η in the spectroscopic notation). This global phase information is not allowed in $\mathbf{M}$ or $\mathbf{L}$ (only κ survives). In a subsequent paper, we will show that this is useful in some calculations.

B. Inverse of the Z Matrix

We first calculate the determinant of $\mathbf{Z}$:

$$\det(\mathbf{Z}) = [\tau^2 - \alpha^2 - \beta^2 - \gamma^2]^2 \ge 0. \tag{48}$$

Equality is satisfied for pure polarizers. If $\det(\mathbf{Z})$ is non-zero there exists an inverse matrix $\mathbf{Z}^{-1}$ such that

$$\mathbf{Z}\mathbf{Z}^{-1} = \mathbf{Z}^{-1}\mathbf{Z} = \mathbf{I}_4, \tag{49}$$

where $\mathbf{I}_4$ is the 4×4 identity.

We also calculate the explicit form of the $\mathbf{Z}^{-1}$ matrix by following the usual matrix inversion procedure:

$$\mathbf{Z}^{-1} = \frac{1}{\tau^2 - \alpha^2 - \beta^2 - \gamma^2}\begin{pmatrix} \tau & -\alpha & -\beta & -\gamma \\ -\alpha & \tau & i\gamma & -i\beta \\ -\beta & -i\gamma & \tau & i\alpha \\ -\gamma & i\beta & -i\alpha & \tau \end{pmatrix}. \tag{50}$$

As it can be seen from Eq. (50), in order to obtain $\mathbf{Z}^{-1}$, it is not necessary to follow the tedious matrix inversion procedure, it is enough to reverse the signs of α, β, and γ, apart from the factor $1/(\tau^2 - \alpha^2 - \beta^2 - \gamma^2)$. Once we get $\mathbf{Z}^{-1}$, it is straightforward to write the inverse of the associated Mueller matrix:

$$\mathbf{M}^{-1} = \mathbf{Z}^{-1}(\mathbf{Z}^{-1})^* = (\mathbf{Z}^{-1})^*\mathbf{Z}^{-1}. \tag{51}$$

C. Hermitian Z Matrix

From the explicit form of the matrix $\mathbf{Z}$, it can be directly observed that, if and only if the parameters $\tau, \alpha, \beta, \gamma$ are real, $\mathbf{Z}$ is Hermitian and the associated nondepolarizing Mueller matrix is also Hermitian. And because $\mathbf{M}$ is real, a Hermitian $\mathbf{M}$ is symmetric. In this case the Mueller matrix takes the following simple form:

$$\mathbf{M}_h = \mathbf{Z}_h\mathbf{Z}_h^* = \mathbf{Z}_h^*\mathbf{Z}_h, \tag{52}$$

$$\mathbf{M}_h = \begin{pmatrix} M_{00} & 2\tau\alpha & 2\tau\beta & 2\tau\gamma \\ 2\tau\alpha & M_{11} & 2\alpha\beta & 2\alpha\gamma \\ 2\tau\beta & 2\alpha\beta & M_{22} & 2\beta\gamma \\ 2\tau\gamma & 2\alpha\gamma & 2\beta\gamma & M_{33} \end{pmatrix}, \tag{53}$$

where the subscript h stands for Hermitian and

$$M_{00} = \tau^2 + \alpha^2 + \beta^2 + \gamma^2,$$
$$M_{11} = \tau^2 + \alpha^2 - \beta^2 - \gamma^2,$$
$$M_{22} = \tau^2 - \alpha^2 + \beta^2 - \gamma^2,$$
$$M_{33} = \tau^2 - \alpha^2 - \beta^2 + \gamma^2.$$

This Mueller matrix is equivalent to the general diattenuation matrix $\mathbf{M}_D$ given in [12].

D. Unitary Z Matrix

For $\mathbf{Z}$ to be unitary, by definition,

$$\mathbf{Z}\mathbf{Z}^\dagger = \mathbf{Z}^\dagger\mathbf{Z} = \mathbf{I}_4, \qquad \text{hence } \mathbf{Z}^{-1} = \mathbf{Z}^\dagger. \tag{54}$$

If we choose τ to be real, this can be true if and only if α, β, and γ are pure imaginary numbers. In this case, the term $(\tau^2 - \alpha^2 - \beta^2 - \gamma^2)$ becomes equal to $\mathrm{tr}(\mathbf{H})$. If the Mueller matrix is normalized $\mathrm{tr}(\mathbf{H}) = M_{00} = 1$, then the inverse (or the Hermitian adjoint) of a unitary $\mathbf{Z}$ matrix can be obtained by simply inverting the signs of the three parameters α, β, and γ.

If we let $\alpha = i\tilde{\alpha}, \beta = i\tilde{\beta}, \gamma = i\tilde{\gamma}$ ($\tilde{\alpha}, \tilde{\beta}, \tilde{\gamma}$ are pure real numbers), we can write a nondepolarizing unitary Mueller matrix (and because $\mathbf{M}$ is real, a unitary $\mathbf{M}$ is orthogonal) as

$$\mathbf{M}_u = \mathbf{Z}_u\mathbf{Z}_u^* = \mathbf{Z}_u^*\mathbf{Z}_u, \tag{55}$$

$$\mathbf{M}_u = \begin{pmatrix} M_{00} & 0 & 0 & 0 \\ 0 & M_{11} & 2\tilde{\alpha}\tilde{\beta}+2\tilde{\gamma}\tau & 2\tilde{\alpha}\tilde{\gamma}-2\tilde{\beta}\tau \\ 0 & 2\tilde{\alpha}\tilde{\beta}-2\tilde{\gamma}\tau & M_{22} & 2\tilde{\beta}\tilde{\gamma}+2\tilde{\alpha}\tau \\ 0 & 2\tilde{\alpha}\tilde{\gamma}+2\tilde{\beta}\tau & 2\tilde{\beta}\tilde{\gamma}-2\tilde{\alpha}\tau & M_{33} \end{pmatrix}, \tag{56}$$

where the subscript u stands for unitary and

$$M_{00} = \tau^2 + \breve{\alpha}^2 + \breve{\beta}^2 + \breve{\gamma}^2,$$

$$M_{11} = \tau^2 + \breve{\alpha}^2 - \breve{\beta}^2 - \breve{\gamma}^2,$$

$$M_{22} = \tau^2 - \breve{\alpha}^2 + \breve{\beta}^2 - \breve{\gamma}^2,$$

$$M_{33} = \tau^2 - \breve{\alpha}^2 - \breve{\beta}^2 + \breve{\gamma}^2.$$

This Mueller matrix is equivalent to the general retarder Mueller matrix $\mathbf{M}_R$ given in [12].

E. Polar Decomposition of Z Matrix

Any complex matrix $\mathbf{Z}$ can be written as a product of Hermitian and unitary matrices:

$$\mathbf{Z} = \mathbf{Z}_h \mathbf{Z}_u \text{ or } \mathbf{Z} = \mathbf{Z}_u \mathbf{Z}'_h, \qquad (57)$$

where $\mathbf{Z}_h$ and $\mathbf{Z}'_h$ are Hermitian matrices associated with the amplitude anisotropy and $\mathbf{Z}_u$ is a unitary matrix associated with the phase anisotropy. Because of the noncomutativity of Hermitian and unitary parts, $\mathbf{Z}_h$ and $\mathbf{Z}'_h$ are not identical, and they are related to each other through the following relations:

$$\mathbf{Z}'_h = \mathbf{Z}^{\mathbf{T}}_u \mathbf{Z}_h \mathbf{Z}_u \qquad \text{and} \qquad \mathbf{Z}_h = \mathbf{Z}_u \mathbf{Z}'_h \mathbf{Z}^{\mathbf{T}}_u. \qquad (58)$$

In the following we follow the other route. We assume that $\mathbf{Z}_h$ and $\mathbf{Z}_u$ matrices are given, and we write the two alternative ways of multiplying them:

$$\mathbf{Z} = \mathbf{Z}_h \mathbf{Z}_u, \qquad \mathbf{Z}' = \mathbf{Z}_u \mathbf{Z}_h. \qquad (59)$$

It can be shown that $\mathbf{Z}$ and $\mathbf{Z}'$ lead to the polar decompositions of the associated Mueller matrices

$$(\mathbf{Z}_h \mathbf{Z}_u)(\mathbf{Z}_h \mathbf{Z}_u)^* = (\mathbf{Z}_h \mathbf{Z}_u)(\mathbf{Z}^*_h \mathbf{Z}^*_u)$$
$$= (\mathbf{Z}_h \mathbf{Z}^*_h)(\mathbf{Z}_u \mathbf{Z}^*_u) = \mathbf{M}_h \mathbf{M}_u = \mathbf{M}, \qquad (60)$$

$$(\mathbf{Z}_u \mathbf{Z}_h)(\mathbf{Z}_u \mathbf{Z}_h)^* = (\mathbf{Z}_u \mathbf{Z}_h)(\mathbf{Z}^*_u \mathbf{Z}^*_h)$$
$$= (\mathbf{Z}_u \mathbf{Z}^*_u)(\mathbf{Z}_h \mathbf{Z}^*_h) = \mathbf{M}_u \mathbf{M}_h = \mathbf{M}', \qquad (61)$$

where we use the following commutation relations:

$$\mathbf{Z}_u \mathbf{Z}^*_h = \mathbf{Z}^*_h \mathbf{Z}_u, \qquad \mathbf{Z}_h \mathbf{Z}^*_u = \mathbf{Z}^*_u \mathbf{Z}_h. \qquad (62)$$

4. NUMERICAL EXAMPLE

We can illustrate the calculation of the covariance vector $|h\rangle$ and the matrix $\mathbf{Z}$ with the following Mueller matrix:

$$\mathbf{M} = \frac{1}{30} \begin{pmatrix} 30 & 8 & 4 & 12 \\ 8 & 26 & 8 & 0 \\ 12 & 0 & 12 & 26 \\ 4 & 8 & -22 & 12 \end{pmatrix}. \qquad (63)$$

$\mathbf{M}$ is nondepolarizing because it satisfies the trace condition $\text{tr}(\mathbf{M}^T \mathbf{M}) = 4M^2_{00}$ [13,14]. The corresponding covariance matrix, given in Eq. (6), is

$$\mathbf{H} = \frac{1}{30} \begin{pmatrix} 20 & 4-12i & 4-2i & 4-2i \\ 4+12i & 8 & 2+2i & 2+2i \\ 4+2i & 2-2i & 1 & 1 \\ 4+2i & 2-2i & 1 & 1 \end{pmatrix}. \qquad (64)$$

It can be shown that $\text{rank}(\mathbf{H}) = 1$ and $\text{tr}(\mathbf{H}) = 1$; hence, the covariance vector $|h\rangle$, i.e., the normalized eigenvector corresponding to the nonzero eigenvalue, is

$$|h\rangle = \begin{pmatrix} \tau \\ \alpha \\ \beta \\ \gamma \end{pmatrix} = \frac{1}{\sqrt{600}} \begin{pmatrix} 20 \\ 4+12i \\ 4+2i \\ 4+2i \end{pmatrix}. \qquad (65)$$

With these values of the parameters, τ, α, β, and γ, we can find the anisotropy parameters defined by Arteaga *et al.* [6]:

$$\alpha_A = \sqrt{0.8}, \qquad \beta_A = \sqrt{0.1}, \qquad \gamma_A = \sqrt{0.1}. \qquad (66)$$

Because $\mathbf{M}$ is nondepolarizing $\alpha^2_A + \beta^2_A + \gamma^2_A = 1$, and because the $|h\rangle$ vector is normalized,

$$|\tau|^2 + |\alpha|^2 + |\beta|^2 + |\gamma|^2 = \frac{400 + 160 + 20 + 20}{600} = 1. \qquad (67)$$

The corresponding $\mathbf{Z}$ matrix is

$$\mathbf{Z} = \frac{1}{\sqrt{600}} \begin{pmatrix} 20 & 4+12i & 4+2i & 4+2i \\ 4+12i & 20 & 2-4i & -2+4i \\ 4+2i & -2+4i & 20 & 12-4i \\ 4+2i & 2-4i & -12+4i & 20 \end{pmatrix}. \qquad (68)$$

By direct matrix multiplication it can be shown that $\mathbf{Z}\mathbf{Z}^* = \mathbf{Z}^*\mathbf{Z} = \mathbf{M}$.

5. CONCLUSIONS

In this work, we have shown how the information contained in nondepolarizing Mueller matrices can be expressed in terms of a covariance vector or a generating 4×4 matrix. These two representations have in common that they are built around three complex parameters (α, β, γ), which are unequivocally linked to different forms of anisotropy and one additional parameter of isotropy, τ, that is real if it is calculated from a Mueller matrix. This representation is closely related to the coefficients of anisotropy, which were identified with geometric arguments in a previous paper, and provides a systematic classification of all possible Mueller matrix symmetries.

The 4×4 $\mathbf{Z}$ matrix is a mathematical entity, intimately related to a nondepolarizing Mueller matrix, which preserves many of its properties, and, with the advantage, it can deal with a global phase. It acts as a matrix state generator for pure (i.e., nondepolarizing) Mueller matrices, much like $|h\rangle$ is the vector state of a rank 1 $\mathbf{H}$. In a subsequent paper, we will detail how these mathematical tools turn out to be useful for the polarimetric description of coherent or incoherent superposition processes.

REFERENCES

1. P. Soleillet, "Sur les paramètres caractérisant la polarisation partielle de la lumière dans les phénomènes de fluorescence," Ann. Phys. **12**, 23–59 (1929).

2. S. R. Cloude, "Group theory and polarisation algebra," Optik **75**, 26–36 (1986).

3. J. J. Gil and I. S. José, "Polarimetric subtraction of Mueller matrices," J. Opt. Soc. Am. A **30**, 1078–1088 (2013).

4. J. J. Gil, "Review on Mueller matrix algebra for the analysis of polarimetric measurements," J. Appl. Remote Sens. **8**, 081599 (2014).

5. A. Aiello and J. P. Woerdman, "Linear algebra for Mueller calculus," arXiv:math-ph/0412061 (2006).

6. O. Arteaga, E. Garcia-Caurel, and R. Ossikovski, "Anisotropy coefficients of a Mueller matrix," J. Opt. Soc. Am. A **28**, 548–553 (2011).

7. E. Kuntman and O. Arteaga, "Decomposition of a depolarizing Mueller matrix into its nondepolarizing components by using symmetry conditions," Appl. Opt. **55**, 2543–2550 (2016).

8. R. Ossikovski, "Differential matrix formalism for depolarizing anisotropic media," Opt. Lett. **36**, 2330–2332 (2011).

9. O. Arteaga and A. Canillas, "Analytic inversion of the Mueller-Jones polarization matrices for homogeneous media," Opt. Lett. **35**, 559–561 (2010).

10. C. R. Jones, "New calculus for the treatment of optical systems. VII. Properties of the N-matrices," J. Opt. Soc. Am. **38**, 671–685 (1948).

11. R. Barakat, "Exponential versions of the Jones and Mueller-Jones polarization matrices," J. Opt. Soc. Am. A **13**, 158–163 (1996).

12. O. Arteaga, "Mueller matrix polarimetry of anisotropic chiral media," Ph.D. thesis (University of Barcelona, 2010).

13. J. J. Gil and E. Bernabeu, "A depolarization criterion in Mueller matrices," Opt. Acta **32**, 259–261 (1985).

14. J. J. Gil and E. Bernabeu, "Depolarization and polarization indices of an optical system," Opt. Acta **33**, 185–189 (1986).

Formalism of optical coherence and polarization based on material media states

Ertan Kuntman,[1] M. Ali Kuntman,[2] Jordi Sancho-Parramon,[3] and Oriol Arteaga[1,*]

[1]*Departament de Física Aplicada, Institute of Nanoscience and Nanotechnology (IN2UB), Feman Group,*
Universitat de Barcelona, C/ Martí i Franquès 1, Barcelona 08030, Spain
[2]*Independent Researcher, Ankara 06830, Turkey*
[3]*Rudjer Boskovic Institute, Bijenicka cesta 54, Zagreb 10000, Croatia*
(Received 2 January 2017; published 15 June 2017)

The fluctuations or disordered motion of the electromagnetic fields are described by statistical properties rather than instantaneous values. This statistical description of the optical fields is underlying in the Stokes-Mueller formalism that applies to measurable intensities. However, the fundamental concept of optical coherence, which is assessed by the ability of waves to interfere, is not treatable by this formalism because it omits the global phase. In this work we show that using an analogy between deterministic matrix states associated with optical media and quantum mechanical wave functions, it is possible to construct a general formalism that accounts for the additional terms resulting from the coherency effects that average out for incoherent treatments. This method generalizes further the concept of coherent superposition to describe how deterministic states of optical media can superpose to generate another deterministic media state. Our formalism is used to study the combined polarimetric response of interfering plasmonic nanoantennas.

I. INTRODUCTION

In optics, interference is the phenomena that occurs when two coherent waves superpose. The celebrated example is the Young's double slit experiment with a beam of light, but coherence and interference are not restricted to photons. Any moving particle is susceptible to interference with another if they keep a well-defined and constant phase relation, as it can occur for example between two oscillating dipoles [1]. In optics this is one of the most fundamental interactions. When a material medium is irradiated by an electromagnetic wave, molecular electric charges are set in oscillatory motion by the electric field of the wave, producing secondary radiation in a form of refracted, reflected, diffracted, or scattered light with certain polarization attributes.

Polarized light was the only quantum phenomenon that was understood quantitatively before the birth of quantum mechanics in 1900. Many mathematical tools of quantum mechanics appear in the classical description of a polarized electromagnetic wave and, for example, Malus's law, which was postulated in 1809, is also obeyed at the single-photon level and allows a quantum mechanical interpretation in terms of probability amplitudes [2]. In quantum mechanics, the observable values are the eigenvalues of Hermitian operators associated with the observable quantity. The observable corresponding to the optical phenomena occurring in light-matter interactions is the 4×4 scattering matrix with 16 real elements also known as the Mueller matrix that describes the linear transformation of the Stokes parameters of a light beam upon interaction with a linear medium.

In this work, we first demonstrate how alternative representations of nondepolarizing (deterministic) optical systems that were recently presented [3] can be used to make the analogy between the Mueller-Jones *states* of optical systems and the quantum mechanical wave function. We also show

that quantum coherence in material media can be represented by a coherent linear superposition of matrix (or vector) states associated with nondepolarizing Mueller matrices. This linear combination is generally understood as a sum of Jones matrices of nondepolarizing component systems [4,5]. But here, instead of Jones matrices, we propose a linear combination of matrix (or vector) *states* with *complex* coefficients that play the role of probability amplitudes of quantum mechanics.

Even though the relationship between polarization optics and quantum mechanics has been studied by several previous authors [6–9], these works are mainly focused on the description of the polarization states of a light wave, and they do not consider light-matter interactions through material media states. Ossikovski *et al.* [10] recently presented a treatment of spatial coherency in polarimetry and ellipsometry with Mueller matrices, albeit their formulation is fully based on classical electromagnetic tools. In general, available theories about coherence and polarization [11–13] require a direct consideration of electromagnetic fields. Nevertheless, our formalism is entirely based on the description of material media with Mueller-Jones states, and it provides a complete analogy between the phenomenological Stokes-Mueller formalism describing the interaction of light with a material medium and quantum mechanics.

The overall effect of the interaction of light with a deterministic, i.e., nondepolarizing, medium or optical system can be described by a 2×2 complex matrix **J**, referred to as the Jones matrix [14]. The 4×4 real matrix for transforming the Stokes vectors is the Mueller matrix **M** that is directly connected with the experimental work in polarization optics. If the medium is deterministic then the associated Mueller matrix (also known as the Mueller-Jones matrix) can be analytically obtained from the Jones matrix [15]. As opposed to the Jones matrix, a Mueller matrix does not contain information about the overall phase change introduced by a material medium, because it is not an observable.

Sometimes it is convenient to study the properties of a general Mueller matrix **M** (nondepolarizing or depolarizing)

---

*oarteaga@ub.edu

by transforming $\mathbf{M}$ into a Hermitian matrix $\mathbf{H}$ which is called the covariance matrix [16].[1] If and only if the Mueller matrix of the system is nondepolarizing, the associated covariance matrix will be of rank 1. In this case, it is always possible to define a covariance vector $|h\rangle$ such that

$$\mathbf{H} = |h\rangle\langle h|, \tag{1}$$

where the vector $|h\rangle$ is the eigenvector of $\mathbf{H}$ corresponding to the single nonzero eigenvalue [17–19].

As its mathematical form suggests, $\mathbf{H} = |h\rangle\langle h|$ is an analog of the pure state of quantum mechanics expressed in the density matrix form, where the covariance vector $|h\rangle$ plays the role of a quantum mechanical state vector $|\Psi\rangle$. In a suitable basis that we defined in a previous work [3], the dimensionless components of $|h\rangle$ are $\tau, \alpha, \beta,$ and γ:

$$|h\rangle = (\tau, \alpha, \beta, \gamma)^T, \tag{2}$$

where α, β, γ are complex parameters and τ can be chosen to be real because the global phase is not an experimental observable.

A deterministic state can be alternatively given by a Jones matrix $\mathbf{J}$, a Mueller-Jones matrix $\mathbf{M}_J$, covariance vector $|h\rangle$, or a 4×4 complex matrix $\mathbf{Z}$ defined as [3][2]

$$\mathbf{Z} = \begin{pmatrix} \tau & \alpha & \beta & \gamma \\ \alpha & \tau & -i\gamma & i\beta \\ \beta & i\gamma & \tau & -i\alpha \\ \gamma & -i\beta & i\alpha & \tau \end{pmatrix}. \tag{3}$$

This matrix has a remarkable property [3]:

$$\mathbf{M}_J = \mathbf{Z}\mathbf{Z}^* = \mathbf{Z}^*\mathbf{Z}, \tag{4}$$

where $\mathbf{M}_J$ is a Mueller-Jones matrix.

Here, the analogy between the $\mathbf{Z}$ matrix and a quantum mechanical *wave function*, usually denoted as ψ, is evident. The $\mathbf{Z}$ matrix is a complex matrix state that, when multiplied with its complex conjugate, gives a real valued Mueller-Jones matrix with elements that are observable quantities in experimental polarization optics. In the following, $\mathbf{Z}$ matrices will be referred to as Mueller-Jones states, and we will show that it is also possible to think of a linear superposition of $\mathbf{Z}$ matrices in a way very similar to the superposition of quantum mechanical wave functions.

II. COHERENT SUPERPOSITION OF POLARIZATION STATES

The coherent superposition of polarization states of light can be introduced with Young's double slit experiment. The wave function of the combined beam can be written as a linear superposition of wave functions of light emerging from each slit:

$$\psi = a\psi_a + b\psi_b. \tag{5}$$

---

[1]Note we call this covariance matrix $\mathbf{H}$ while other authors use $\mathbf{C}$. Our notation is defined in detail in [3].

[2]This matrix was also defined in the Ph.D. thesis of R. Chipman (University of Arizona, 1987) with the name of "polarization coupling matrix," but its properties were not studied.

The phenomenon of interference of light comes into play if ψ_j are, in all respects, identical to each other except relative phases. For example, if $\psi_b = e^{i\phi}\psi_a$ ($0 \leqslant \phi < 2\pi$), and if we let $a = b = \frac{1}{\sqrt{2}}$, then the probability distribution function at a given detection point displays a typical $\cos\phi$ dependence:

$$\begin{aligned} \psi\psi^* &= \tfrac{1}{2}\psi_a\psi_a^*(1 + e^{i\phi})(1 + e^{-i\phi}) \\ &= \psi_a\psi_a^*(1 + \cos\phi). \end{aligned} \tag{6}$$

If we consider an extended detector, the probability density at the detector will vary accordingly with the cosine term as a function of position, because the optical path (and therefore the value of ϕ) changes with the detection point. On the other hand, if we set a vertical and a horizontal polarizer before each slit, there will be no sign of interference at all. Thus, it is worth remarking that the lack of visibility of interference fringes does not necessarily indicate absence of coherence.

A. Superposition of Z matrices

A superposition of optical media states may take place during a light-matter interaction experiment. When a light beam simultaneously illuminates different parts of the material medium, each part having different optical properties, the light emerging from different parts, in general with different polarizations, may coherently recombine into a single beam. If the studied material medium is composed of several nondepolarizing (deterministic) systems, each system with a well-defined Jones matrix, then the Jones matrix of the combined system is simply given by a linear combination of the Jones matrices of the component systems [4,5,20]:

$$\mathbf{J} = \sum_i \mathbf{J}_i. \tag{7}$$

For the analogies with quantum mechanics that we are tracing in this work it is more practical to rewrite Eq. (7) with normalized Jones component matrices, so that each term of the superposition is preceded by a complex coefficient that accounts for the relative amplitude and phase:

$$\mathbf{J} = a\mathbf{J}_a + b\mathbf{J}_b + c\mathbf{J}_c + \cdots, \tag{8}$$

and satisfies the normalization condition $|a|^2 + |b|^2 + |c|^2 + \cdots = 1$. By means of definition $\mathbf{Z} = \mathbf{A}(\mathbf{I} \otimes \mathbf{J})\mathbf{A}^{-1}$ (where $\mathbf{A}$ is a constant unitary matrix [3]), this coherent linear combination can be directly translated to the $\mathbf{Z}$ matrix states with the same complex coefficients:

$$\mathbf{Z} = a\mathbf{Z}_a + b\mathbf{Z}_b + c\mathbf{Z}_c + \cdots. \tag{9}$$

Complex coefficients $a, b, c, \ldots$, here play the role of probability amplitudes of quantum mechanics. Obviously, this is a coherent summation and the resultant matrix state $\mathbf{Z}$ corresponds to the nondepolarizing Mueller matrix of the combined system. The complex coefficients can generally be functions of space, time, and frequency. These dependencies can entail depolarization effects if the measurement system cannot resolve these variations, as will be discussed later.

Without loss of generality we may restrict our presentation to a two-term coherent parallel combination. It can be shown that Eqs. (8) and (9) lead to the same Mueller-Jones matrix of the combined nondepolarizing system, $\mathbf{M}_J$. For instance, from

Eq. (9), $\mathbf{M}_J$ can be written in terms of $\mathbf{Z}$ matrices as follows:

$$\mathbf{M}_J = \mathbf{Z}\mathbf{Z}^* = aa^*\mathbf{Z}_a\mathbf{Z}_a^* + bb^*\mathbf{Z}_b\mathbf{Z}_b^* + ab^*\mathbf{Z}_a\mathbf{Z}_b^* + ba^*\mathbf{Z}_b\mathbf{Z}_a^*. \tag{10}$$

In this expansion, $\mathbf{Z}_a\mathbf{Z}_a^*$ and $\mathbf{Z}_b\mathbf{Z}_b^*$ are the Mueller-Jones matrices of the nondepolarizing component systems, whereas $\mathbf{Z}_a\mathbf{Z}_b^*$ and $\mathbf{Z}_b\mathbf{Z}_a^*$ are the matrices resulting from coherence that cannot be interpreted as Mueller matrices in the usual sense. The combined term $ab^*\mathbf{Z}_a\mathbf{Z}_b^* + ba^*\mathbf{Z}_b\mathbf{Z}_a^*$ turns out to be a real matrix; but it still is not a Mueller matrix. The result provided by means of Eq. (8) is mathematically equivalent to Eq. (10) under the transformation $\mathbf{A}(\mathbf{J}_m \otimes \mathbf{J}_n^*)\mathbf{A}^{-1} = \mathbf{Z}_m\mathbf{Z}_n^*$ [3]. Besides rendering the mathematics compact and simple, the advantage of the $\mathbf{Z}$ matrix approach is that, in contrast to Jones formalism, it also permits treating incoherent or partially coherent processes by, respectively, truncating or attenuating the coherence terms $\mathbf{Z}_a\mathbf{Z}_b^*$ and $\mathbf{Z}_b\mathbf{Z}_a^*$.

B. Superposition of $|h\rangle$ states

The Jones and the $\mathbf{Z}$ matrix approaches are equivalent descriptions for a coherent parallel combination of deterministic systems. However, sometimes it may be convenient to work with vectors rather than matrices, and to formulate the coherent parallel combination process in terms of the covariance vectors of the associated systems:

$$|h\rangle = a|h_a\rangle + b|h_b\rangle + c|h_c\rangle + \cdots, \tag{11}$$

where $|a|^2 + |b|^2 + |c|^2 + \cdots = 1$ and the complex vectors $|h_i\rangle$ are defined in Eq. (2).

For a two-term coherent parallel combination, the covariance matrix $\mathbf{H}$ of the combined system can be written as

$$
\begin{aligned}
\mathbf{H} &= |h\rangle\langle h| \\
&= aa^*|h_a\rangle\langle h_a| + bb^*|h_b\rangle\langle h_b| + ab^*|h_a\rangle\langle h_b| \\
&\quad + ba^*|h_b\rangle\langle h_a|,
\end{aligned}
\tag{12}
$$

where $|h_a\rangle\langle h_a|$ and $|h_b\rangle\langle h_b|$ are the covariance matrices corresponding to the Mueller-Jones matrices of the nondepolarizing component systems; $|h_b\rangle\langle h_a|$ and $|h_b\rangle\langle h_a|$ are the mixed *coherence* terms which cannot be related to the usual Mueller matrices. The covariance matrix $\mathbf{H}$ leads directly to the Mueller-Jones matrix of the combined system.

In quantum mechanics, any state vector (pure state) can be written as a linear combination of basis states (pure states) which are, in general, a complete set of eigenvectors of a Hermitian operator that corresponds to an observable quantity:

$$|\Psi\rangle = \sum_{i=1}^{N} a_i|\psi\rangle_i, \tag{13}$$

where a_i are complex numbers (amplitudes) and $|\psi\rangle_i$ are the eigenvectors of a Hermitian operator that constitute a complete set of basis system. The covariance vector $|h\rangle$ is the analog of the quantum mechanical state vector $|\Psi\rangle$, and it is also possible to decompose a given vector $|h\rangle$ with respect to a complete basis set of component systems. We simply apply the ordinary vector decomposition procedure:

$$|h\rangle = a_1|h_1\rangle + a_2|h_2\rangle + a_3|h_3\rangle + a_4|h_4\rangle, \tag{14}$$

where a_i are complex coefficients and $|h_i\rangle$ constitute a complete set of basis vectors. The vectorial decomposition of $|h\rangle$ is not unique: for a given $|h\rangle$ there may exist infinitely many decompositions with respect to different sets of complete basis. Basis vectors $|h_i\rangle$ can define an orthogonal or nonorthogonal basis. For example, if $|h_1\rangle$ and $|h_2\rangle$ correspond, respectively, to orthonormal covariance vectors of a linear horizontal polarizer and a linear vertical polarizer, then the following expansion of $|h\rangle$ will correspond to a horizontal quarter-wave-plate state:

$$|h\rangle = \frac{1+i}{2}|h_1\rangle + \frac{1-i}{2}|h_2\rangle. \tag{15}$$

The algebra of Mueller-Jones formalism admits a superposition of $|h\rangle$ states as given in Eq. (14). Therefore, at least mathematically, we can consider an ideal quarter-wave-plate state as a coherent linear combination of two orthogonal linear polarizer states. In practice, this means that it is possible to combine two orthogonal polarizers coherently with the associated complex coefficients as given in Eq. (15) to obtain an "artificial" quarter wave plate that effectively responds to the incident light just like a genuine one (e.g., a crystal plate). In fact, this is intimately related to the common model for an optical linear retarder which resolves a light wave into two orthogonal linear polarization components and produces a phase shift between them.

In general, we can use a nonorthogonal basis to decompose a given covariance vector $|h\rangle$. However, decomposition with respect to a nonorthogonal basis is more involved: we have to take into account covariant and contravariant types of vectors and expansion coefficients. As an example, the covariance vector of an ideal partial polarizer can be decomposed into nonorthogonal basis states, one of them being the direct beam state which corresponds to the identity Mueller matrix, and the other component being a horizontal linear polarizer state, with suitable coefficients.

III. PARTIAL COHERENCE AND DEPOLARIZATION

In a real experiment, the measuring apparatus may be unable to resolve the fluctuations in the phases of the electromagnetic fields arising during the interaction of the light beam with a sample, then the measured scattering matrix of the combined system turns out to be a depolarizing Mueller matrix that can be considered as a mixture of nondepolarizing Mueller-Jones matrices. Kim *et al.* [21] consider an *ensemble* average of Jones matrix realizations in order to explain depolarization. Gil gives a more detailed depolarization scheme based on an *incoherent* convex sum of Mueller-Jones matrices [4]: if we let $I^{(i)}$ be the intensity of the portion of light that interacts with the i element, and denote $\mathbf{J}^{(i)}$, $\mathbf{M}_J^{(i)}$ the respective Jones and Mueller-Jones matrices representing the i element, the Jones vector ϵ of the light pencil emerging from each element will be given by

$$\epsilon_i' = \mathbf{J}^{(i)}[\sqrt{p_i}\epsilon], \tag{16}$$

where $p_i = I^{(i)}/I$, I being the total intensity. The corresponding Stokes vector s' of the complete emerging beam, obtained through the *incoherent superposition* of the beams emerging

from the different elements s_i', can be written as

$$s' = \sum_i s_i' = \left(\sum_i p_i \mathbf{M}_J^{(i)} \right) s = \mathbf{M}s, \qquad (17)$$

where $\mathbf{M}$ is the depolarizing Mueller matrix of the incoherently combined system.

In this result the system is considered as an ensemble, so that each realization i characterized by a well-defined Mueller-Jones matrix $\mathbf{M}_J^{(i)}$, occurs with probability p_i; hence, the optical system can be considered as a proper mixture of Muller-Jones realizations at the outset. However, even when the fluctuations in phases in each of the elements take place, instantaneous realizations are still deterministic. In other words, at a given time, space, and frequency all phases can be considered as constants, therefore the linear superposition is *instantaneously* coherent and the Mueller matrix of the combined optical system is instantaneously *nondepolarizing* (here the adverb *instantaneously* does not only imply a temporal meaning). Only when we begin to take into account the statistical averages (time average, spatial average, and/or frequency average), coherence terms will be washed out and the result will be depolarizing. For example, consider a simple case where the $\mathbf{Z}$ matrix of the combined system is formed by a linear combination of $\mathbf{Z}$ matrices of two subsystems at a given instant:

$$\mathbf{Z} = \frac{1}{\sqrt{2}}\mathbf{Z}_a + \frac{e^{i\phi}}{\sqrt{2}}\mathbf{Z}_b, \qquad (18)$$

where $\mathbf{Z}_a$, $\mathbf{Z}_b$ are the matrix states of the subsystems, and ϕ is a constant phase angle. The nondepolarizing Mueller matrix corresponding to $\mathbf{Z}$ will be

$$\mathbf{M}_J = \frac{1}{2}\mathbf{M}_a + \frac{1}{2}\mathbf{M}_b + \frac{e^{-i\phi}}{2}\mathbf{Z}_a\mathbf{Z}_b^* + \frac{e^{i\phi}}{2}\mathbf{Z}_b\mathbf{Z}_a^*, \qquad (19)$$

where $\mathbf{Z}_a\mathbf{Z}_b^*$ and $\mathbf{Z}_a^*\mathbf{Z}_b$ are the coherence terms.

Now consider another instance:

$$\mathbf{Z}' = \frac{1}{\sqrt{2}}\mathbf{Z}_a - \frac{e^{i\phi}}{\sqrt{2}}\mathbf{Z}_b. \qquad (20)$$

In this case there is an additional phase, $e^{i\pi} = -1$. Then the nondepolarizing Mueller matrix corresponding to $\mathbf{Z}'$ is

$$\mathbf{M}'_J = \frac{1}{2}\mathbf{M}_a + \frac{1}{2}\mathbf{M}_b - \frac{e^{-i\phi}}{2}\mathbf{Z}_a\mathbf{Z}_b^* - \frac{e^{i\phi}}{2}\mathbf{Z}_b\mathbf{Z}_a^*. \qquad (21)$$

In the arithmetic mean of $\mathbf{M}_J$ and $\mathbf{M}'_J$,

$$\mathbf{M}_{\text{average}} = \tfrac{1}{2}\mathbf{M}_a + \tfrac{1}{2}\mathbf{M}_b, \qquad (22)$$

the coherence terms are totally truncated, and the result is a *depolarizing* Mueller matrix which turns out to be a convex sum of nondepolarizing Mueller matrices of the component systems.

The matrices $\mathbf{M}$ and $\mathbf{M}'$ are the instantaneous (in the sense of constant phase) realizations of the measurement process. Now consider a continuum of similar instantaneous realizations and assume that the phase relations between the component systems change very rapidly during the exposure time T. For example, let the phase angle ϕ be a function of time so that the orientation of unit vector $e^{i\phi}$ randomly fluctuates with a

vanishing integral $\int_0^T e^{i\phi} \, dt$, then, due to the temporal average of the instantaneous realizations, the coherence terms will be truncated in the case of incoherence or attenuated in the case of partial coherence and depolarization effects will appear. Here we have discussed temporal averaging in these two limiting cases, but similar results would be obtained for spatial and frequency averaging.

In general, when the phases of the complex coefficients of a system with two components fluctuate we may replace Eq. (10) by

$$\mathbf{M} = |a|^2\mathbf{Z}_a\mathbf{Z}_a^* + |b|^2\mathbf{Z}_b\mathbf{Z}_b^* + \langle ab^*\rangle\mathbf{Z}_a\mathbf{Z}_b^* + \langle ba^*\rangle\mathbf{Z}_b\mathbf{Z}_a^*, \quad (23)$$

where the brackets $\langle ...\rangle$ denote averaging over space, time, or frequency. Clearly, the degree of coherence is then controlled by the terms $\langle ab^*\rangle$ and $\langle ba^*\rangle$. In the case of total coherence, $\langle ab^*\rangle = ab^*$ and $\langle ba^*\rangle = ba^*$, and there will be no depolarization [the Mueller matrix will be given by Eq. (10)], while for total incoherence $\langle ab^*\rangle = \langle ba^*\rangle = 0$. In between these two limiting cases there will be partial coherence. It is therefore possible to quantify the degree of coherence with the following parameter:

$$p = \sqrt{\frac{\langle ab^*\rangle\langle ba^*\rangle}{|a|^2|b|^2}}, \qquad (24)$$

where p takes values between 0 (total incoherence) and 1 (total coherence). Note that p is similar but not exactly equal to the *Coherence Index* proposed in [10].

Interference. Consider now the development of an interference pattern on the screen of Young's double slit experiment, photon by photon. The arrival of each photon at a point detector is an instantaneous realization of the superposed probability waves. But, if the coherency of light cannot be preserved in a long period of time, the interference pattern will be washed out, in spite of the fact that the instantaneous detection of a single photon still obeys the well-defined superposition principle of quantum mechanics.

We may observe interference effects in the overall detected intensity if in Eq. (18) $\mathbf{Z}_a = \mathbf{Z}_b$:

$$\mathbf{Z} = \frac{1}{\sqrt{2}}\mathbf{Z}_a + \frac{e^{i\phi}}{\sqrt{2}}\mathbf{Z}_a = \frac{1}{\sqrt{2}}\mathbf{Z}_a(1 + e^{i\phi}). \qquad (25)$$

This is an analog of Young's double slit with two equivalent component systems with a relative phase between them. The corresponding Mueller-Jones matrix is

$$\mathbf{M}_J = \mathbf{Z}_a\mathbf{Z}_a^*(1 + \cos\phi) = \mathbf{M}_a(1 + \cos\phi), \qquad (26)$$

where $\mathbf{M}_a$ is the nondepolarizing Mueller matrix (Mueller-Jones matrix) of the equivalent component systems. Note that Eq. (26) is an analog of Eq. (6), but here the interference is given in terms of Mueller-Jones matrices associated with optical media.

Interference effects can only be observed if the value of ϕ can be preserved during the measurement. If ϕ varies drastically, on the average, the $\cos\phi$ term will tend to vanish but the Mueller-Jones matrix of the combined system will be still equal to $\mathbf{M}_a$. For depolarization effects, uncontrollable

random fluctuations in the phases are not enough: at least two systems with *distinct* states should be combined in parallel.

IV. EXAMPLE: COHERENT EFFECTS BETWEEN DIPOLES

Superposition of distinct states can be illustrated by small (much smaller than the wavelength of light) spherical particles with isotropic polarizability that can be put in oscillatory motion when they are placed in a periodic electric field, producing secondary radiation. If, in an oriented material medium, dipoles are constrained to vibrate only along a certain direction, the forward-scattering matrix of the dipole coincides with the Mueller matrix of a linear polarizer. Therefore, for vertical and horizontal dipoles we have, respectively,

$$\mathbf{M_V} = \begin{pmatrix} 1 & -1 & 0 & 0 \\ -1 & 1 & 0 & 0 \\ 0 & 0 & 0 & 0 \\ 0 & 0 & 0 & 0 \end{pmatrix},$$

$$\mathbf{M_H} = \begin{pmatrix} 1 & 1 & 0 & 0 \\ 1 & 1 & 0 & 0 \\ 0 & 0 & 0 & 0 \\ 0 & 0 & 0 & 0 \end{pmatrix}. \quad (27)$$

The corresponding $\mathbf{Z_V}$ and $\mathbf{Z_H}$ Matrices are

$$\mathbf{Z_V} = \frac{1}{\sqrt{2}} \begin{pmatrix} 1 & -1 & 0 & 0 \\ -1 & 1 & 0 & 0 \\ 0 & 0 & 1 & i \\ 0 & 0 & -i & 1 \end{pmatrix},$$

$$\mathbf{Z_H} = \frac{1}{\sqrt{2}} \begin{pmatrix} 1 & 1 & 0 & 0 \\ 1 & 1 & 0 & 0 \\ 0 & 0 & 1 & -i \\ 0 & 0 & i & 1 \end{pmatrix}. \quad (28)$$

The superposed state is given by $\mathbf{Z} = a_V \mathbf{Z_V} + a_H \mathbf{Z_H}$. If the two particles are identical and with the same complex weights a_V and a_H ($a_V = a_H = a$), the coherent superposed state will be given by

$$\mathbf{M_{coh}} = |a|^2 (\mathbf{Z_V Z_V^*} + \mathbf{Z_H Z_H^*} + \mathbf{Z_V Z_H^*} + \mathbf{Z_H Z_V^*}) = 2|a|^2 \mathbf{I}, \quad (29)$$

where $\mathbf{I}$ is the 4×4 identity matrix, meaning that the coherent superposed system is able to maintain the polarization state of any incoming beam. In fact, this is a general result when superposing $\mathbf{Z}$ matrices that correspond to orthogonal directions of anisotropy. For example, the same identity matrix is recovered when superposing left- and right-handed circular polarizers. As discussed earlier, equivalent results for coherent superposition are also obtained by the summation of Jones matrices shown in Eq. (7), but that approach cannot describe the incoherent or partially coherent cases discussed below.

If a_V and a_H have the same amplitude ($|a_V| = |a_H| = |a|$) but different and fluctuating phases the coherence terms may average to zero and an incoherent superposition will be
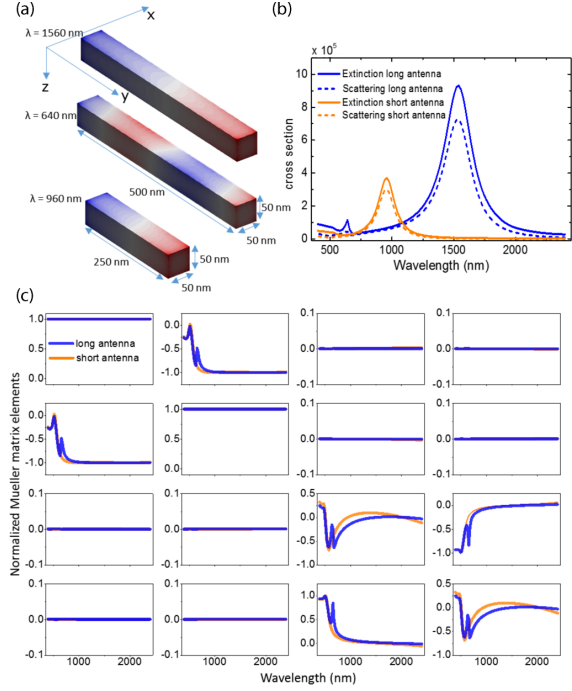

FIG. 1. (a) Surface charge distributions (positive charges in red and negatives in blue) for the long and short nanoantennas at the indicated wavelengths. (b) Calculated extinction and scattering cross sections for the two types of nanoantennas. Due to the different aspect ratio, the resonances occur at different wavelengths. (c) Normalized Mueller matrix for each structure when the long axis is oriented along y.

obtained:

$$\mathbf{M_{incoh}} = |a|^2 (\mathbf{Z_V Z_V^*} + \mathbf{Z_H Z_H^*}) = 2|a|^2 \begin{pmatrix} 1 & 0 & 0 & 0 \\ 0 & 1 & 0 & 0 \\ 0 & 0 & 0 & 0 \\ 0 & 0 & 0 & 0 \end{pmatrix}. \quad (30)$$

Note that regardless of the characteristics of the component particles, $\mathbf{M_{incoh}}$ will only be affected by the amplitudes of a_V and a_H but not by their phases. Any intermediate situation between the limiting cases of Eqs. (29) and (30) can be represented by Eq. (23) and will correspond to partial coherence.

The case of plasmonic nanoantennas. The coherent superposition of dipoles can be well illustrated for visible or near-IR light by analyzing the optical response of thin strips of gold with the nanoantenna geometry shown in Fig. 1(a). These metallic rectangular structures have a width and thickness of 50 nm and a length of 500 nm (for the long nanoantenna) and 250 nm (for the short nanoantenna). The electromagnetic response of such antenna-like particles is calculated using the boundary element method (BEM) [22,23]. We used the MATLAB implementation of the BEM method developed by Hohenester *et al.* [23]. The optical constants of Au are taken from Johnson and Christy [24] with the data extrapolated to
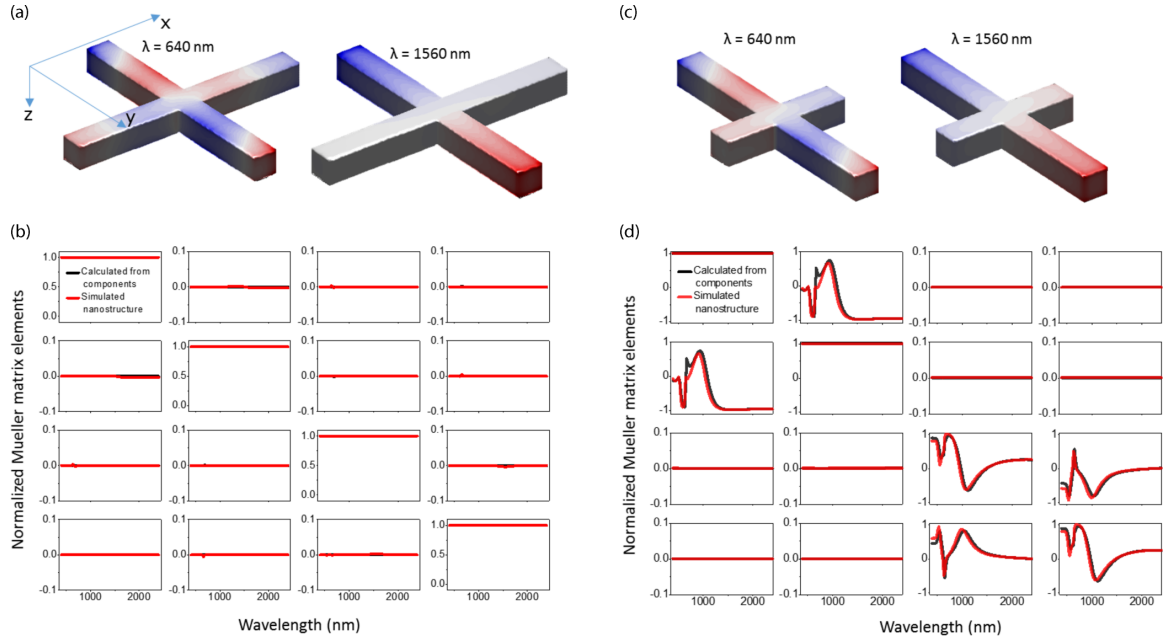
FIG. 2. (a) Surface charge distributions for a cross made of two long nanoantennas at the indicated wavelengths. (b) Comparison between the normalized Mueller matrix obtained from BEM simulation (red) of the structure in (a) and the calculation (black). (c) Surface charge distributions for a cross made of a long and a short nanoantenna. (d) Comparison between the normalized Mueller matrix obtained from BEM simulation (red) of (c) and the calculation (black).

the infrared range by the Drude model. The extinction spectra of the long nanoantenna [Fig. 1(b)] shows a dipolar resonance at 1560 nm and a secondary quadrupolar resonance around 640 nm, as it is shown by the surface charge distributions of Fig. 1(a). The short nanoantenna [Fig. 1(b)] has a single dipole resonance located at shorter wavelengths (960 nm), corresponding to a smaller aspect ratio [25]. The simulated Mueller matrices for the vertically oriented short and long nanoantennas are shown in Fig. 1(c). At long wavelengths, the Mueller matrix for both structures is very close to a vertical polarizer [$\mathbf{M}_V$ in Eq. (27)], while at the shortest wavelengths energy of light is no longer confined in a dipolar resonance, and the nanoantennas behave more like retarders.

In the next step, we analyze the superposed effect of two combined nanoantennas that are not necessarily aligned. This combined effect can be calculated from Eq. (10) by using the component $\mathbf{Z}$ matrices derived from the Mueller matrices of Fig. 1. We simply rotate the simulated Mueller matrices of vertical nanoantennas to obtain their Mueller matrix at an angle θ: $\mathbf{R}(-\theta)\mathbf{MR}(\theta)$. First we consider two perpendicularly crossed nanoantennas, which are illustrated by cross-like structures in Figs. 2(a) and 2(c). For a cross formed by two equal nanoantennas, the complex coefficients associated with each component antenna are the same, then the coherent superposition of orthogonal $\mathbf{Z}$ matrix states leads to an identity Mueller matrix [Fig. 2(b)], as it was anticipated by Eq. (29). However, even if the Mueller matrices of long and short nanoantennas are very similar [Fig. 1(c)], the combined effect of perpendicularly crossed long and short

antennas strongly differs from the identity Mueller matrix [Fig. 2(d)] because, in this case, the complex coefficients are not the same. For any of these perpendicularly crossed configurations, the Mueller matrices simulated by the BEM method are in good agreement with the matrices calculated from the data of component nanoantennas.

In a cross made by orthogonal nanoantennas there is no significant electronic interaction between the dipole modes of the antennas, and the extinction spectrum is, qualitatively, an addition of the spectra of the individual antennas. However, the situation can be different if the dipole moments of the antennas are parallel or partially parallel because, in this case, they can significantly couple to each other. According to the plasmon hybridization theory of particle dimers, coupling of the individual resonances results in a lower energy mode with the dipole moments of the individual particles being in phase, and results in a higher energy mode with the dipole moments out of phase [26]. This second case has an overall lower dipole moment and hence scatters less light. The surface charge distribution calculated at the resonances confirms the nature of these coupled modes (see Fig. 1 of the Supplemental Material [27]).

In Fig. 3 we consider the superposed effect of the nanoantennas with a relative orientation of $45°$. Since in this configuration the dipole moments are oblique, the coupled modes substantially modify the individual responses of the antennas. The intensity of the coupling depends on the distance between the antennas (see Fig. 2 of the Supplemental Material). When the coupling is significant, the calculated Mueller matrices [with Eq. (10)] from the
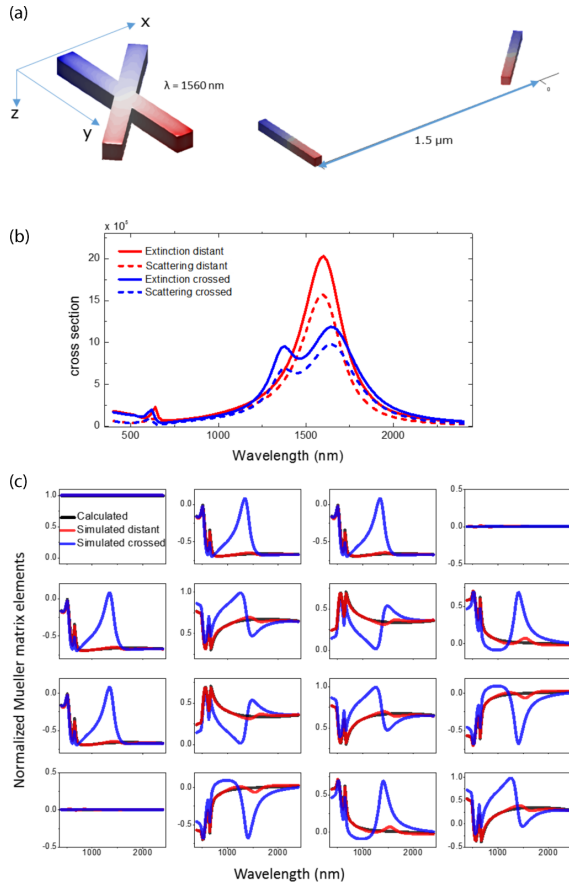
FIG. 3. (a) Surface charge distributions for crossed and distant (1.5 μm of separation) oblique nanoantennas. (b) Extinction and scattering cross section for the systems shown in (a). The strong coupling in the oblique crosses results in low and high energy modes that do not appear for the distant dipoles, when coupling is not significant. (c) The calculated Mueller matrix from the component nanoantenna states is in agreement with BEM simulation for distant dipoles.

associated component nanoantenna matrix states do not match the BEM simulations of the combined nanostructure. However, instead of simulating crossed antennas, when we consider separated antennas, as shown in Fig. 3, the results of the BEM simulations show good agreement with the coherent superposition calculations of Eq. (10), because the coupling effects are minimized. Extending our interference formalism by incorporating specific dynamical laws of interaction will be the subject of future work.

V. CONCLUSIONS

In this work, it is shown that the coherent (constant phase) parallel combination of deterministic systems can be written as a linear combination of **Z** matrices with complex coefficients. In practice this means that we can synthesize any nondepolarizing optical system as a coherent linear superposition of a complete set of nondepolarizing basis systems. When the component Mueller-Jones states are the same but have different relative phases, interference effects are expected to be observed. It is also shown that depolarization can arise from temporal, spatial, or frequency averaging over fluctuating and distinct Mueller-Jones matrices. If the parallel combination process is incoherent at the outset, this averaging totally cancels out the coherence terms, and the Mueller matrix of the combined system reduces simply to the convex sum of Mueller-Jones matrix realizations.

The mathematical formalism we have described is based on the linear light-matter interactions described in Mueller matrices. It allows us to introduce the concept of "superposition of Mueller-Jones states" of optical media, and makes an analogy between the quantum mechanical wave function ψ and the matrix material media state **Z**. This constitutes a theory of optical coherence that has the particularity that is grounded on the 16 observable quantities (elements of a Mueller matrix) that characterize an optical media, as opposed to the single observable quantity (intensity of light) around which other theories are built. Note that the analogy with quantum mechanics allows us to directly formulate the optical superposition of Mueller-Jones states pertaining to optical media without need of an explicit consideration of the superposition of electromagnetic fields, which is the starting point of other formulations of optical coherence. We think that this formalism introduces a unified theory of coherence and polarization that can be specially useful for experimental techniques that explore polarized light and material media interactions such as polarimetry or ellipsometry. In these techniques the polarization of light is affected by coherent, partially coherent, and incoherent superposition processes which often can coexist. In nanophotonic applications our formalism may also provide theoretical means to tailor the light emission of nanostructures embedded in large area domains with the desired polarization response and functionality.

ACKNOWLEDGMENT

[1] Z. Ficek and S. Swain, *Quantum Interference and Coherence: Theory and Experiments* (Springer, Berlin, 2005).

[2] K. Wódkiewicz, Phys. Rev. A **51**, 2785 (1995).

[3] E. Kuntman, M. Ali Kuntman, and O. Arteaga, J. Opt. Soc. Am. A **34**, 80 (2017).

[4] J. J. Gil, Eur. Phys. J. Appl. Phys. **40**, 1 (2007).

[5] N. G. Parke, J. Math. Phys. **28**, 131 (1949).

[6] A. Peres, *Quantum Theory: Concepts and Methods* (Springer, Berlin, 2002).

[7] U. Fano, J. Opt. Soc. Am. **39**, 859 (1949).

[8] U. Fano, Phys. Rev. **93**, 121 (1954).

[9] E. Wolf, Phys. Lett. A **312**, 263 (2003).

[10] R. Ossikovski and K. Hingerl, Opt. Lett. **41**, 4044 (2016).

[11] F. Gori, M. Santarsiero, S. Vicalvi, R. Borghi, and G. Guattari, Pure Appl. Opt **7**, 941 (1998).

[12] L. Mandel and E. Wolf, *Optical Coherence and Quantum Optics* (Cambridge University Press, Cambridge, England, 1995).

[13] T. Setälä, A. Shevchenko, M. Kaivola, and A. T. Friberg, Phys. Rev. E **66**, 016615 (2002).

[14] R. C. Jones, J. Opt. Soc. Am. **31**, 488 (1941).

[15] D. Goldstein, *Polarized Light, Revised and Expanded (Optical Science and Engineering)*, 2nd ed. (CRC Boca Raton, FL, 2003).

[16] S. R. Cloude, in *Polarization Considerations for Optical Systems II*, edited by R. A. Chipman, Proc. Soc. PhotoOpt. Instrum. Eng. (SPIE, San Diego, 1989), Vol. 1166, pp. 177–185.

[17] J. J. Gil and I. S. José, J. Opt. Soc. Am. A **30**, 1078 (2013).

[18] J. J. Gil, J. Appl. Remote Sens. **8**, 081599 (2014).

[19] A. Aiello and J. P. Woerdman, arXiv:math-ph/0412061.

[20] S. M. Nichols, O. Arteaga, A. T. Martin, and B. Kahr, Appl. Surf. Sci. (2016), doi: 10.1016/j.apsusc.2016.10.146.

[21] K. Kim, L. Mandel, and E. Wolf, J. Opt. Soc. Am. A **4**, 433 (1987).

[22] F. J. G. de Abajo and A. Howie, Phys. Rev. B **65**, 115418 (2002).

[23] U. Hohenester and A. Trügler, Comput. Phys. Commun. **183**, 370 (2012).

[24] P. B. Johnson and R. W. Christy, Phys. Rev. B **6**, 4370 (1972).

[25] G. W. Bryant, F. J. G. de Abajo, and J. Aizpurua, Nano Lett. **8**, 631 (2008).

[26] P. Nordlander, C. Oubre, E. Prodan, K. Li, and M. I. Stockman, Nano Lett. **4**, 899 (2004).

[27] See Supplemental Material at http://link.aps.org/supplemental/10.1103/PhysRevA.95.063819 for simulations and calculations of the coupling between oblique optical nanoantennas.

Supplementary Material to: Formalism of optical coherence and polarization based on material media states

Ertan Kuntman[1]**, M. Ali Kuntman**[2]**, Jordi Sancho-Parramon**[3]**, and Oriol Arteaga**[1,+]

[1]Departament de Física Aplicada, Feman Group, IN2UB, Universitat de Barcelona, C/ Martí i Franquès 1, Barcelona 08030, Spain
[2]Independent Researcher, Ankara, Turkey.
[3]Rudjer Boskovic Institute, Bijenicka cesta 54, 10000, Zagreb, Croatia
[*]oarteaga@ub.edu

Coupled modes in oblique nanoantennas
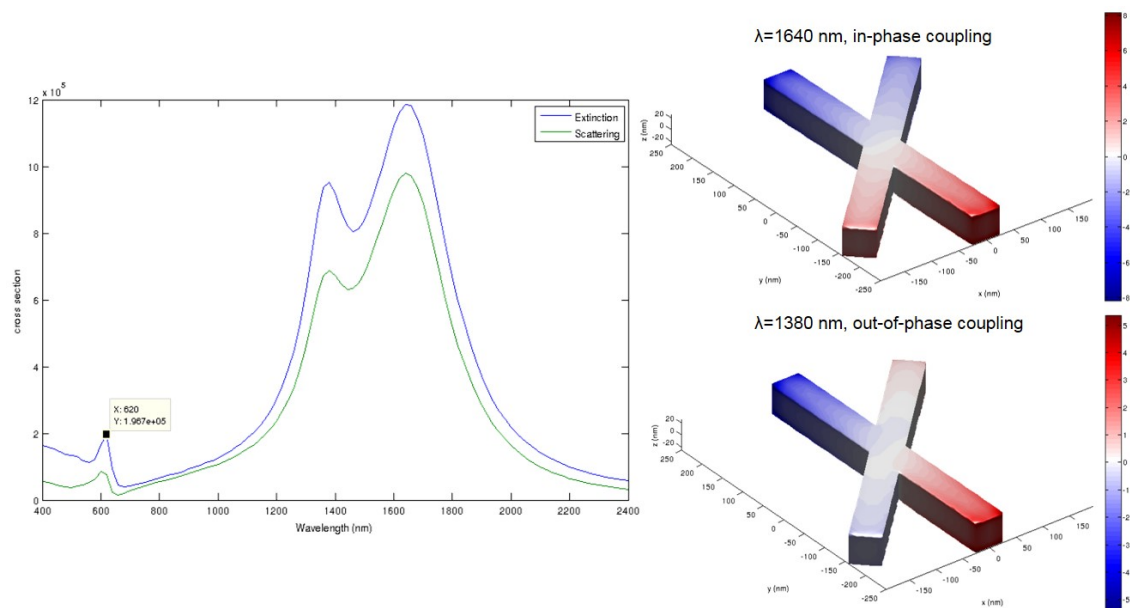
Figure 1. Low and high energy modes (λ=1640 nm and λ=1380, respectively) that appear due to the interaction between oblique nanoantennas. The surface charge distributions show that the low energy scattering peak corresponds to an in-phase coupled mode while the high energy peak corresponds to out-of-phase coupling.

Coupling between plasmonic nanoantennas as function of their distance
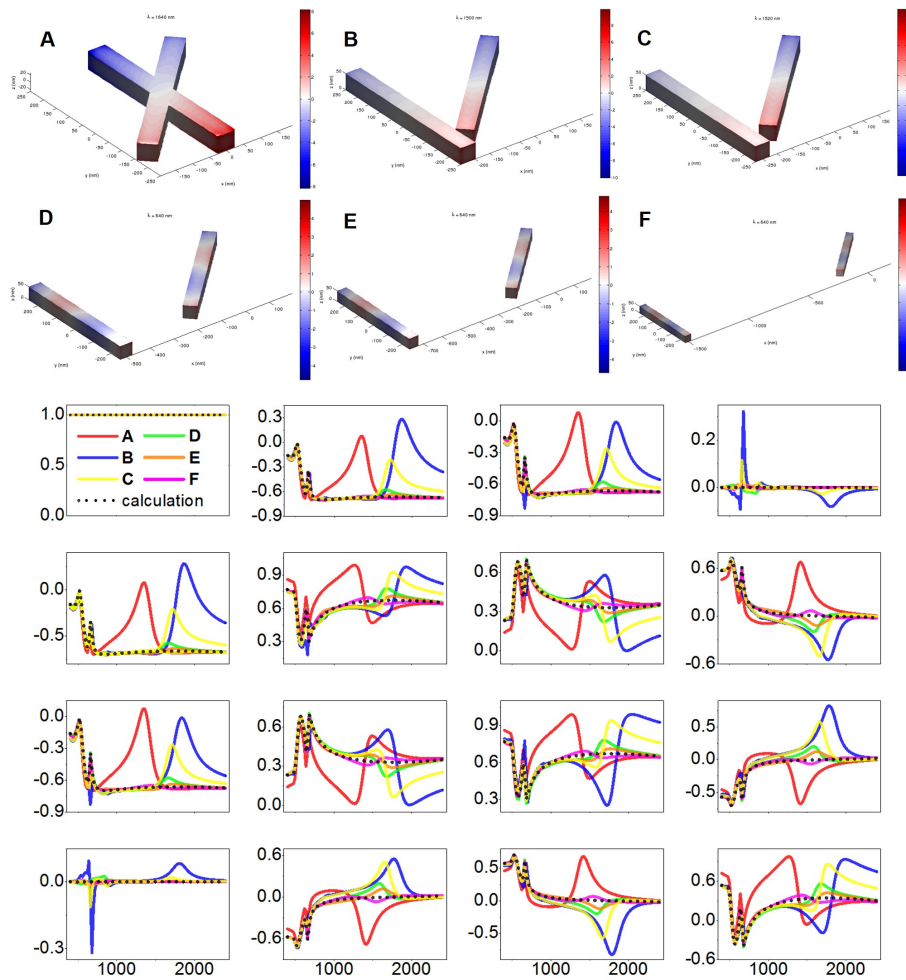
Figure 2. Mueller matrix simulations using the BEM method for different geometrical configurations of two nanoantennas that have a relative orientation of 45°. Each simulated configuration is identified with a letter (A, B, C, D, E or F) and the calculated Mueller matrix using each nanoantenna Mueller-Jones state (and neglecting interaction between antennas) is indicated with a dotted line. Clearly, results A and B are those that differ more from the calculation because, in these configurations, the interaction between nanoantennas is strong. As the distance between the antennas increases, the results of the simulation re-conciliate with the non-interacting calculation.

Coupling between long and short nanoantennas
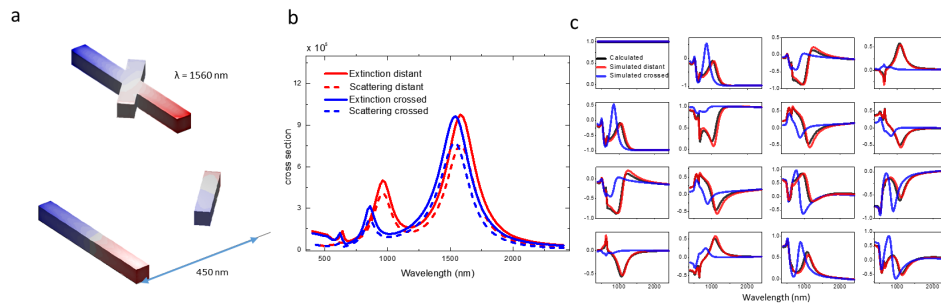
Figure 3. a, Surface charge distributions for crossed and distant (450 nm of separation) oblique long and short nanoantennas **b**, Extinction and scattering cross section for the systems shown in **a**. **c**, The calculated Mueller matrix from the component nanoantenna states is in agreement with the simulated Mueller matrix of distant dipoles.

Optics Letters

Mueller matrix polarimetry on a Young's double-slit experiment analog

Oriol Arteaga,[1,*] ⓘ Razvigor Ossikovski,[2] Ertan Kuntman,[1] Mehmet A. Kuntman,[3] Adolf Canillas,[1] and Enric Garcia-Caurel[2]

[1]Department de Física Aplicada, IN2UB, Feman Group, Universitat de Barcelona, C/ Martí i Franqués 1, Barcelona 08030, Spain
[2]LPICM, CNRS, Ecole Polytechnique, Université Paris-Saclay, 91128 Palaiseau, France
[3]Independent Scholar, Ankara 06830, Turkey
*Corresponding author: oarteaga@ub.edu

In this Letter we describe an experiment in which coherent light is sent through a calcite crystal that separates the photons by their polarization. The two beams are then let to superpose, and this recombined beam is used to measure the Mueller matrix of the system. Results are interpreted according to our recent formalism of coherent superposition in material media. This is the first experimental implementation of a Young's experiment with complete polarimetry, and it is demonstrated that our method can be used for the experimental synthesis of optical devices with on-demand optical properties. © 2017 Optical Society of America

OCIS codes: (260.3160) Interference; (260.5430) Polarization; (260.2130) Ellipsometry and polarimetry.

https://doi.org/10.1364/OL.42.003900

Coherence is related to the ability of waves to interfere. Most optical interference effects occur in the micro- or nano-scale (e.g., thin films) and we do not have access to a macroscopic control of the two or more beams that coherently superpose. With the high temporal and spatial coherence of lasers it is easy to merge two or more macroscopic beams in a well-controlled manner in an interferometer. However, it is usually difficult to have a precise control of the polarization state of light at the different arms of an interferometer, because beam splitters tend to produce some change in the polarization of light (even those marketed as non-polarizing), making accurate polarimetric measurements often problematic [1–3].

In this work we use a different approach to achieve the superposition of two macroscopically distinguishable beams. When light goes through a crystal slab of calcite, or any other crystal with strong birefringence, it splits by polarization into two rays that take slightly different paths in a phenomenon long known as double refraction. If the two emerging beams, carrying orthogonal polarizations, are not very distant one from the other it is easy to merge them again (at least partially) by using a lens that focuses the light on the exit window of the crystal that makes the beams diverge afterwards. A scheme of the process is

shown in Fig. 1(a). Effectively, this method recombines two beams that are juxtaposed in the space [4] avoiding the non-idealities associated with beam splitters, and it allows us to keep the experimental device simple, as it is not necessary to consider multiple arms. Despite the fact that our experimental setup does not involve two slits, the optical outcome is analog to the famous Young's double-slit experiment when the slits are covered by orthogonal polarizers as it was first suggested in 1819 by Fresnel and Arago [5,6] and as we have recently demonstrated [7]. Our experimental data was analyzed according to a new formalism of optical coherence and polarization [8] that is useful to describe superposition processes taking place during a polarimetric experiment. It is based on a quantum mechanical analogy and uses complex Mueller–Jones matrix states, $\mathbf{Z}$, that relate to Mueller–Jones matrices as $\mathbf{M} = \mathbf{Z}\mathbf{Z}^*$ or covariance vectors, $|h\rangle$ [8,9].

Measurements were done with the 4-PEM Mueller polarimeter described in [10]. It uses four photoelastic modulators of different frequencies to determine simultaneously all Mueller matrix (MM) elements from frequency analysis of the intensity
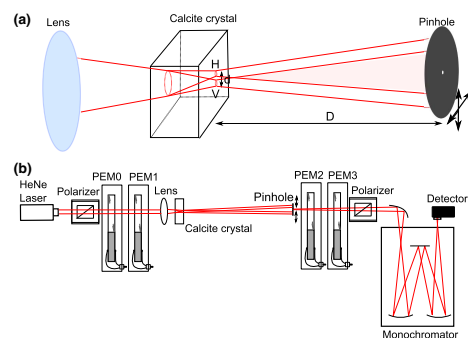

Fig. 1. (a) Double refraction in the crystal generates two point-like sources separated by a distance d with horizontal (H) and vertical (V) polarizations. A mobile pinhole is placed at a distance D to scan the superposed beams. (b) Detail of the setup when mounted in the 4-PEM Mueller polarimeter.

of light at the photomultiplier detector. Two basic modifications of the instrument (with respect to the basic description of [10]) were required in this experiment. First, the incoherent light source of the polarimeter was replaced by a He–Ne laser (632.8 nm). Second, in front of the polarization state analyzer (PSA) a pinhole of 20 μm (or 30 μm in other measurements) has been inserted, as it is shown in Fig. 1(b). This pinhole, which is displaceable with a motorized x–y translator, controls the spatial resolution of the measurement.

With this method it is possible to obtain MM maps with good spatial resolution. Displacing the pinhole is equivalent to studying a different point of a hypothetical "measurement screen" placed at position of the pinhole. When the distances between the pinhole and the two emerging beams from the crystal are exactly the same, the beams reach the pinhole with the same phase, while for other positions of the pinhole there will be a phase difference that will result in fringes in some MM elements. The distance between two successive fringes is given by $\Delta x = D\lambda/d$, where λ is the wavelength, d is the distance between two emerging beams in calcite, and D is the distance to the pinhole. In our experiment $d \simeq 1.5$ mm and $D \simeq 420$ mm.

As a preliminary check, we measured the MM corresponding to each individual beam (by blocking its partner). The crystal behaves as a polarizer and the two beams carry orthogonal polarizations. The crystal was then carefully rotated until the MMs of horizontal and vertical polarizers, $\mathbf{M_H}$ and $\mathbf{M_V}$, were respectively obtained, within the experimental error. Then we let the two diverging beams superpose and set the pinhole to map, point-by-point, an area of 1×1 mm^2. The result is presented in the color map of Fig. 2(a).

Fringes appear at particular MM elements approximately as horizontal lines. This orientation is due to the experimental configuration, because the two emerging beams appear one
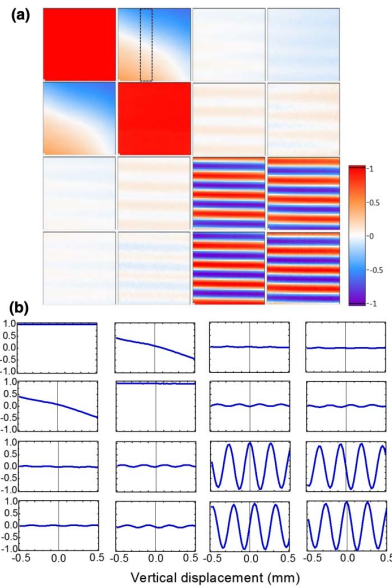
in the top of the other and with H and V polarizations, as it is shown in Fig. 1(a). The orientation of the fringes, as well as the MM itself, rotates if the crystal is rotated. In Fig. 2(b), we plot the evolution of the MM as a function of the vertical displacement of the pinhole (1 mm in total). The central point does not correspond exactly to the position where the distances between the pinhole and the two beam spots are the same since there is an initial phase shift caused by the different path lengths of the two beams through the crystal [7].

The superposition shown in Fig. 2 can be mathematically presented using $\mathbf{Z}$ matrices as [8]

$$\mathbf{Z}_0 = \frac{1}{\sqrt{2}}\mathbf{Z}_H + \frac{e^{i\phi}}{\sqrt{2}}\mathbf{Z}_V, \qquad (1)$$

where the phase ϕ accounts for the phase difference between the two beams. ϕ depends on the position of the pinhole because it is given by the difference in the optical path between the two beams. As

$$\mathbf{Z_V} = \frac{1}{\sqrt{2}}\begin{pmatrix} 1 & -1 & 0 & 0 \\ -1 & 1 & 0 & 0 \\ 0 & 0 & 1 & i \\ 0 & 0 & -i & 1 \end{pmatrix},$$

$$\mathbf{Z_H} = \frac{1}{\sqrt{2}}\begin{pmatrix} 1 & 1 & 0 & 0 \\ 1 & 1 & 0 & 0 \\ 0 & 0 & 1 & -i \\ 0 & 0 & i & 1 \end{pmatrix}, \qquad (2)$$

then

$$\mathbf{Z}_0 = \frac{1}{\sqrt{2}}\begin{pmatrix} 1+e^{i\phi} & 1-e^{i\phi} & 0 & 0 \\ 1-e^{i\phi} & 1+e^{i\phi} & 0 & 0 \\ 0 & 0 & 1+e^{i\phi} & -i(1-e^{i\phi}) \\ 0 & 0 & i(1-e^{i\phi}) & 1+e^{i\phi} \end{pmatrix}. \qquad (3)$$

And the corresponding MM is

$$\mathbf{M}_0 = \mathbf{Z}_0\mathbf{Z}_0^* = \begin{pmatrix} 1 & 0 & 0 & 0 \\ 0 & 1 & 0 & 0 \\ 0 & 0 & \cos\phi & -\sin\phi \\ 0 & 0 & \sin\phi & \cos\phi \end{pmatrix}, \qquad (4)$$

which is close to the experimental matrix of Fig. 2. When ϕ is zero or is a multiple of 2π an identity MM is obtained while, for other values, it progressively evolves between a horizontal quarter-wave plate MM ($\phi = -\pi/2$), a vertical quarter-wave plate ($\phi = \pi/2$), and a half-wave plate ($\phi = \pi$).

The only significant difference between the results of Fig. 2 and Eq. (4) can be seen in the spatial dependence of elements m_{01} and m_{10}. This occurs when two beams are not balanced and they do not superpose with exactly the same amplitude, as it was assumed in our theoretical description [Eq. (1)]. In fact, assuming Gaussian beams in the crystal, only when the pinhole is equidistant from the two beams a superposition with the same amplitude is expected.

The measured MMs are modified when other optical elements are added in the experiment. In Fig. 3 we show three color maps in which other optical elements are added in the optical path. Figure 3(a) corresponds to a measurement in

Fig. 2. (a) Spatial evolution of the MM (in a region of 1×1 mm^2 and with a pixel resolution of 20 μm). (b) The area boxed in (a) plotted as a function of pinhole's vertical displacement. In the point identified with zero vertical displacement the identity MM is measured.
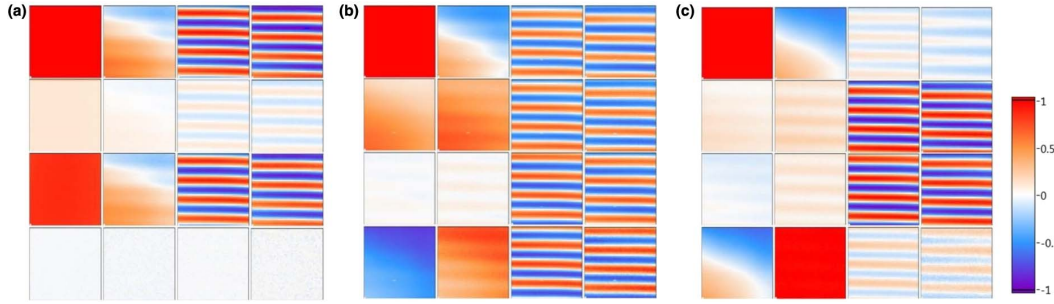
Fig. 3. Color maps of the spatial evolution of the MM in a region of 1×1 mm^2. In (a) the beams emerging from the crystal have gone through a polarizer with transmission axis at approximately 45°. In (b) only the lower beam has gone through a quarter-wave plate with the fast axis at –45°. In (c) both beams have gone through a quarter-wave plate with the fast axis at –45°.

which the two beams separated by the crystal have gone through a film polarizer with the transmission axis at 45°. This superposition can be mathematically presented as

$$\mathbf{Z}_a = \frac{1}{\sqrt{2}}\mathbf{Z}_{45}\mathbf{Z}_H + \frac{e^{i\phi}}{\sqrt{2}}\mathbf{Z}_{45}\mathbf{Z}_V = \mathbf{Z}_{45}\mathbf{Z}_0. \qquad (5)$$

And, as $\mathbf{Z}$ matrices commute [9],

$$\mathbf{M}_a = \mathbf{Z}_a\mathbf{Z}_a^* = \mathbf{M}_{45}\mathbf{M}_0 = \begin{pmatrix} 1 & 0 & \cos\phi & -\sin\phi \\ 0 & 0 & 0 & 0 \\ 1 & 0 & \cos\phi & -\sin\phi \\ 0 & 0 & 0 & 0 \end{pmatrix}, \quad (6)$$

where $\mathbf{M}_{45}$ is the MM of the polarizer with the transmission axis at 45°.

In Fig. 3(b) the vertically polarized beam emerging from the crystal has traversed a quarter-wave plate with the fast axis at –45°. This superposition can be presented as

$$\mathbf{Z}_b = \frac{1}{\sqrt{2}}\mathbf{Z}_H + \frac{e^{i\phi}}{\sqrt{2}}\mathbf{Z}_R\mathbf{Z}_V,$$

$$\text{with } \mathbf{Z}_R = \frac{1}{\sqrt{2}}\begin{pmatrix} 1 & 0 & i & 0 \\ 0 & 1 & 0 & -1 \\ i & 0 & 1 & 0 \\ 0 & 1 & 0 & 1 \end{pmatrix}, \qquad (7)$$

$$\mathbf{M}_b = \mathbf{Z}_b\mathbf{Z}_b^* = \begin{pmatrix} 1 & 0 & -\sin\phi/\sqrt{2} & -\cos\phi/\sqrt{2} \\ 1/2 & 1/2 & -\sin\phi/\sqrt{2} & -\cos\phi/\sqrt{2} \\ 0 & 0 & \cos\phi/\sqrt{2} & -\sin\phi/\sqrt{2} \\ -1/2 & 1/2 & \sin\phi/\sqrt{2} & \cos\phi/\sqrt{2} \end{pmatrix}. \quad (8)$$

In Fig. 3(c) the two beams emerging from the crystal have gone though a quarter-wave plate with the fast axis at –45°. This superposition can be presented as

$$\mathbf{Z}_c = \frac{1}{\sqrt{2}}\mathbf{Z}_R\mathbf{Z}_H + \frac{e^{i\phi}}{\sqrt{2}}\mathbf{Z}_R\mathbf{Z}_V = \mathbf{Z}_R\mathbf{Z}_0, \qquad (9)$$

and the Mueller matrix is

$$\mathbf{M_c} = \mathbf{Z}_c\mathbf{Z}_c^* = \mathbf{M}_R\mathbf{M}_0 = \begin{pmatrix} 1 & 0 & 0 & 0 \\ 0 & 0 & -\sin\phi & -\cos\phi \\ 0 & 0 & \cos\phi & -\sin\phi \\ 0 & 1 & 0 & 0 \end{pmatrix}. \quad (10)$$

All the above results concern the coherent superposition and the measured MMs are, within the experimental uncertainty, non-depolarizing. One way to reduce the coherence of these measurements is to increase the size of the pinhole, so that the fringes cannot be well resolved. To describe this partially coherent case we may use Eq. (1) to write

$$\mathbf{M} = \frac{1}{2}\mathbf{M}_H + \frac{1}{2}\mathbf{M}_V + \frac{\langle e^{-i\phi(x,y)}\rangle}{2}\mathbf{Z}_V\mathbf{Z}_H^* + \frac{\langle e^{i\phi(x,y)}\rangle}{2}\mathbf{Z}_H\mathbf{Z}_V^*,$$
$$(11)$$

where $\phi(x, y)$ makes explicit the dependence of the phase with the position in the space and

$$\langle e^{\pm i\phi(x,y)}\rangle = \frac{1}{A_P}\int_{A_P} e^{\pm i\phi(x,y)}\mathrm{d}S. \qquad (12)$$

This surface integral extends over the area of the pinhole, A_P. Small pinholes provide good spatial resolution that translate in coherent measurements, but if the pinhole size increases, the phase variations are averaged over the measurement area leading to partially coherent or incoherent results that exhibit depolarization effects [8]. In general, when the spatial resolution is poor, several periods of fringes will be averaged thus giving $\langle e^{\pm i\phi(x,y)}\rangle \approx 0$ and only the two first terms of Eq. (11) will remain. The partially coherent experimental results can be likewise interpreted using the classic Jones and K-matrix formalism from [4].

In Fig. 4 we study the variation of the measurement as a function of the spatial resolution. The initial mapping was made in the experimental setup of Fig. 1 with a 30 μm pinhole over an area of 2.3×3.67 mm^2 in order to collect several periods of fringes. No depolarization is observed (depolarization index, *DI*, equal to 1 [11]) in this image. In the second map, we have done 8×8 binning, which is approximately equivalent to using a pinhole with a diameter of 240 μm. With this lateral resolution it is no longer possible to resolve the fringes and the depolarization is maximum in a rather thin region at the middle of the image. In this region the intensity of the two superposing beams is roughly the same (i.e., 50%–50% superposition) while for points above and below this region one of the beams clearly predominates over the other. In the last map we have averaged all pixels of the map, which is roughly equivalent to a measurement without a pinhole. The poor spatial resolution (~3 mm) leads to an incoherent result that is approximately given by the convex sum of the MMs of a
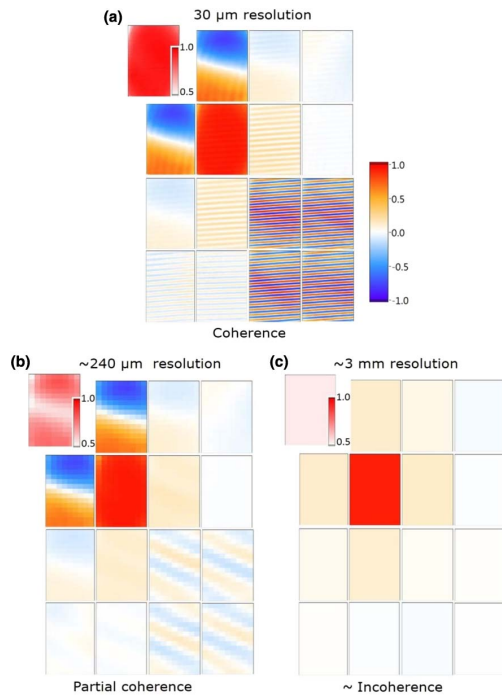
Fig. 4. Spatial evolution of the normalized MM in a region of 2.30×3.67 mm^2 for different spatial resolutions. In the top left corner of each MM appears the depolarization index, *DI* [11].

horizontal and vertical polarizer [Eq. (11) with truncated coherence terms].

For the Mueller matrices displayed in Figs. 2 and 3, interference fringes will not be visible in the overall transmitted intensity when illuminating with unpolarized light. This is in agreement with the third Fresnel–Arago law of interference [5,6]. However in [8] we showed that, when the two superposing **Z** matrix states are equal, the resulting MM will be globally scaled by a factor that depends on their phase difference:

$$\mathbf{M}' = \mathbf{ZZ}^*(1 + \cos\phi) = \mathbf{M}(1 + \cos\phi), \qquad (13)$$

indicating that, in this case, interference fringes would be observed for any incoming Stokes vector. To study this situation we set a new experiment in calcite (outside of the polarimeter) to image with a camera the interference fringes generated for different superpositions of **Z** states. Here, to avoid the effects of laser speckle in the captured images, we used a monochromatized Xe lamp as a light source. The results are shown in Fig. 5. In Fig. 5(a) (that corresponds to the same type of superposition as in Fig. 2) no interference fringes are detected, but they become visible [Fig. 5(b)] when two polarizers at 45° are added at each side of the calcite crystal, because $\mathbf{Z}_{45}\mathbf{Z}_H\mathbf{Z}_{45} = \mathbf{Z}_{45}\mathbf{Z}_V\mathbf{Z}_{45}$ and Eq. (13) holds. This situation makes the experiment completely analog to Young's double-slit experiment, as discussed in [7]. In Fig. 5(c) the first polarizer is turned to –45° and, as in this configuration $\mathbf{Z}_{45}\mathbf{Z}_H\mathbf{Z}_{-45} = -\mathbf{Z}_{45}\mathbf{Z}_V\mathbf{Z}_{-45}$ the interference fringes are similar to those in Fig. 5(b) but shifted by 180°. In this case, this additional phase shift, which is different from ϕ, can be understood as a
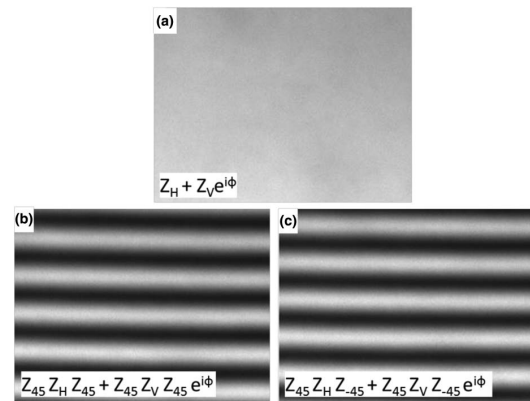
Fig. 5. Intensity of the transmitted beam, as seen with a camera, for the superpositions indicated at the bottom of each panel.

Pancharatman phase [12], i.e., it is a geometrical phase that depends on the trajectory of the polarization state in the Poincaré sphere.

In this Letter we have described an alternative version of Young's experiment in which coherent light is sent through a calcite crystal that separates the photons by their polarization. The two beams are then let to superpose and this recombined beam is used to measure the MM of the system. To our knowledge this is the first time that a version of Young's experiment has been experimentally analyzed with Mueller polarimetry. The experimental results are easily described by our recent formalism of coherence and polarization. This work demonstrates that by using coherent light and having a macroscopic control of the phase difference between two beams it is possible to effectively synthesize in the space Mueller–Jones matrices with on-demand optical properties. This method provides a simple pathway to control and modulate spatially the polarization of a light beam from combinations of two basic optical elements with a well-controlled phase difference.

REFERENCES

1. H. F. Hazebroek and A. A. Holscher, J. Phys. E **6**, 822 (1973).
2. C. H. Lin, C. Chou, and K. S. Chang, Appl. Opt. **29**, 5159 (1990).
3. F. Barroso, S. Bosch, N. Tort, O. Arteaga, J. Sancho-Parramon, E. Jover, E. Bertran, and A. Canillas, Thin Solid Films **519**, 2801 (2011).
4. R. Ossikovski and K. Hingerl, Opt. Lett. **41**, 4044 (2016).
5. F. Arago and A. Fresnel, Ann. Chim. Phys. **10**, 288 (1819).
6. R. Barakat, J. Opt. Soc. Am. A **10**, 180 (1993).
7. R. Ossikovski, O. Arteaga, J. Vizet, and E. Garcia-Caurel, J. Opt. Soc. Am. A **34**, 1309 (2017).
8. E. Kuntman, M. A. Kuntman, J. Sancho-Parramon, and O. Arteaga, Phys. Rev. A **95**, 063819 (2017).
9. E. Kuntman, M. Ali Kuntman, and O. Arteaga, J. Opt. Soc. Am. A **34**, 80 (2017).
10. O. Arteaga, J. Freudenthal, B. Wang, and B. Kahr, Appl. Opt. **51**, 6805 (2012).
11. J. J. Gil and R. Ossikovski, *Polarized Light and the Mueller Matrix Approach* (CRC Press, 2016).
12. S. Pancharatman, Proc. Indian Acad. Sci. A **44**, 247 (1956).

Light scattering by coupled oriented dipoles: Decomposition of the scattering matrix

M. Ali Kuntman,[1] Ertan Kuntman,[2] Jordi Sancho-Parramon,[3] and Oriol Arteaga[2,4,*]

[1]*Independent researcher, Ankara, Turkey*
[2]*Departament de Física Aplicada, IN2UB, Enphocamat Group, Universitat de Barcelona, C/ Martí i Franquès 1, Barcelona 08030, Spain*
[3]*Rudjer Boskovic Institute, Bijenicka cesta 54, 10000, Zagreb, Croatia*
[4]*LPICM, École Polytechnique, Université Paris-Saclay, 91128 Palaiseau, France*

We study the optical response of two coupled oriented dipoles with the dimer axis perpendicular to the wave vector of light by analyzing how their scattering matrix can be decomposed. The scattering matrix can be written as a linear combination of three terms with a clear physical meaning: one for each particle and another that is responsible for the coupling and that vanishes for noninteracting or distant particles. We show that the interaction term may generate optical activity for certain scattering directions and that this effect manifests itself mostly in the near field. This simple and intuitive theory based on matrix and vector states of oriented dipoles also describes hybridization processes and Fano resonances. The decomposition method can be also formulated in terms of a hybrid basis that allows us to quantitatively determine the individual contribution of the in-phase and out-of-phase coupling modes to the overall intensity. Our method can help to understand the optical response of more complex nanostructures that can be decomposed into dipole terms. The results are illustrated in gold nanoantenna dimers which exhibit a strong dipolar resonance.

I. INTRODUCTION

Dipole interactions occur when two dipoles interact with each other through the space. For example dipolar interactions are responsible for electrostatic interactions inside molecules or between molecules which have permanent dipole(s): The partially negative portion of one polar molecule can be attracted to the partially positive portion of a second polar molecule. Dipole interactions are also very important for optical interactions in nanoscale particles. Since the oscillating electric field of a light wave acts on the charges of a particle, causing them to oscillate at the same frequency, the particle becomes a small radiating dipole whose radiation is seen as scattered light.

In optics, the interaction between induced dipoles is usually treated considering their mutual interaction potential [1]. This approach has also been generalized for the calculation of the light scattering by arbitrarily shaped particles, as a numerical technique known as the coupled dipole method or discrete dipole approximation (DDA) [2–4]. The method is based on a finite volume discretization of the scattering object, in which each volume element is modeled by an oscillating electric dipole that acts as receiver and emitter of electromagnetic radiation. Each dipole of the collection interacts with all the others, so that the fields at each dipole are determined by the incident field and interactions among all the dipoles of the collection. Similar approaches can also be used to study radiative heat transfer in systems of multiple dipoles [5].

In this paper we study analytically the simpler but relevant case of interaction between two oriented dipoles that form a dipole dimer. Despite that there are in the literature several

methods (both analytic and numeric) to predict the optical response of coupled dipoles [2,6–9], usually these methods provide the overall optical response and do not permit us to distinguish the contribution of the individual dipoles from the coupling contribution. We propose a study of the dipole interaction based on a decomposition of the scattering matrix. In our model the two dipoles are excited in phase by the incident wave that drives the system and we consider that the polarizabilities of the two particles are fully anisotropic, i.e., they can only be polarized in a predefined direction, in contrast to the classical consideration of a dimer made of isotropic spherical particles [10–12]. The existence of well defined directions of polarization brings our optical scattering problem closer to real nanostructures or metamaterials, where the direction of polarization is given by the morphology and orientation of the objects. The simplest example perhaps is the interaction between two plasmonic nanoantennas (a plasmonic dimer). Dipolar nano-objects (e.g., nanoparticles, nanorods, etc.) are generally regarded as most elementary components to build more complex composite nanostructures [13–16]. They are also the simplest "plasmonic molecules" and the possibility of controlling and measuring their chiroptical properties has created a growing interest in the usage of plasmonic dimers in biological applications such as DNA based nanostructures [17] or intracellular localization [18].

Our decomposition shows that the scattering matrix of oriented dipole dimers can be written as a linear combination of three scattering matrix terms with a clear physical meaning: one for each particle and the remaining one for the interaction. Despite the simplicity of the theory, it allows us to understand subtle effects such as the emergence of optical activity in certain achiral dimer configurations. Our decomposition method also allows for an easy representation of

*oarteaga@ub.edu

hybridization processes and of Fano resonances in anisotropic plasmonic nanostructures. In particular we show that the decomposition can be also formulated in terms of a hybrid basis which allows us to determine the individual contribution of each hybrid mode to the overall intensity. Finally, we apply our decomposition method to study the scattering matrix of oriented gold nanoantenna dimers in the spectral region where they exhibit a strong dipolar resonance. With this method we can quantify the relative contribution of coupled modes in the nanoantenna dimer and analyze how the interaction modifies the optical properties of the individual nanoantennas.

II. GENERAL FRAMEWORK

The induced electric dipole moment vector, $\mathbf{p}$, on a particle is proportional to the corresponding incident electric field, $\mathbf{E}_0(\mathbf{r})$:

$$\mathbf{p} = \varepsilon\tilde{\boldsymbol{\alpha}}\mathbf{E_0}(\mathbf{r}), \tag{1}$$

where $\tilde{\boldsymbol{\alpha}}$ is the electric polarizability of the particle, and ε is the permittivity of the medium where the dipole is located. When we put two particles close to each other we have to consider mutual interactions. In this case, each one of the dipoles will experience the induced field of the other dipole. This coupling effect can be taken into account to find the actual dipole of each particle as follows [14]:

$$\mathbf{p_1} = \tilde{\boldsymbol{\alpha}_1}\varepsilon\mathbf{E_0}(\mathbf{r_1}) + \tilde{\boldsymbol{\alpha}_1}k^2\bar{\bar{\mathbf{G}}}_\mathbf{E}(\mathbf{r_1} - \mathbf{r_2}) \cdot \mathbf{p_2}, \tag{2}$$

$$\mathbf{p_2} = \tilde{\boldsymbol{\alpha}_2}\varepsilon\mathbf{E_0}(\mathbf{r_2}) + \tilde{\boldsymbol{\alpha}_2}k^2\bar{\bar{\mathbf{G}}}_\mathbf{E}(\mathbf{r_2} - \mathbf{r_1}) \cdot \mathbf{p_1}, \tag{3}$$

where $\bar{\bar{\mathbf{G}}}_\mathbf{E}$ is the free-space electric dyadic Green's function, k is the wave number, and $\tilde{\boldsymbol{\alpha}_1}$, $\tilde{\boldsymbol{\alpha}_2}$ are the polarizability tensors of the associated particles. Explicit form of dyadic Green's function is given by

$$\bar{\bar{\mathbf{G}}}_\mathbf{E}(\mathbf{r}) \cdot \mathbf{p} = \left[\left(1 + \frac{i}{kr} - \frac{1}{k^2r^2}\right)\mathbf{p}\right.$$
$$\left. + \left(-1 - \frac{3i}{kr} + \frac{3}{k^2r^2}\right)(\mathbf{u_r} \cdot \mathbf{p})\mathbf{u_r}\right]g(r), \tag{4}$$

where $\mathbf{u_r}$ is the unit vector along $\mathbf{r}$ and $g(r) = e^{ikr}/4\pi r$. The notation can be simplified if we let:

$$A(r) \equiv \left(1 + \frac{i}{kr} - \frac{1}{k^2r^2}\right)g(r), \tag{5a}$$

$$B(r) \equiv \left(-1 - \frac{3i}{kr} + \frac{3}{k^2r^2}\right)g(r). \tag{5b}$$

Thus,

$$\bar{\bar{\mathbf{G}}}_\mathbf{E}(\mathbf{r}) \cdot \mathbf{p} = A(r)\mathbf{p} + B(r)(\mathbf{u_r} \cdot \mathbf{p})\mathbf{u_r}. \tag{6}$$

Now let us consider the scattered far field at an observation point z. The total scattered field can be considered as a sum of the fields due to the interacting dipoles.

$$E_{\text{scat},j} = \frac{k^2}{\varepsilon}[(\bar{\bar{\mathbf{G}}}_E(\mathbf{r}_f - \mathbf{r_1}) \cdot \mathbf{p_1})_j + (\bar{\bar{\mathbf{G}}}_E(\mathbf{r}_f - \mathbf{r_2}) \cdot \mathbf{p_2})_j], \tag{7}$$

where $j = x, y, z$. Note, however, that the z component vanishes for a far-field detector in the z axis.

In the following we will show that, according to the above-mentioned dipole-dipole interaction scheme, the total 2×2 scattering matrix (or Jones matrix) of the whole process can be written as a linear combination of three Jones matrices, two of them corresponding to the usual Jones matrices of noninteracting dipoles and the third one being the Jones matrix due to the interaction. The interaction Jones matrix is scaled by a factor which is a function of the distance between the interacting dipoles so that for distant dipoles this coupling term consistently vanishes.

III. DECOMPOSITION OF THE SCATTERING MATRIX OF THE COUPLED DIPOLE SYSTEM

Let us consider a coherent parallel combination of interacting dipoles as given in Fig. 1. d is the distance between the dipoles, which are located in the same z plane, and are excited simultaneously by a plane wave. According to the figure the unit vectors $\mathbf{u}(\mathbf{r_2} - \mathbf{r_1})$ and $\mathbf{u}(\mathbf{r_1} - \mathbf{r_2})$ will be

$$\mathbf{u}(\mathbf{r_2} - \mathbf{r_1}) = (0, -1, 0), \quad \mathbf{u}(\mathbf{r_1} - \mathbf{r_2}) = (0, 1, 0). \tag{8}$$

We consider that the polarizability of the dipoles is fully anisotropic, i.e., they can only polarize along a certain direction. The polarizability tensor of each dipole, $\tilde{\boldsymbol{\alpha}_1}$ and $\tilde{\boldsymbol{\alpha}_2}$, will be:

$$\tilde{\boldsymbol{\alpha}_i} = \alpha_i\begin{pmatrix} a_i & b_i \\ b_i & c_i \end{pmatrix} \tag{9}$$

with $i = 1, 2$. α_1 are α_2 are the Lorentzian polarizabilities of the dipoles and $\tilde{\boldsymbol{\alpha}_1}$, $\tilde{\boldsymbol{\alpha}_2}$ are given by the following rotation:

$$\tilde{\boldsymbol{\alpha}_i} = \mathbf{R}(-\phi_i)\alpha_i\begin{pmatrix} 1 & 0 \\ 0 & 0 \end{pmatrix}\mathbf{R}(\phi_i), \tag{10}$$

where

$$\mathbf{R}(\phi) = \begin{pmatrix} \cos\phi & \sin\phi \\ -\sin\phi & \cos\phi \end{pmatrix}, \tag{11}$$

and ϕ_1 and ϕ_2 are the rotation angles as defined in Fig. 1. Then

$$a_i = \cos^2(\phi_i), \tag{12a}$$

$$b_i = \cos(\phi_i)\sin(\phi_i), \tag{12b}$$
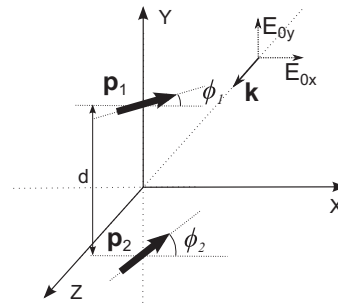
$$c_i = \sin^2(\phi_i). \tag{12c}$$

FIG. 1. Scheme of the geometry. Dimer axis and dipole vectors are perpendicular to the direction of propagation of incident light.

From Eqs. (2) and (3) we can calculate the dipole vectors, whose components are given by:

$$p_{1x} = \varepsilon\alpha_1 a_1 E_{1x} + \varepsilon\alpha_1 b_1 E_{1y} + \alpha_1 a_1 \delta_1 p_{2x} + \alpha_1 b_1 \delta_2 p_{2y},$$
(13a)

$$p_{1y} = \varepsilon\alpha_1 b_1 E_{1x} + \varepsilon\alpha_1 c_1 E_{1y} + \alpha_1 b_1 \delta_1 p_{2x} + \alpha_1 c_1 \delta_2 p_{2y},$$
(13b)

$$p_{2x} = \varepsilon\alpha_2 a_2 E_{2x} + \varepsilon\alpha_2 b_2 E_{2y} + \alpha_2 a_2 \delta_1 p_{1x} + \alpha_2 b_2 \delta_2 p_{1y},$$
(13c)

$$p_{2y} = \varepsilon\alpha_2 b_2 E_{2x} + \varepsilon\alpha_2 c_2 E_{2y} + \alpha_2 b_2 \delta_1 p_{1x} + \alpha_2 c_2 \delta_2 p_{1y},$$
(13d)

where $k^2 A \equiv \delta_1$, $k^2(A + B) \equiv \delta_2$. We can solve these coupled equations for the components of the dipole vectors:

$$p_{1x} = \varepsilon\alpha_1 C_1 \frac{\mathcal{E}_1 + \alpha_2 \Delta \mathcal{E}_2}{1 - \alpha_1\alpha_2\Delta^2},$$
(14)

$$p_{1y} = \varepsilon\alpha_1 S_1 \frac{\mathcal{E}_1 + \alpha_2 \Delta \mathcal{E}_2}{1 - \alpha_1\alpha_2\Delta^2},$$
(15)

$$p_{2x} = \varepsilon\alpha_2 C_2 \frac{\mathcal{E}_2 + \alpha_1 \Delta \mathcal{E}_1}{1 - \alpha_1\alpha_2\Delta^2},$$
(16)

$$p_{2y} = \varepsilon\alpha_2 S_2 \frac{\mathcal{E}_2 + \alpha_1 \Delta \mathcal{E}_1}{1 - \alpha_1\alpha_2\Delta^2},$$
(17)

where

$$C_i = \cos\phi_i, \quad S_i = \sin\phi_i,$$
(18)

$$\mathcal{E}_i = C_i E_{ix} + S_i E_{iy},$$
(19)

and

$$\Delta = C_1 C_2 \delta_1 + S_1 S_2 \delta_2.$$
(20)

Note that Δ is the only term that is related to coupling. A far field detection point, z, has characteristic vector $\mathbf{r}_f$ with a module much larger than those of the dipole vectors: $r_f \gg r_1, r_2$. In these conditions $\mathbf{r}_f$ will be perpendicular to $\mathbf{r}_1$ and $\mathbf{r}_2$,

$$(\bar{\bar{\mathbf{G}}}_E(\mathbf{r}_f - \mathbf{r}_i) \cdot \mathbf{p}_i)_j = \frac{e^{ikz}}{4\pi z} p_{ij},$$
(21)

where $i = 1, 2$ and $j = x, y$. If the detection point is equidistant to the dipoles we simply get:

$$E_{\text{scat}x} = \beta(p_{1x} + p_{2x}),$$
(22a)

$$E_{\text{scat}y} = \beta(p_{1y} + p_{2y}),$$
(22b)

where

$$\beta = \frac{k^2 e^{ikz}}{4\pi\varepsilon z}.$$
(23)

According to Fig. 1, it is reasonable to assume that $\mathbf{E}_1(r_1) = \mathbf{E}_2(r_2) = \mathbf{E}_0$ as it corresponds to a plane wave propagating in the z direction. Then the scattering problem can be directly formulated with a 2×2 scattering matrix $\mathbf{T}$ that transforms the fields as follows:

$$\begin{pmatrix} E_{\text{scat}x} \\ E_{\text{scat}y} \end{pmatrix} = \begin{pmatrix} T_{11} & T_{12} \\ T_{21} & T_{22} \end{pmatrix} \begin{pmatrix} E_{0x} \\ E_{0y} \end{pmatrix} = \begin{pmatrix} T_{11}E_{0x} + T_{12}E_{0y} \\ T_{21}E_{0x} + T_{22}E_{0y} \end{pmatrix}.$$
(24)

From Eqs. (22a) and (22b) we find that the 2×2 scattering matrix $\mathbf{T}$ can be presented as:

$$\mathbf{T} = \gamma[\alpha_1 \mathbf{J}_1 + \alpha_2 \mathbf{J}_2 + \alpha_1\alpha_2\Delta\mathbf{J}_{\text{int}}],$$
(25)

where $\mathbf{J}_1$, $\mathbf{J}_2$, and $\mathbf{J}_{\text{int}}$ are Jones matrices given by

$$\mathbf{J}_i = \begin{pmatrix} C_i^2 & C_i S_i \\ C_i S_i & S_i^2 \end{pmatrix},$$
(26)

$$\mathbf{J}_{\text{int}} = \begin{pmatrix} 2C_1 C_2 & C_1 S_2 + C_2 S_1 \\ C_1 S_2 + C_2 S_1 & 2S_1 S_2 \end{pmatrix},$$
(27)

and

$$\gamma = \frac{\varepsilon\beta}{1 - \alpha_1\alpha_2\Delta^2}.$$
(28)

γ can be understood as an overall (polarization independent) complex amplitude of scattering. Note that it is also affected by the coupling term Δ.

In Eq. (25), $\mathbf{J}_1$ and $\mathbf{J}_2$ are the Jones matrices of the individual, noninteracting dipoles. As seen in Eq. (26), the scattering matrix of a horizontal ($\phi = 0°$) or vertical ($\phi = 90°$) dipolar particle is diagonal. $\mathbf{J}_{\text{int}}$ is a combined term that contributes only when there is interaction ($\Delta \neq 0$). Therefore, whenever the dipoles are sufficiently separated the contribution of the interaction matrix $\mathbf{J}_{\text{int}}$ will be negligible. It is also possible that still for small separations between the dipoles the system has a vanishing Δ due to their particular orientations in the plane. This happens whenever the dipoles are orthogonal and the line joining the dipole centers is parallel to one of the dipole vectors as, for example, when $\phi_1 = 0°$ and $\phi_2 = 90°$ in Eq. (20). This situation will be discussed in more detail in Sec. III B.

Instead of using 2×2 scattering matrices it is sometimes useful to rearrange the information contained in the scattering matrix in a so-called four-component covariance vector. The covariance vector that corresponds to a Jones matrix is defined as follows:

$$|h\rangle_{\mathbf{J}} = \frac{1}{2} \begin{pmatrix} J_{11} + J_{22} \\ J_{11} - J_{22} \\ J_{12} + J_{21} \\ i(J_{12} - J_{21}) \end{pmatrix},$$
(29)

where J_{ij} are the elements of 2×2 the scattering matrix. We use the standard bra-ket notation of quantum mechanics, where the bra is the Hermitian conjugate of the ket and represented by a row vector. As it was discussed in Refs. [19,20] the outer product $|h\rangle\langle h|$ generates a 4×4 covariance scattering matrix of rank 1 that can be considered as an analog of a pure state in quantum mechanics. In terms of covariance vectors we can, alternatively, write the decomposition in Eq. (25) as:

$$|h\rangle = \gamma[\alpha_1 |h\rangle_1 + \alpha_2 |h\rangle_2 + \alpha_1\alpha_2\Delta|h\rangle_{\text{int}}],$$
(30)

where:

$$|h\rangle_i = \frac{1}{2} \begin{pmatrix} 1 \\ \cos^2(\phi_i) - \sin^2(\phi_i) \\ 2\sin(\phi_i)\cos(\phi_i) \\ 0 \end{pmatrix},$$
(31)

and

$$|h\rangle_{\text{int}} = \begin{pmatrix} \cos(\phi_1 - \phi_2) \\ \cos(\phi_1 + \phi_2) \\ \sin(\phi_1 + \phi_2) \\ 0 \end{pmatrix}. \tag{32}$$

Note that because the matrices in Eqs. (26) and (27) are symmetric, the fourth component of these covariance vectors is always zero. This reads as an absence of circular polarization effects [19,21].

IV. OPTICAL PROPERTIES OF DIMERS OF ANISOTROPIC PARTICLES

The above presented decomposition of the scattering matrix or the covariance vector allows us to study several relevant optical properties characteristic of dipolar dimer systems. In particular, in the next subsections we will use our decomposition method to discuss circular polarization effects, hybrid modes, and Fano resonances. All these are well-known optical properties that have been previously analyzed in the context of dimer systems [6–11,13,22–27]. The advantage of the decomposition method that we have introduced is that it distinguishes the contribution of the individual dipoles from the coupling contribution and that works for dimers of anisotropic particles at any relative orientation in the plane, allowing, for example, the derivation of generalized analytic expressions for the dipole coupling that are a function of the orientation angles.

A. Circular polarization effects

Chiroptical effects with plasmonic dimers have been considered in several recent publications [28–31] as they are relatively easy to fabricate with modern techniques. The geometry considered in most of these works is different from Fig. 1, as they consider two misaligned dipoles in which the dimer axis is completely parallel to the wave vector of light. This is a chiral configuration that gives rise to optical activity in these plasmonic samples. In essence, this corresponds to the coupled oscillator model of Born and Kuhn (Born-Kuhn model) [31,32] which, when applied to a chiral geometry, is the basis for the classical theory of optical activity. This model provides an intuitive way to understand the generation of optical activity (circular dichroism and circular birefringence) in chiral media.

In general, the serial combination of two misaligned particles with a dipolar response leads to circular polarization effects, or chiroptical effects in the far-field detection. This can be intuitively seen by considering the Jones matrix product associated to a sequence of dipolar elements, e.g., $\mathbf{J}_2\mathbf{J}_1$, and transforming it into its associated covariance vector:

$$|h\rangle_{\mathbf{J}_2\mathbf{J}_1} = \begin{pmatrix} \cos(\phi_1 - \phi_2) \\ \cos(\phi_1 + \phi_2) \\ \sin(\phi_1 + \phi_2) \\ i\sin(\phi_1 - \phi_2) \end{pmatrix}, \tag{33}$$

in which the fourth component, associated to these circular effects or chiroptical effects [20,21], is nonvanishing. But this case of serial (sequential) combination of elements is totally different from the geometry given in Fig. 1. In Eqs. (31) and (32) the fourth components of the vectors were zero, which

reads as an absence of circular effect as it could be expected from the achiral geometry of the problem.

However, depending on the location of the observation point, there may exist a varying phase difference between the radiation fields of the dipoles. Earlier, in Eqs. (22a) and (22b) we considered that both dipoles radiate to a point of the far field with the same complex factor β [Eq. (23)], but if the detection point is not equidistant from the dipoles, we have to consider different phases.

$$E_{\text{scatx}} = \beta p_{1x} + \beta' p_{2x}, \tag{34a}$$

$$E_{\text{scaty}} = \beta p_{1y} + \beta' p_{2y}, \tag{34b}$$

where $\beta' = \beta e^{i\chi}$. χ is an additional phase term that accounts for the different optical paths from each dipole to the detector.

In this situation Eq. (25) must be replaced by

$$\mathbf{T} = \gamma[\alpha_1\mathbf{J}_1 + e^{i\chi}\alpha_2\mathbf{J}_2 + \alpha_1\alpha_2\Delta\mathbf{J}'_{\text{int}}], \tag{35}$$

where

$$\mathbf{J}'_{\text{int}} = \begin{pmatrix} C_1C_2(1 + e^{i\chi}) & C_1S_2 + C_2S_1e^{i\chi} \\ C_1S_2e^{i\chi} + C_2S_1 & S_1S_2(1 + e^{i\chi}) \end{pmatrix}. \tag{36}$$

Then the covariance vector associated with this interaction matrix is:

$$|h\rangle'_{\text{int}} = \begin{pmatrix} \cos(\phi_1 - \phi_2)(1 + e^{i\chi}) \\ \cos(\phi_1 + \phi_2)(1 + e^{i\chi}) \\ \sin(\phi_1 + \phi_2)(1 + e^{i\chi}) \\ -i\sin(\phi_1 - \phi_2)(1 - e^{i\chi}) \end{pmatrix}, \tag{37}$$

where the fourth component now is different from zero if the dipoles are not parallel to each other ($\phi_1 \neq \phi_2$). Note that when $\chi = \pi$ only the fourth component of $|h\rangle'_{\text{int}}$ survives and the interaction term displays pure circular effects.

This emergence of chiroptical signals from achiral systems is an interferencelike phenomenon that arises when there is a phase (path) difference to the observation point. Translating the point of detection will also modify the values of optical activity signals, eventually also switching their signs. There are two other important aspects that need to be highlighted:

(i) The effect may manifest itself only for interacting dipoles. In noninteracting systems ($\Delta = 0$) with the geometry of Fig. 1, the superposition of the dephased dipolar scattering contributions is not sufficient to generate chiroptical effects in the scattering matrix. Note that the only matrix modified in Eq. (35) is the interaction matrix.

(ii) This effect is not observed in the far field unless large scattering angles are considered. When the detection distance is large compared to the separation of the dipoles d, the phase difference will be given by $\chi = 2\pi dx/\lambda D$ [33], where D is the distance between the plane of the dipoles and the parallel plane that includes the detector, λ is the wavelength, and x is the position of the observation point along the axis parallel to the line connecting the two point dipoles. As in the far field $D \gg d$, this phase difference tends to be negligible in far field realizations unless one considers sufficiently large scattering angles (implying large x).

We believe that the progress in the near field microscopy offers new perspectives for exploiting this effect for biosensing.
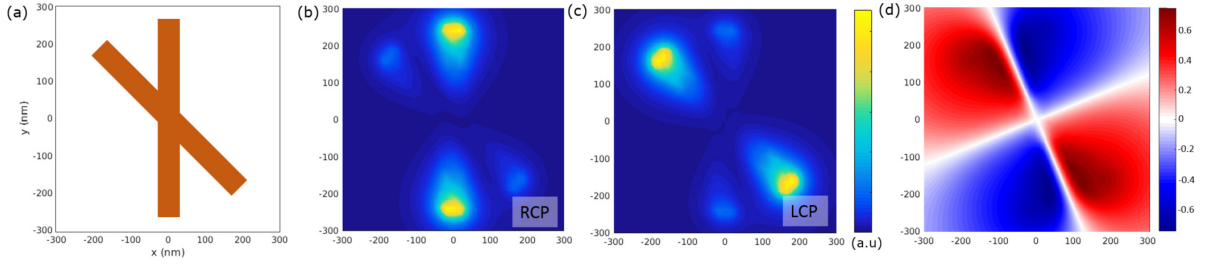
FIG. 2. Simulated response of two equal gold nanoantennas forming a cross by $45°$. (a) shows the geometry and dimensions of the cross structure, which has a thickness of 50 nm. (b) and (c) show the scattered field $|E|^2$ in a plane at 10 nm above the cross when the structure is illuminated with a plane wave of 1640 nm with right-and left-circular polarizations, respectively. In (d) we calculate the ratio $(I_{LCP} - I_{RCP})/(I_{LCP} + I_{RCP})$.

For example, this means that the near-field scattering fingerprint for such an arrangement of dipoles can be drastically modified by only adjusting the handedness of the incoming polarization, but without substantially affecting the far-field response. To illustrate this we have simulated the near field scattering of two crossed thin strips of gold with the nanoantenna geometry shown in Fig. 2(a). The simulation has been made with the boundary element method (BEM) [34,35] considering light with a wavelength that corresponds to the dipolar resonance of nanoantennas with this geometry (1640 nm). The plane wave is polarized in the xy plane and propagates along $+z$. The obvious differences between Fig. 2(b) and Fig. 2(c) show that the near field response of the structure (the figures show it in a plane 10 nm above the nanostructure) is strongly sensitive to the handedness of the incoming circular polarization, as it is anticipated by Eq. (37).

The ratio $(I_{LCP} - I_{RCP})/(I_{LCP} + I_{RCP})$, shown in Fig. 2(c), quantifies the differential scattering between left- and right-handed circular polarization. Note that it vanishes along two well defined orthogonal lines that cross the center of the nanostructure. These points correspond to zones that are equidistant from both nanoantennas, and there is no added phase χ ($\chi = 0$). As we have previously pointed out, the strong circular effects [Fig. 2(c)] wash out in the far field because χ becomes negligible. In fact we already gave the far field response for this nanostructure in terms of the Mueller matrix in Ref. [19] and it was not sensitive to the handedness of the incoming polarization.

The emergence of chiroptical signals in certain systems with achiral geometries has been previously considered in molecules [36,37], crystals [38], and metamaterials [39,40]. Perhaps the most paradigmatic example is the water molecule [37] (point group C_{2v}) where, due to the difference in electronegativity between the oxygen (O) and hydrogen (H) atoms, there is a dipole moment pointing from each H to the O. These two permanent dipoles are misaligned by $104.45°$ and they are both in the same plane, so it is the same type of geometry that we have considered. Our results can also be used to understand, at least qualitatively, the emergence of chiroptical signals in such planar systems for certain directions of observation. In fact optical activity in these achiral molecules and crystals is determined by an optical activity tensor, that when plotted, has the same twofold symmetry with alternating signs as the one displayed in Fig. 2(d).

B. Hybrid modes

Let us consider a coupling process as given in Fig. 1. Equations (13) can be rearranged as follows:

$$p_{1x} - \alpha_1 a_1 \delta_1 p_{2x} - \alpha_1 b_1 \delta_2 p_{2y} = \varepsilon \alpha_1 a_1 E_{1x} + \varepsilon \alpha_1 b_1 E_{1y}$$
(38a)

$$p_{1y} - \alpha_1 b_1 \delta_1 p_{2x} - \alpha_1 c_1 \delta_2 p_{2y} = \varepsilon \alpha_1 b_1 E_{1x} + \varepsilon \alpha_1 c_1 E_{1y}$$
(38b)

$$p_{2x} - \alpha_2 a_2 \delta_1 p_{1x} - \alpha_2 b_2 \delta_2 p_{1y} = \varepsilon \alpha_2 a_2 E_{2x} + \varepsilon \alpha_2 b_2 E_{2y}$$
(38c)

$$p_{2y} - \alpha_2 b_2 \delta_1 p_{1x} - \alpha_2 c_2 \delta_2 p_{1y} = \varepsilon \alpha_2 b_2 E_{2x} + \varepsilon \alpha_2 c_2 E_{2y}.$$
(38d)

Here we consider p_{1x}, p_{1y}, p_{2x}, and p_{2y} as independent variables. Right hand side of the equations are the external fields, i.e., the driving forces of the dipoles, and we assume that the dipoles can be described as Lorentzian oscillators with a profile of the form:

$$\alpha_i(\omega) = \frac{\eta_i \omega_i}{\omega_i^2 - \omega^2 - i \Gamma_i \omega},$$
(39)

where ω is the frequency of the incoming radiation, ω_i is the frequency of resonance, η_i is the amplitude of oscillation which depends on the particle size, and Γ_i is the damping. For the analytical calculus of this section we will assume that there is no damping ($\Gamma_i = 0$).

The coupled Eqs. (38) can be written as a matrix equation:

$$\mathbf{AP} = \mathbf{E},$$
(40)

where $\mathbf{P}$ is a four-dimensional vector consisting of the components of the dipole vectors $\mathbf{p}_1$ and $\mathbf{p}_2$, $\mathbf{E}$ is also a four-dimensional vector associated with the right hand side of the coupled equations, and $\mathbf{A}$ is the following matrix:

$$\mathbf{A} = \begin{pmatrix} \lambda_1 & 0 & -\delta_1 a_1 & -\delta_2 b_1 \\ 0 & \lambda_1 & -\delta_1 b_1 & -\delta_2 c_1 \\ -\delta_1 a_2 & -\delta_2 b_2 & \lambda_2 & 0 \\ -\delta_1 b_2 & -\delta_2 c_2 & 0 & \lambda_2 \end{pmatrix},$$
(41)

where $\lambda_1 = 1/\alpha_1$, $\lambda_2 = 1/\alpha_2$. This problem can be treated as the well known problem of coupled mechanical (harmonic) oscillators [41]. Here the components of the electric dipole

vectors play the role of position coordinates and the external fields are associated with the driving forces. Normal modes of the coupled system of oscillating dipoles can be found by equating the determinant of matrix **A** to zero, which leads to the equation:

$$\lambda_1^2 \lambda_2^2 - \Delta^2 \lambda_1 \lambda_2 = 0, \qquad (42)$$

where Δ is defined in Eq. (20).

There are four roots. Two of them are trivially given by $\lambda_1 \lambda_2 = 0$, i.e., either λ_1 or λ_2 is zero. Nonzero roots are

$$\lambda_1 \lambda_2 = \Delta^2. \qquad (43)$$

Note that this is also the condition that makes the denominator of γ [Eq. (28)] vanish, so that there is a resonance in the scattering [Eq. (25)]. We can analytically examine the conditions for this resonance if the Lorentzian profile given in Eq. (39) (without damping) is assumed for the polarizabilities:

$$\lambda_1 \lambda_2 = \left(\frac{\omega_1^2 - \omega^2}{\eta_1 \omega_1^2} \right)\left(\frac{\omega_2^2 - \omega^2}{\eta_2 \omega_2^2} \right) = \Delta^2. \qquad (44)$$

We solve now for ω. Roots with $\lambda_1 \lambda_2 = 0$ give $\omega = \omega_1$ and $\omega = \omega_2$ that correspond to trivial cases with no interaction between the dipoles. Nonzero roots give the frequencies for two hybridized modes:

$$\omega^{\pm} = \sqrt{\frac{\omega_1^2 + \omega_2^2 \pm \sqrt{(\omega_1^2 - \omega_2^2)^2 + 4\omega_1^2\omega_2^2 \eta_1 \eta_2 \Delta^2}}{2}}. \quad (45)$$

If the dipoles are identical ($\alpha_1 = \alpha_2$) we have

$$\omega^{\pm} = \omega_0 \sqrt{1 \pm \eta \Delta}. \qquad (46)$$

For any pair of angles, ϕ_1 and ϕ_2, we always have two hybrid modes. For example, if we choose $\phi_1 = \phi_2 = 0$

$$\omega^{\pm} = \omega_0 \sqrt{1 \pm \eta \delta_1}, \qquad (47)$$

if we choose $\phi_1 = \phi_2 = \frac{\pi}{2}$

$$\omega^{\pm} = \omega_0 \sqrt{1 \pm \eta \delta_2}. \qquad (48)$$

The strength of the coupling may be evaluated with the aid of the parameter

$$\omega_{cc} = \sqrt{\eta_1 \eta_2 \omega_1 \omega_2 \Delta^2}. \qquad (49)$$

If the coupling is weak ($\omega_{cc} \ll |\omega_1 - \omega_2|$), the solutions of Eq. (45) reduce to

$$\omega^{+} \approx \omega_1 + \frac{\omega_{cc}^2}{4(\omega_1 - \omega_2)}, \qquad (50)$$

$$\omega^{-} \approx \omega_2 - \frac{\omega_{cc}^2}{4(\omega_1 - \omega_2)}, \qquad (51)$$

and in the case of strong coupling ($\omega_{cc} \gg |\omega_1 - \omega_2|$), the approximate solutions are

$$\omega^{\pm} \approx \frac{\omega_1 + \omega_2}{2} \pm \frac{\omega_{cc}}{2}. \qquad (52)$$

These formulas coincide with the resonances predicted by the plasmon hybridization model for two plasmonic particles given in Ref. [42], which the advantage that here we know how the coupling parameter ω_{cc} varies with the dipole orientation.

Figure 3 shows the switch of the energy of resonance for two coupled dipoles with equal polarizabilities ($\alpha_1 = \alpha_2$) as a function of the distance between them for six different geometrical arrangements. Their hybridization can be evaluated with Eq. (46). In both, a ($\phi_1 = \phi_2 = 0°$) and b ($\phi_1 = \phi_2 = 90°$), particles oscillate in phase but a corresponds to a π-type stacking (dimer axis perpendicular to the dipole direction), while b is a σ-type stacking (dimer axis parallel to the dipole direction). In this case the shift in energy is stronger than in a and the resonance evolves to lower frequencies. Note that for a and b, the incoming plane wave can only excite one of the two hybrid modes, the in-phase mode. The energy splitting of the in-phase and out-of-phase modes for these two cases are schematically shown in Fig. 4. The scattering matrices corresponding to these two cases (assuming the more general case $\alpha_1 \neq \alpha_2$) are:

(i) *Case (a)*, dipoles perpendicular to the dimer axis:

$$\mathbf{T}_a = \varepsilon\beta \frac{\alpha_1 + \alpha_2 + 2\alpha_1\alpha_2\delta_1}{1 - \alpha_1\alpha_2\delta_1^2}\begin{pmatrix} 1 & 0 \\ 0 & 0 \end{pmatrix}, \qquad (53)$$

(ii) *Case (b)*, dipoles parallel to the dimer axis:

$$\mathbf{T}_b = \varepsilon\beta \frac{\alpha_1 + \alpha_2 + 2\alpha_1\alpha_2\delta_2}{1 - \alpha_1\alpha_2\delta_2^2}\begin{pmatrix} 0 & 0 \\ 0 & 1 \end{pmatrix}. \qquad (54)$$

If only the near-field contribution of A and B (i.e., only the d^{-3} term) is retained in the coupling parameters δ_1 and δ_2, we have that $\delta_1 \propto -1/d^3$ and $\delta_2 \propto 2/d^3$, and we may define the polarizabilities of the coupled systems for cases (a) and (b), respectively, as follows:

$$\alpha_a = \frac{\alpha_1 + \alpha_2 - 2\alpha_1\alpha_2/d^3}{1 - \alpha_1\alpha_2/d^6}, \qquad (55a)$$

$$\alpha_b = \frac{\alpha_1 + \alpha_2 + 4\alpha_1\alpha_2/d^3}{1 - 4\alpha_1\alpha_2/d^6}, \qquad (55b)$$

that respectively correspond to π and σ type bonding/antibonding. The polarizabilites for the coupled dimer system were first defined in Ref. [43]. When $\alpha_1 = \alpha_2 \equiv \alpha$ and if only the near-field contributions of δ_1 and δ_2 are considered, far field scattering matrices given by Eqs. (53) and (54) simplify to:

$$\mathbf{T}_a = \varepsilon\beta \frac{2\alpha}{1 + \alpha/d^3}\begin{pmatrix} 1 & 0 \\ 0 & 0 \end{pmatrix}, \qquad (56a)$$

$$\mathbf{T}_b = \varepsilon\beta \frac{2\alpha}{1 - 2\alpha/d^3}\begin{pmatrix} 0 & 0 \\ 0 & 1 \end{pmatrix}. \qquad (56b)$$

Therefore for $\mathbf{T}_a$ only the in-phase mode that corresponds to $\alpha/d^3 = -1$ (antibonding configuration) can be excited, and the out-of-phase mode (bonding configuration) is dark. Meanwhile, for $\mathbf{T}_b$ the in-phase mode corresponds to $2\alpha/d^3 = 1$ and the out-of-phase mode (antibonding configuration) is dark. Dark modes cannot be optically activated with a plane wave, since it always generates an in-phase situation. Indeed, an out-of-phase mode could be activated if the dipoles were not located in the same z plane, so that the incident electric field is not the same for both dipoles [44]. Another possibility to excite the out-of-phase mode, even for dipoles located in the same z plane, is using inhomogeneous excitation, such as focused radiation [45].
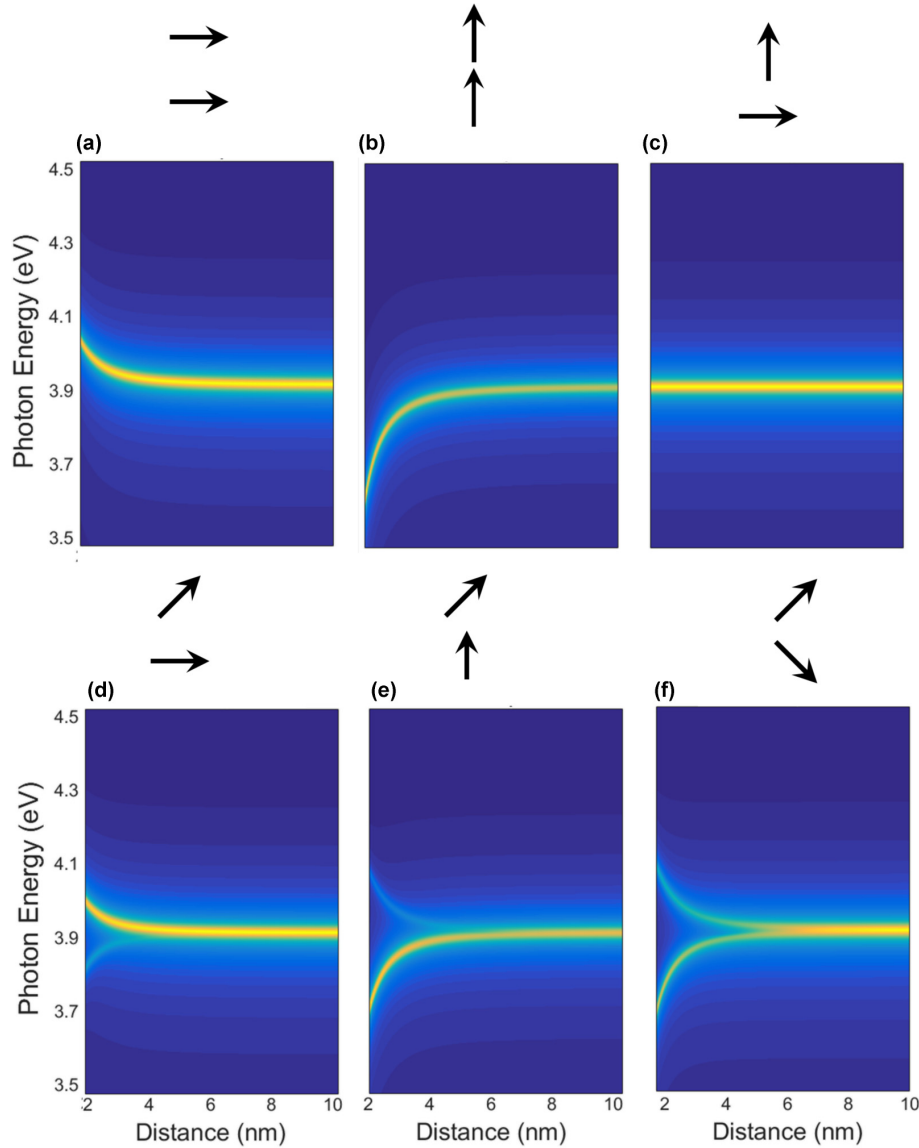
FIG. 3. Calculated intensity for the scattering of two coupled dipoles as a function of the distance between them. The dipoles can only polarize along the orientations shown by the arrows drawn at the top of each panel. These calculations correspond to illumination with a left-handed circularly polarized plane wave. The two particles were assumed to have polarizabilities of the same magnitude ($\alpha_1 = \alpha_2$) but different orientation. The spectroscopic values of the polarizability that we have used in this example are those that result from applying Clausius Mossotti relation to spherical silver particles in vacuum with a radii of 1 nm and using the Drude model of silver. Note that these spectroscopic values of polarizability are chosen for illustration purposes only and that the calculation is not describing a coupled system of spheres.

The remaining panels of Fig. 3 show misaligned dipoles. In (c) ($\phi_1 = 0°$ and $\phi_2 = 90°$) there is no hybridization because $\Delta = 0$ due to the orthogonality. Panels (d) ($\phi_1 = 0°, \phi_2 = 45°$) and (e) ($\phi_1 = 90°, \phi_2 = 45°$) show configurations which are, respectively, rather close to (a) and (b), but here both hybrid modes, in-phase and out-of-phase, can appear, despite that the in-phase is still much more intense than the other. In (f) ($\phi_1 = -45°, \phi_2 = 45°$) the directions of oscillation are orthogonal, like in (c), but here both particles have dipolar

component parallel and perpendicular to the dimer axis and Δ is no longer vanishing. Note also that a rotation of the dipole arrows in (c) does not lead to the arrangement in (f). In this arrangement the two hybrid modes have a very similar intensity.

The availability of the scattering matrix together with the knowledge of the geometry of the problem provides very valuable information for the study of the hybridization. Suppose that we measure the transfer matrix of the whole system. Call
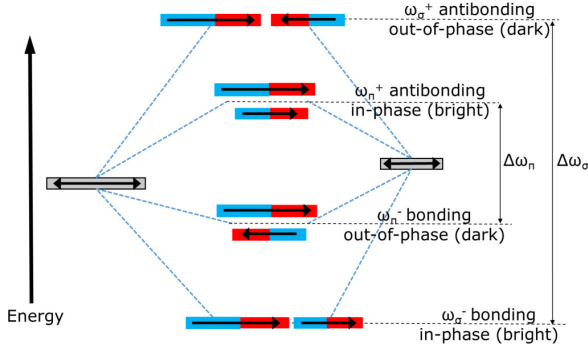
FIG. 4. Energy splitting in hybrid modes for a dipole dimer perpendicular (π-type stacking) and parallel (σ-type stacking) to the dimer axis. Red and blue colors, respectively, indicate positive and negative charge distribution.

this measured matrix, $\mathbf{T}_m$, and let the associated covariance vector be $|t\rangle_m$. If the orientation of the interacting dipoles with respect to the measurement coordinates are known then the matrices $\mathbf{J}_1$, $\mathbf{J}_2$, and $\mathbf{J}_{\text{int}}$ are also known [defined by Eqs. (26) and (27)], as well as their associated vectors $|h\rangle_1$, $|h\rangle_2$, and $|h\rangle_{\text{int}}$. Therefore, we can either decompose $\mathbf{T}_m$ or $|t\rangle_m$:

$$\mathbf{T}_m = g_1\mathbf{J}_1 + g_2\mathbf{J}_2 + g_{\text{int}}\mathbf{J}_{\text{int}}, \tag{57a}$$

$$|t\rangle_m = g_1|h\rangle_1 + g_2|h\rangle_2 + g_{\text{int}}|h\rangle_{\text{int}}, \tag{57b}$$

where g_1, g_2, and g_{int} are complex amplitudes (expansion coefficients) that can be determined algebraically. Note that this three term decomposition of an interacting two-component system was already suggested in Ref. [19]. Comparing with Eq. (25) gives

$$g_1 = \gamma\alpha_1, \quad g_2 = \gamma\alpha_2, \quad g_{\text{int}} = \gamma\alpha_1\alpha_2\Delta. \tag{58}$$

Therefore,

$$\frac{g_{\text{int}}^2}{g_1 g_2} = \alpha_1\alpha_2\Delta^2. \tag{59}$$

We can then rewrite γ in terms of the complex coefficients g_1, g_2, and g_{int}:

$$\gamma \propto \frac{1}{1 - \left(\frac{g_{\text{int}}}{g_1 g_2}\right)^2} = \frac{g_1 g_2}{(\sqrt{g_1 g_2} - g_{\text{int}})(\sqrt{g_1 g_2} + g_{\text{int}})}, \tag{60}$$

where we can define

$$\nu^{\pm} = \sqrt{g_1 g_2} \pm g_{\text{int}}. \tag{61}$$

The maxima of γ [i.e., the resonant conditions for the hybridized modes given by Eq. (43)] occur when either $\nu^+ = 0$ or $\nu^- = 0$. Note that $\nu^{\pm}$ are in general complex numbers and their real and imaginary parts may not vanish simultaneously. We assume in our analysis of hybridization that $\text{Re}(\nu^{\pm}) = 0$ is a condition of resonance if at the same time $\text{Im}(\nu^{\pm})$ is small or slowly varying.

We may now use ν^+ and ν^- to define a new basis, $|h^+\rangle$ and $|h^-\rangle$, in which $|t\rangle_m$ can be formulated as

$$|t\rangle_m = \nu^+|h^+\rangle + \nu^-|h^-\rangle, \tag{62}$$

where $|t\rangle_m$ is now written as a two term decomposition of hybrid modes, so that it is no longer necessary to make an explicit consideration of the interaction term. We may call $|h^+\rangle$ and $|h^-\rangle$ the *hybrid basis*.

From direct comparison between Eqs. (57b), (62), and (61) we can find:

$$|h^{\pm}\rangle = \frac{g_1|h\rangle_1 + g_2|h\rangle_2}{2\sqrt{g_1 g_2}} \pm \frac{|h\rangle_{\text{int}}}{2}, \tag{63}$$

where, as g_1 and g_2 can vary with frequency, the definition of the basis is frequency dependent. Note however that when $g_1 = g_2$ the definition of the hybrid basis becomes merely geometrical and energy independent:

$$|h^{\pm}\rangle = \frac{|h\rangle_1 + |h\rangle_2}{2} \pm \frac{|h\rangle_{\text{int}}}{2}. \tag{64}$$

C. Fano resonances

Fano resonances in hybridized systems arise due to interference effects between the radiating states of the system [25,26]. We have shown that our interacting dimer system can be described as the superposition of three matrix or vector states. The most favorable condition for interference occurs when the superposed states are identical (fully overlapping), and this occurs when the states are characterized by the same normalized 2×2 scattering matrix or covariance vector.

Consider the case of dipoles parallel to the dimer axis, already presented in Eq. (54), which can be now written as

$$\mathbf{T}_b = \gamma\left[\alpha_1\begin{pmatrix}0 & 0\\0 & 1\end{pmatrix} + \alpha_2\begin{pmatrix}0 & 0\\0 & 1\end{pmatrix} + 2\alpha_1\alpha_2\delta_2\begin{pmatrix}0 & 0\\0 & 1\end{pmatrix}\right], \tag{65}$$

to highlight that $\mathbf{J}_1 = \mathbf{J}_2 = \mathbf{J}_{\text{int}}$. Alternatively, this can be also presented by a covariance vector:

$$|h\rangle_b = \gamma(\alpha_1 + \alpha_2 + 2\alpha_1\alpha_2\delta_2)\begin{pmatrix}1/2\\-1/2\\0\\0\end{pmatrix}. \tag{66}$$

The scattering intensity is given by

$$\langle h|h\rangle_b = |\gamma(\alpha_1 + \alpha_2 + 2\alpha_1\alpha_2\delta_2)|^2/2. \tag{67}$$

In the previous section we have shown that the denominator of γ is a key to analyze the hybrid resonances, but γ is an overall factor that is not taking into account interferences between the states. Interference takes place in the superposition term $\alpha_1 + \alpha_2 + 2\alpha_1\alpha_2\delta_2$ and, for example, one can expect a Fano dip when the real part of this superposition term vanishes and the imaginary part is small or slowly varying. This happens when there is destructive interference between the states. Figure 5 shows an example of this effect by considering the same calculus as in Fig. 3(b) but know with $\alpha_1 \neq \alpha_2$. One can observe dips in the radiated intensity in between the two resonant modes.

Note that, in this configuration, no interference can occur if $\alpha_1 = \alpha_2 \equiv \alpha$ because then the scattering matrix simplifies to:

$$\mathbf{T}_b = \frac{\varepsilon\beta\alpha}{1 - \alpha\delta_2}\begin{pmatrix}0 & 0\\0 & 1\end{pmatrix}, \tag{68}$$

which does not allow interference because it contains just a single state. Indeed, symmetry breaking between coupling dipoles
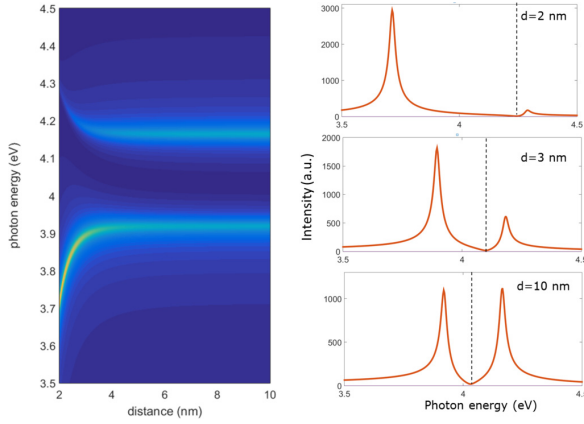
FIG. 5. Scattering intensity as a function of the distance for two parallel dipoles with different polarizabilities. Because of the interference, there is Fano dip (dashed line) in between the two resonant modes.

is a standard requirement for the generation of Fano resonances [46,47]. A more in-depth analysis of Fano resonances in other dimer configurations will be the subject of a future work.

V. APPLICATION TO PLASMONIC NANOANTENNAS

The analytic theory of light scattering by two coupled oriented dipoles that we have developed thus far can be useful to describe light-matter interaction processes which involve material structures that have dipolar responses. One good example is the case of plasmonic nanoantennas that we have already used in Sec. III A. Of particular interest is studying how the interaction affects the outcomes of optical measurements, since this analytic method may eventually permit us to distinguish the interaction contribution from the overall measured far-field optical response. With modern Mueller matrix polarimetry approaches it is possible to measure the complete scattering matrix in different plasmonic systems [48,49], even for single particles [50].

We apply this analytic method of the interaction to the far field response of a nanoantenna dimer made of gold and we analyze the same basic geometry as in Fig. 2, but for cases that differ in the distance between nanoantennas, as shown in Fig. 6(a). The far-field 2×2 Jones scattering matrix for these six configurations is calculated with the BEM method and then converted into a covariance vector to apply the decomposition of Eq. (57b).

The covariance vectors $|h\rangle_1$, $|h\rangle_2$, and $|h\rangle_{\rm int}$ are simply given by the geometry of the considered nanoantenna dimer. As in our example $\phi_1 = 90°$ and $\phi_2 = 135°$, the covariance vectors [defined in Eqs. (31) and (32)] will be:

$$|h\rangle_1 = \frac{1}{2}\begin{pmatrix} 1 \\ -1 \\ 0 \\ 0 \end{pmatrix}, \quad |h\rangle_2 = \frac{1}{2}\begin{pmatrix} 1 \\ 0 \\ -1 \\ 0 \end{pmatrix}, \quad |h\rangle_{\rm int} = \frac{1}{\sqrt{2}}\begin{pmatrix} 1 \\ -1 \\ -1 \\ 0 \end{pmatrix}.$$

$$(69)$$
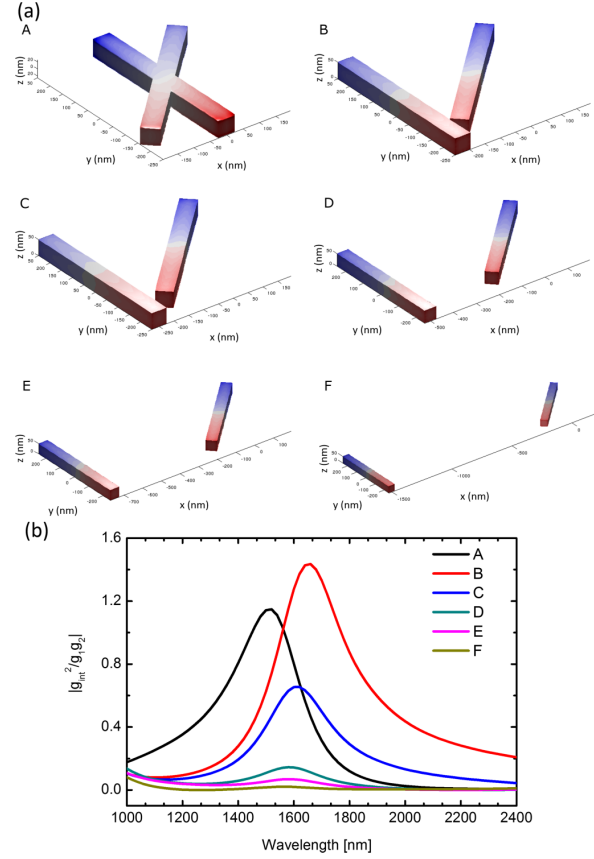
FIG. 6. (a) Different geometries of nanoantenna dimers considered in the BEM simulations. The only difference between the considered cases is the distance between the center of the nanoantennas (d), which is respectively set at 0 nm, 225 nm, 250 nm, 500 nm, 750 nm, and 1500 nm in A, B, C, D, E, and F. (b) Spectroscopic values of $|g_{\rm int}^2/g_1 g_2|$ for the six different configurations.

In this basis, Eq. (57b) leads to a system of three equations and three unknowns (note that the fourth equation is trivial because, for the present simulations of the nanoantennas, the fourth component of the covariance vector $|t\rangle_m$ is always zero), hence, it is possible to find g_1, g_2, and $g_{\rm int}$:

$$g_1 = 2(h_0 + h_2), \quad g_2 = 2(h_0 + h_1),$$
$$g_{\rm int} = -\sqrt{2}(h_0 + h_1 + h_2),$$

$$(70)$$

where h_0, h_1, and h_2 are, respectively, the first, second and third complex elements of the covariance vector $|t\rangle_m$ corresponding to the simulated scattering Jones matrix with the BEM method.

Therefore we can write:

$$\frac{g_{\rm int}^2}{g_1 g_2} = \frac{(h_0 + h_1 + h_2)^2}{2(h_0 + h_1)(h_0 + h_2)}.$$

$$(71)$$

The results of this analysis for the six cases presented in Fig. 6(a) are given in Fig. 6(b). We plot $|g_{\rm int}^2/g_1 g_2|$ (where the bars $|...|$ denote the complex modulus) as a function of the wavelength. The most obvious result is that $|g_{\rm int}^2/g_1 g_2|$ diminishes as the distance between the nanoantennas increases.
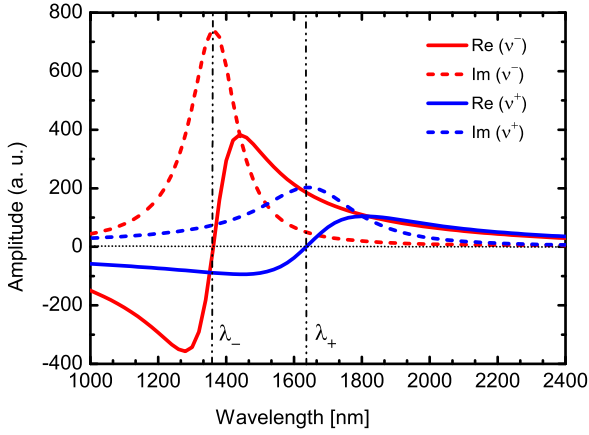
FIG. 7. Complex coefficients ν^+ and ν^- corresponding to simulation A. The vertical lines indicate the position of the hybridization resonances.

Note that for cases D, E, and F $|g_{int}^2/g_1 g_2|$ is very small across all the spectrum, which indicates that interaction is weak. Only for cases A and B the interaction leads to a marked hybridization in the overall scattering intensity. For the remaining cases, hybridization mostly manifests itself as peak broadening, and the two hybrid contributions are not clearly distinguishable in the overall intensity unless ν^+ and ν^- are calculated.

Hybridized frequencies can be calculated by analyzing the complex amplitudes ν^+ and ν^- of the hybrid basis. As discussed earlier, the resonances appear when the real part of $\nu^\pm$ is zero and the imaginary part is small or slowly varying (i.e., maxima of gamma). This is illustrated in Fig. 7, which displays the spectroscopic values of ν^+ and ν^- and the spectral position of the resonances for Simulation A. The resonant peaks found for all the simulated cases are summarized in Table I.

The values in Table I show that the hybrid frequencies are very sensitive to the distance between the nanoantennas. The spectral response can be therefore analyzed and designed by changing the interparticle distance, without need to modify the particle shape and orientation. This could be important for potential applications in near-field biosensing, in which small changes of distance translate in abrupt changes of light intensity. This is the basis of nanometrology tools such as plasmon rulers [13,51,52]. In fact our analytic approach allows

TABLE I. Spectral position of the in-phase (λ_+) and out-of-phase (λ_-) hybridization resonances for the considered cases.

Case	λ_+ (nm)	λ_- (nm)	$|\lambda_+ - \lambda_-|$ (nm)
A	1635	1360	275
B	1484	1828	344
C	1499	1692	193
D	1522	1620	98
E	1532	1614	82
F	1594	1545	49
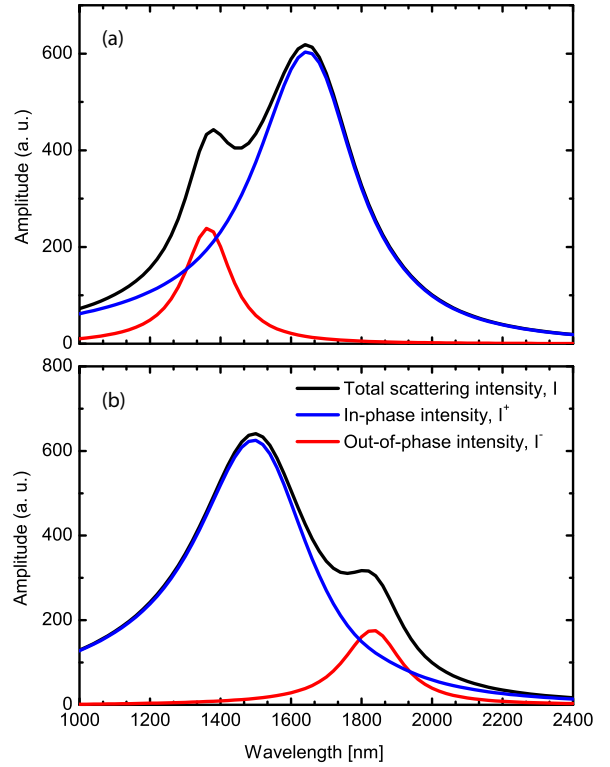
FIG. 8. Comparison of the in-phase and out-phase calculated intensities (I^+ and I^-, respectively) with respect to the overall simulated scattering intensity (I) for simulations A (a) and B (b).

us to determine the position of the hybrid frequencies and study their intensity. The intensity of scattering for each hybrid mode is

$$I^\pm = \nu^\pm \nu^{\pm *} \langle h^\pm | h^\pm \rangle, \tag{72}$$

where * indicates the complex conjugate and

$$|h^\pm\rangle = \frac{1}{4\sqrt{2}} \begin{pmatrix} 2\sqrt{2} \pm 2 \\ -\sqrt{2} \pm 2 \\ -\sqrt{2} \pm 2 \\ 0 \end{pmatrix}, \tag{73}$$

corresponding to the basis in Eqs. (69). Note that for an orthogonal hybrid basis like this one $\langle h^+ | h^- \rangle = 0$. In fact the hybrid bases are orthogonal whenever $g_1 = g_2$, and when this occurs:

$$I = I^+ + I^-, \tag{74}$$

where I is the overall scattering intensity ($I = \langle h | h \rangle$). Figure 8 shows how the decomposition in the hybrid basis clearly differentiates the contributions of the in-phase and out-of-phase modes to overall scattered intensity. Notably, the amplitudes I^+ and I^- can perfectly account for the position in energy and amplitude of the in-phase and out-of-phase hybridized peaks. This shows the usefulness of the proposed three term decomposition method for dimer systems.

VI. CONCLUSION

We have shown that the scattering matrix of a coupled dipole dimer can be written as a linear combination of three states which have a clear physical (and geometrical) meaning. The study of the interaction term $\Delta\mathbf{J}_{int}$ and the complex factor γ permits a clear understanding of phenomena occurring in some particle dimers, such as the emergence of optical activity in certain achiral configurations, hybridization effects, and Fano resonances. The application of the formalism has been illustrated by studying the dipolar resonance of coupled plasmonic nanoantennas which were simulated by elaborated numerical methods. Some of the results given by our analytic calculus are:

(i) The near-field scattering fingerprint for an achiral dipole dimer can be drastically modified by only adjusting the handedness of the incoming polarization, but this will not substantially alter far-field response for small scattering angles.

(ii) We have obtained an analytic expression [Eq. (45)] that provides the frequencies of the hybrid modes for any geometric arrangement of dipoles in a plane. Fano-like resonances can be also explained from the interference between the matrix states of our decomposition.

(iii) We have shown that the hybridization-induced spectral splitting in coupled oriented dimers can be well explained by our decomposition method. The hybrid basis that we have defined allows us to quantitatively distinguish the contribution of the in-phase and out-of-phase modes to the overall scattering intensity in particles with anisotropic polarizability, something that, to our knowledge, has never been achieved with prior descriptions of plasmonic hybridization processes. This is possible even for weakly coupled particles, where no evident peak splitting is observed in the scattering cross sections.

Our analytical model provides a simple framework to understand and quantify the relative contribution of coupled modes in complex nanostructures. We think that this analytic method can be particularly useful in nanophotonic applications that make use of small antennalike elements for controlling electromagnetic waves such as optical trapping, single-molecule localization, and recognition or surface-enhanced spectroscopy.

[1] J. D. Jackson, *Classical electrodynamics* (Wiley, India, 2011).

[2] E. M. Purcell and C. R. Pennypacker, Astrophys. J. **186**, 705 (1973).

[3] S. B. Singham and C. F. Bohren, J. Opt. Soc. Am. A **5**, 1867 (1988).

[4] B. T. Draine and P. J. Flatau, J. Opt. Soc. Am. A **11**, 1491 (1994).

[5] R. Messina, M. Tschikin, S.-A. Biehs, and P. Ben-Abdallah, Phys. Rev. B **88**, 104307 (2013).

[6] B. Rolly, B. Stout, and N. Bonod, Phys. Rev. B **84**, 125420 (2011).

[7] V. V. Klimov and D. V. Guzatov, Appl. Phys. A **89**, 305 (2007).

[8] W. Rechberger, A. Hohenau, A. Leitner, J. R. Krenn, B. Lamprecht, and F. R. Aussenegg, Opt. Commun. **220**, 137 (2003).

[9] P. Nordlander, C. Oubre, E. Prodan, K. Li, and M. I. Stockman, Nano Lett. **4**, 899 (2004).

[10] R. Ruppin, Phys. Rev. B **26**, 3440 (1982).

[11] I. Olivares, R. Rojas, and F. Claro, Phys. Rev. B **35**, 2453 (1987).

[12] M. Schmeits and L. Dambly, Phys. Rev. B **44**, 12706 (1991).

[13] P. K. Jain, W. Huang, and M. A. El-Sayed, Nano Lett. **7**, 2080 (2007).

[14] P. Albella, M. A. Poyli, M. K. Schmidt, S. A. Maier, F. Moreno, J. J. Sáenz, and J. Aizpurua, J. Phys. Chem. C **117**, 13573 (2013).

[15] E. Prodan, C. Radloff, N. J. Halas, and P. Nordlander, Science **302**, 419 (2003).

[16] P. R. Wiecha, L.-J. Black, Y. Wang, V. Paillard, C. Girard, O. L. Muskens, and A. Arbouet, Sci. Rep. **7**, 40906 (2017).

[17] A. Cecconello, L. V. Besteiro, A. O. Govorov, and I. Willner, Nat. Rev. Mater. **2**, 17039 (2017).

[18] M. Sun, L. Xu, J. H. Banhg, H. Kuang, S. Alben, N. A. Kotov, and C. Xu, Nat. Commun. **8**, 1847 (2017).

[19] E. Kuntman, M. A. Kuntman, J. Sancho-Parramon, and O. Arteaga, Phys. Rev. A **95**, 063819 (2017).

[20] E. Kuntman, M. Ali Kuntman, and O. Arteaga, J. Opt. Soc. Am. A **34**, 80 (2016).

[21] O. Arteaga and A. Canillas, Opt. Lett. **35**, 559 (2010).

[22] F. Capolino, *Theory and Phenomena of Metamaterials*, edited by F. Capolino (CRC Press, Boca Raton, FL, 2009).

[23] V. V. Gozhenko, L. G. Grechko, and K. W. Whites, Phys. Rev. B **68**, 125422 (2003).

[24] A. Pinchuk and G. Schatz, Nanotechnology **16**, 2209 (2005).

[25] A. E. Miroshnichenko, S. Flach, and Y. S. Kivshar, Rev. Mod. Phys. **82**, 2257 (2010).

[26] K. C. Woo, L. Shao, H. Chen, Y. Liang, J. Wang, and H.-Q. Lin, ACS Nano **5**, 5976 (2011).

[27] D. Lin and J.-S. Huang, Opt. Express **22**, 7434 (2014).

[28] J. Wu, X. Lu, Q. Zhu, J. Zhao, Q. Shen, L. Zhan, and W. Ni, Nano-Micro Lett. **6**, 372 (2014).

[29] L.-Y. Wang, K. W. Smith, S. Dominguez-Medina, N. Moody, J. M. Olson, H. Zhang, W.-S. Chang, N. Kotov, and S. Link, ACS Photonics **2**, 1602 (2015).

[30] B. Auguié, J. L. Alonso-Gómez, A. Guerrero-Martínez, and L. M. Liz-Marzán, J. Phys. Chem. Lett. **2**, 846 (2011).

[31] X. Yin, M. Schäferling, B. Metzger, and H. Giessen, Nano Lett. **13**, 6238 (2013).

[32] W. Kuhn, Zeitschr. Physikal. Chem. **4B**, 14 (1929).

[33] R. Ossikovski, O. Arteaga, S. H. Yoo, E. Garcia-Caurel, and K. Hingerl, Opt. Lett. **42**, 4740 (2017).

[34] U. Hohenester and A. Trügler, Comput. Phys. Commun. **183**, 370 (2012).

[35] F. J. G. de Abajo and A. Howie, Phys. Rev. B **65**, 115418 (2002).

[36] K. Claborn, C. Isborn, W. Kaminsky, and B. Kahr, Angew. Chem., Int. Ed. **47**, 5706 (2008).

[37] C. Isborn, K. Claborn, and B. Kahr, J. Phys. Chem. A **111**, 7800 (2007).

[38] O. Arteaga, Opt. Lett. **40**, 4277 (2015).

[39] T. W. H. Oates, T. Shaykhutdinov, T. Wagner, A. Furchner, and K. Hinrichs, Opt. Mater. Express **4**, 2646 (2014).

[40] T. W. H. Oates, T. Shaykhutdinov, T. Wagner, A. Furchner, and K. Hinrichs, Adv. Mater. **26**, 7197 (2014).

[41] J. R. Taylor, *Classical Mechanics* (University Science Books, Herndon, VA, 2005).

[42] M. Schäferling, Chiral nanophotonics: chiral optical properties of plasmonic systems (Springer, New York, 2017).

[43] B. Khlebtsov, A. Melnikov, V. Zharov, and N. Khlebtsov, Nanotechnology **17**, 1437 (2006).

[44] J. P. Kottmann and O. J. F. Martin, Opt. Lett. **26**, 1096 (2001).

[45] J. Sancho-Parramon, Opt. Lett. **36**, 3527 (2011).

[46] F. Hao, Y. Sonnefraud, P. V. Dorpe, S. A. Maier, N. J. Halas, and P. Nordlander, Nano Lett. **8**, 3983 (2008).

[47] B. Luk'yanchuk, N. I. Zheludev, S. A. Maier, N. J. Halas, P. Nordlander, H. Giessen, and C. T. Chong, Nat. Mater. **9**, 707 (2010).

[48] O. Arteaga, B. M. Maoz, S. Nichols, G. Markovich, and B. Kahr, Opt. Express **22**, 13719 (2014).

[49] O. Arteaga, J. Sancho-Parramon, S. Nichols, B. M. Maoz, A. Canillas, S. Bosch, G. Markovich, and B. Kahr, Opt. Express **24**, 2242 (2016).

[50] S. Chandel, J. Soni, S. K. Ray, A. Das, A. Ghosh, S. Raj, and N. Ghosh, Sci. Rep. **6**, 26466 (2016).

[51] S. Kadkhodazadeh, J. R. de Lasson, M. Beleggia, H. Kneipp, J. B. Wagner, and K. Kneipp, J. Phys. Chem. C **118**, 5478 (2014).

[52] J. I. L. Chen, Y. Chen, and D. S. Ginger, J. Am. Chem. Soc. **132**, 9600 (2010).

Research Article

Journal of the Optical Society of America A

OPTICS, IMAGE SCIENCE, AND VISION

Quaternion algebra for Stokes–Mueller formalism

Ertan Kuntman,[1] **Mehmet Ali Kuntman,**[3] **Adolf Canillas,**[1] **and Oriol Arteaga**[1,2,*]

[1]*Dep. Física Aplicada, Feman Group, IN2UB, Universitat de Barcelona, 08028 Barcelona, Spain*
[2]*LPICM, CNRS, École Polytechnique, Université Paris-Saclay, 91128 Palaiseau, France*
[3]*Independent Researcher, Baran Sitesi F-6, 52200 Ordu, Turkey*
Corresponding author: oarteaga@ub.edu

In this paper, we show that the Stokes–Mueller formalism can be reformulated in terms of quaternions and that the quaternion algebra is a suitable alternative presentation of the formalism of Mueller–Jones states that we have recently described [J. Opt. Soc. Am. A **34**, 80 (2017)]. The vector and matrix states associated with the Mueller matrices of nondepolarizing optical systems are different representations that are isomorphic to the same quaternion state, and this quaternion state turns out to be the rotator of the Stokes quaternion. In this work, we study the properties of this general quaternion state and its application to the calculus of polarization effects. We also show that the coherent linear combination of nondepolarizing optical media states and depolarization phenomena can be reformulated in terms of quaternion states.   © 2019 Optical Society of America

1. INTRODUCTION

The formulation of the problem of interaction between polarization devices/media and polarized light is usually made using the Stokes–Mueller matrix formalism, but it is also possible to use a more abstract, coordinate- and matrix-free algebraic formalism based on quaternions. The use of quaternions in polarization optics is not common, but it was pioneered years ago by Pellat-Finet [1,2] and, more recently, it has also been considered by other authors [3,4]. These works mainly focus on particular uses of quaternions in certain polarization calculus, for example, to simplify the calculation of Jones matrix cascades of birefringent systems, but they do not provide a quaternion representation for the most general polarization operator having all possible forms of birefringence and dichroism. In this work, we show a complete formulation of polarization algebra in terms of quaternions. Through isomorphic properties, it is shown that such formulation is equivalent to other well-known representations given by the Jones calculus, Mueller–Stokes calculus, covariance vectors, etc.

We start recalling several results from polarization theory. The covariance matrix **H** associated with the Mueller matrix **M** is [5]

$$\mathbf{H} = \frac{1}{4}\sum_{i,j=0}^{3} M_{ij}\Pi_{ij}, \tag{1}$$

where $M_{ij}(i,j=0,1,2,3)$ are the elements of the Mueller matrix **M**, $\Pi_{ij} = \mathbf{A}(\boldsymbol{\sigma}_i \otimes \boldsymbol{\sigma}_j^*)\mathbf{A}^{-1}$:

$$\mathbf{A} = \begin{pmatrix} 1 & 0 & 0 & 1 \\ 1 & 0 & 0 & -1 \\ 0 & 1 & 1 & 0 \\ 0 & i & -i & 0 \end{pmatrix},$$

$$\mathbf{A}^{-1} = \frac{1}{2}\mathbf{A}^{\dagger} = \frac{1}{2}\begin{pmatrix} 1 & 1 & 0 & 0 \\ 0 & 0 & 1 & -i \\ 0 & 0 & 1 & i \\ 1 & -1 & 0 & 0 \end{pmatrix}. \tag{2}$$

The superscript † indicates the conjugate transpose (Hermitian conjugate), the superscript * indicates complex conjugate, ⊗ is the Kronecker product, and $\boldsymbol{\sigma}_i$ are the Pauli matrices with the 2×2 identity in the following order:

$$\boldsymbol{\sigma}_0 = \begin{pmatrix} 1 & 0 \\ 0 & 1 \end{pmatrix}, \qquad \boldsymbol{\sigma}_1 = \begin{pmatrix} 1 & 0 \\ 0 & -1 \end{pmatrix}, \tag{3}$$

$$\boldsymbol{\sigma}_2 = \begin{pmatrix} 0 & 1 \\ 1 & 0 \end{pmatrix}, \qquad \boldsymbol{\sigma}_3 = \begin{pmatrix} 0 & -i \\ i & 0 \end{pmatrix}. \tag{4}$$

If and only if the Mueller matrix of the system is nondepolarizing (we can also call it *pure* or *deterministic*), the associated covariance matrix **H** will be of rank one. In this case, it is always possible to define a covariance vector $|h\rangle$ such that [5–10]

$$\mathbf{H} = |h\rangle\langle h|, \tag{5}$$

where $|h\rangle$ is the eigenvector of **H** corresponding to the single nonzero eigenvalue.

In previous works [9,10], we parameterized the dimensionless components of $|b\rangle$ as τ, α, β, and γ:

$$|b\rangle = \begin{pmatrix} \tau \\ \alpha \\ \beta \\ \gamma \end{pmatrix}, \tag{6}$$

where τ, α, β, and γ are generally complex numbers. One of the parameters can be chosen to be real and positive if the global phase is not considered, as it is typically done in polarimetric measurements because it is not accessible.

On the other hand, in [9], we introduced another object, $\mathbf{Z}$, that serves as a Mueller–Jones state in matrix form and that has applications in many calculi [11,12]:

$$\mathbf{Z} = \begin{pmatrix} \tau & \alpha & \beta & \gamma \\ \alpha & \tau & -i\gamma & i\beta \\ \beta & i\gamma & \tau & -i\alpha \\ \gamma & -i\beta & i\alpha & \tau \end{pmatrix}. \tag{7}$$

By direct matrix multiplication, it can be shown that the Mueller matrix of any nondepolarizing optical media can be written as

$$\mathbf{M} = \mathbf{Z}\mathbf{Z}^* = \mathbf{Z}^*\mathbf{Z}. \tag{8}$$

The Mueller matrix transforms the Stokes vector $|s\rangle = (s_0, s_1, s_2, s_3)^T$ into another Stokes vector $|s'\rangle$:

$$|s'\rangle = \mathbf{M}|s\rangle. \tag{9}$$

Similarly, it can be shown that the $\mathbf{Z}$ matrix transforms the associated Stokes matrix according to the following scheme:

$$\mathbf{S}' = \mathbf{Z}\mathbf{S}\mathbf{Z}^\dagger, \tag{10}$$

where the Stokes matrix, $\mathbf{S}$, is defined as

$$\mathbf{S} = \begin{pmatrix} s_0 & s_1 & s_2 & s_3 \\ s_1 & s_0 & -is_3 & is_2 \\ s_2 & is_3 & s_0 & -is_1 \\ s_3 & -is_2 & is_1 & s_0 \end{pmatrix}. \tag{11}$$

We note that the term Stokes matrix has been used previously [6,13] with a different meaning: to refer to 4×4 matrices that transform Stokes vectors into Stokes vectors, so that the set of Mueller matrices is constituted by those Stokes matrices that satisfy the Cloude's criterion. It should not be confused with the different meaning that it has here.

The Stokes matrix $\mathbf{S}$ can also be defined in terms of the polarization matrix Φ:

$$\mathbf{S} = \mathbf{A}(\Phi \otimes \mathbf{I})\mathbf{A}^{-1}, \tag{12}$$

where

$$\Phi = |E\rangle\langle E|, \tag{13}$$

and $|E\rangle$ is the Jones vector:

$$|E\rangle = \begin{pmatrix} E_x \\ E_y \end{pmatrix}. \tag{14}$$

The $\mathbf{Z}$ matrix can be written in terms of the Jones matrix, $\mathbf{J}$, as follows:

$$\mathbf{Z} = \mathbf{A}(\mathbf{J} \otimes \mathbf{I})\mathbf{A}^{-1}. \tag{15}$$

Proof of Eq. (10) immediately follows from the definitions of $\mathbf{Z}$ and $\mathbf{S}$.

Similar to the Jones matrices, $\mathbf{Z}$ matrices can describe the product state of the combined system associated with a serial combination of nondepolarizing optical media:

$$\mathbf{Z} = \mathbf{Z}_N \cdot \mathbf{Z}_{N-1}...\mathbf{Z}_2 \cdot \mathbf{Z}_1. \tag{16}$$

However, such a product state is not possible with $|b\rangle$ vectors. Therefore, $|b\rangle$ vectors and $\mathbf{Z}$ matrices (and by extension Jones matrices), despite containing the same information, appear as different algebraic entities.

In this work, it will be shown that $\mathbf{Z}$ matrices, Jones matrices, and $|b\rangle$ vectors are actually different representations of the same quantity, and they are isomorphic to the same $\boldsymbol{b}$ quaternion. The development of this quaternion algebra is possible thanks to the close relation of these two mathematical representations to Pauli matrices, which are the basis matrices that allow to construct the complex 2×2 matrix operators in polarization optics [14]. Before introducing the quaternion representation, we complete the formalism based on $\mathbf{Z}$ matrix states that we have presented in [9] by describing how it handles optical phases.

2. OPTICAL PHASES AND Z MATRICES

In addition to the intensity, the phase of the electromagnetic waves plays an important role in optics. The Stokes vector, $|s\rangle$, and the Mueller matrix, $\mathbf{M}$, are real; therefore, the transformation $|s'\rangle = \mathbf{M}|s\rangle$ cannot keep track of the phase of the polarization state. The Jones formalism that is based on Jones vectors, $|E\rangle$, and Jones matrices, $\mathbf{J}$, can represent optical phases. For the transformation

$$|E'\rangle = \mathbf{J}|E\rangle, \tag{17}$$

$\arg(\langle E|E'\rangle)$ is the total phase (geometric phase plus dynamic phase) acquired.

In our formalism of $\mathbf{Z}$ matrix states, we can also consider the following transformation:

$$\tilde{\mathbf{S}} = \mathbf{Z}\mathbf{S}, \tag{18}$$

where $\tilde{\mathbf{S}}$ is not a Stokes matrix. By using Eqs. (12), (15), and (17), this identity can be rewritten explicitly as follows:

$$\tilde{\mathbf{S}} = \mathbf{A}(|E'\rangle\langle E|) \otimes \mathbf{I})\mathbf{A}^{-1}. \tag{19}$$

Therefore $\tilde{\mathbf{S}}$ is just the extension of the operator $|E'\rangle\langle E|$, and it carries the same phase contained in $|E'\rangle$.

Similarly, the transformation $\mathbf{Z}|s\rangle$ does not generate a Stokes vector, but it leads to the following theorem:

$$\langle s|\mathbf{Z}|s\rangle = 2\langle E|\mathbf{J}|E\rangle = 2\langle E|E'\rangle. \tag{20}$$

According to this theorem, it is possible to read the phase acquired by the polarization state from $\langle s|\mathbf{Z}|s\rangle$. As it can be seen from the left hand side of Eq. (20), since the Stokes vectors are free from phase, all the additional phase comes from the $\mathbf{Z}$ matrix.

Therefore, we conclude that the $\mathbf{Z}$ matrix can include optical phases information of the Jones formalism, and it can be used as a bookkeeping device for the evolution of the phase. For example, it is possible to keep track of the phase for successive rotations of the polarization state on the Poincare

sphere, and it is possible to calculate the Pancharatnam–Berry phase for closed loops.

3. DEFINITION OF THE *h* QUATERNION STATE

First, we observe that the **Z** matrix can be written as a linear combination of four matrices:

$$\mathbf{Z} = \tau\mathbb{1} + i\alpha\mathbf{I} + i\beta\mathbf{J} + i\gamma\mathbf{K}, \tag{21}$$

where

$$\mathbb{1} = \begin{pmatrix} 1 & 0 & 0 & 0 \\ 0 & 1 & 0 & 0 \\ 0 & 0 & 1 & 0 \\ 0 & 0 & 0 & 1 \end{pmatrix}, \quad \mathbf{I} = \begin{pmatrix} 0 & -i & 0 & 0 \\ -i & 0 & 0 & 0 \\ 0 & 0 & 0 & -1 \\ 0 & 0 & 1 & 0 \end{pmatrix},$$

$$\mathbf{J} = \begin{pmatrix} 0 & 0 & -i & 0 \\ 0 & 0 & 0 & 1 \\ -i & 0 & 0 & 0 \\ 0 & -1 & 0 & 0 \end{pmatrix}, \quad \mathbf{K} = \begin{pmatrix} 0 & 0 & 0 & -i \\ 0 & 0 & -1 & 0 \\ 0 & 1 & 0 & 0 \\ -i & 0 & 0 & 0 \end{pmatrix}. \tag{22}$$

These basis matrices have the following properties:

$$\mathbf{I}^2 = \mathbf{J}^2 = \mathbf{K}^2 = \mathbf{IJK} = -\mathbb{1},$$

$$\mathbf{IJ} = -\mathbf{JI} = \mathbf{K}, \quad \mathbf{JK} = -\mathbf{KJ} = \mathbf{I}, \quad \mathbf{KI} = -\mathbf{IK} = \mathbf{J}. \tag{23}$$

We note that these basis matrices are isomorphic to the basis quaternions defined by Hamilton [15]:

$$\mathbf{i}^2 = \mathbf{j}^2 = \mathbf{k}^2 = \mathbf{ijk} = -1,$$

$$\mathbf{ij} = -\mathbf{ji} = \mathbf{k}, \quad \mathbf{jk} = -\mathbf{kj} = \mathbf{i}, \quad \mathbf{ki} = -\mathbf{ik} = \mathbf{j}. \tag{24}$$

Therefore, the **Z** matrix of Eq. (21) is isomorphic to the *h* quaternion:

$$\mathbf{h} = \tau\mathbf{1} + i\alpha\mathbf{i} + i\beta\mathbf{j} + i\gamma\mathbf{k}, \tag{25}$$

which is directly related with the covariance vector $|h\rangle$. It is worth noting that the Jones matrix, **J**, is also isomorphic to the *h* quaternion. To show this, we write the Jones matrix in terms of Pauli matrices [9,16]:

$$\mathbf{J} = \tau\boldsymbol{\sigma}_0 + \alpha\boldsymbol{\sigma}_1 + \beta\boldsymbol{\sigma}_2 + \gamma\boldsymbol{\sigma}_3, \tag{26}$$

which can be written as

$$\mathbf{J} = \tau\boldsymbol{\sigma}_0 + i\alpha(-i\boldsymbol{\sigma}_1) + i\beta(-i\boldsymbol{\sigma}_2) + i\gamma(-i\boldsymbol{\sigma}_3). \tag{27}$$

The 2×2 matrices $\boldsymbol{\sigma}_0$, $-i\boldsymbol{\sigma}_1$, $-i\boldsymbol{\sigma}_2$, and $-i\boldsymbol{\sigma}_3$ are, respectively, isomorphic to the quaternion basis, $\mathbf{1}, \mathbf{i}, \mathbf{j}$, and $\mathbf{k}$. Therefore, we can write the associated Jones quaternion, **h**, as follows:

$$\mathbf{h} = \tau\mathbf{1} + i\alpha\mathbf{i} + i\beta\mathbf{j} + i\gamma\mathbf{k}, \tag{28}$$

which is identically equal to the quaternion state *h* defined for the **Z** matrix and the $|h\rangle$ vector.

We therefore conclude that the vector state $|h\rangle$, the matrix state **Z**, and the Jones matrix **J** are isomorphic to the same quaternion state, *h*.

4. PROPERTIES OF THE QUATERNION STATE

It is possible to define a polarization formalism based on the quaternionic form of the nondepolarizing media states. The

algebra of this formalism is free from any matrix (or vector) representation. The most relevant properties of the *h* quaternion are described in this section, while other more particular properties are discussed in Appendix A.

A. Multiplication of Quaternion States

We can multiply two (or more) *h* quaternions and those results into another *h* quaternion:

$$\mathbf{h} = \mathbf{h}_2\mathbf{h}_1 = \begin{cases} (\tau_2\tau_1 + \alpha_2\alpha_1 + \beta_2\beta_1 + \gamma_2\gamma_1)\mathbf{1} \\ +i(\tau_2\alpha_1 + \alpha_2\tau_1 + i\beta_2\gamma_1 - i\gamma_2\beta_1)\mathbf{i} \\ +i(\tau_2\beta_1 + \beta_2\tau_1 - i\alpha_2\gamma_1 + i\gamma_2\alpha_1)\mathbf{j} \\ +i(\tau_2\gamma_1 + \gamma_2\tau_1 + i\alpha_2\beta_1 - i\beta_2\alpha_1)\mathbf{k} \end{cases}. \tag{29}$$

It is worth noting that the resultant *h* quaternion is not a four-component column vector, but a single *hypercomplex number* that corresponds to the covariance vector $|h\rangle$ with the following components:

$$|h\rangle = \begin{pmatrix} \tau_2\tau_1 + \alpha_2\alpha_1 + \beta_2\beta_1 + \gamma_2\gamma_1 \\ \tau_2\alpha_1 + \alpha_2\tau_1 + i\beta_2\gamma_1 - i\gamma_2\beta_1 \\ \tau_2\beta_1 + \beta_2\tau_1 - i\alpha_2\gamma_1 + i\gamma_2\alpha_1 \\ \tau_2\gamma_1 + \gamma_2\tau_1 + i\alpha_2\beta_1 - i\beta_2\alpha_1 \end{pmatrix}. \tag{30}$$

The **Z** matrix serves as a short-hand multiplication table for $|h\rangle$ vectors [17]:

$$|h\rangle = \mathbf{Z}_2|h_1\rangle, \tag{31}$$

where $|h\rangle, \mathbf{Z}_2, |h_2\rangle$ correspond to *h* quaternion, $\mathbf{h}_2$ quaternion, and $\mathbf{h}_1$ quaternion of Eq. (29), respectively. The quaternion multiplication algebra of Eq. (29), which exploits the multiplication of two hypercomplex numbers, offers a compact and simple alternative to the matrix–matrix multiplication Eq. (16) or to the matrix–vector multiplication Eq. (31).

B. Transformation of a Stokes Quaternion

An ordinary three-dimensional vector **v** can be rotated about an axis by an angle θ as follows:

$$\mathbf{v}' = \mathbf{q}\mathbf{v}\bar{\mathbf{q}}, \tag{32}$$

where **q** is a unit real quaternion, and $\bar{\mathbf{q}}$ is the Hamilton (quaternion) conjugate of **q**:

$$\mathbf{q} = q_0\mathbf{1} + q_1\mathbf{i} + q_2\mathbf{j} + q_3\mathbf{k},$$

$$\bar{\mathbf{q}} = q_0\mathbf{1} - q_1\mathbf{i} - q_2\mathbf{j} - q_3\mathbf{k}, \tag{33}$$

where q_0, q_1, q_2, and q_3 are real numbers such that $\mathbf{q}\bar{\mathbf{q}} = \bar{\mathbf{q}}\mathbf{q} = q_0^2 + q_1^2 + q_2^2 + q_3^2 = 1$.

From Eq. (10), it immediately follows that a very similar transformation (rotation) applies to the Stokes quaternion (see also Liu *et al.* [3]):

$$\mathbf{s}' = \mathbf{h}\mathbf{s}\mathbf{h}^\dagger, \tag{34}$$

where $\mathbf{h}^\dagger$ is the Hermitian conjugate of the *h* quaternion:

$$\mathbf{h}^\dagger = \tau^*\mathbf{1} + i\alpha^*\mathbf{i} + i\beta^*\mathbf{j} + i\gamma^*\mathbf{k}. \tag{35}$$

s is the Stokes quaternion that corresponds to the Stokes vector $|s\rangle = (s_0, s_1, s_2, s_3)^T$:

$$\mathbf{s} = s_0\mathbf{1} + is_1\mathbf{i} + is_2\mathbf{j} + is_3\mathbf{k}, \tag{36}$$

and **s**' is the transformed (rotated) Stokes quaternion that corresponds to the transformed Stokes vector $|s'\rangle$:

$$|s'\rangle = \mathbf{M}|s\rangle, \tag{37}$$

where $\mathbf{M}$ is a nondepolarizing Mueller matrix. The proof is straightforward but tedious. By direct multiplication of three quaternions in Eq. (34), it can be shown that the transformed Stokes quaternion s' is isomorphic to the transformed Stokes vector $|s'\rangle$. The most general transformation of a Stokes vector by a nondepolarizing optical system state is thus given by the triple quaternion multiplication of Eq. (34).

It can also be shown that the theorem of Eq. (20) can be written in terms of the quaternions as follows:

$$s \cdot hs = \langle s|\mathbf{Z}|s\rangle = 2\langle E|\mathbf{J}|E\rangle, \tag{38}$$

where "." indicates the quaternion dot product.

C. Rotation of the Quaternion State

The Mueller matrix of an optical element can be rotated by an angle θ in a plane perpendicular the light propagation direction:

$$\mathbf{M}(\theta) = \mathbf{R}(\theta)\mathbf{M}\mathbf{R}(-\theta), \tag{39}$$

where

$$\mathbf{R}(\theta) = \begin{pmatrix} 1 & 0 & 0 & 0 \\ 0 & \cos(2\theta) & -\sin(2\theta) & 0 \\ 0 & \sin(2\theta) & \cos(2\theta) & 0 \\ 0 & 0 & 0 & 1 \end{pmatrix}. \tag{40}$$

Similarly, the covariance vector of a nondepolarizing Mueller matrix can be rotated as follows:

$$|h(\theta)\rangle = \mathbf{R}(\theta)|h\rangle, \tag{41}$$

where $|h(\theta)\rangle$ generates $\mathbf{M}(\theta)$.

The covariance vector of the matrix $\mathbf{R}(\theta)$ is $|r(\theta)\rangle = (\cos(\theta), 0, 0, -i\sin(\theta))^T$ with the associated quaternion r:

$$r = \cos(\theta)\mathbf{1} + \sin(\theta)\mathbf{k}. \tag{42}$$

The quaternion r is unitary, and it is the rotator for the quaternion h:

$$h(\theta) = rhr^{\dagger}, \tag{43}$$

where $r^{\dagger} = \bar{r} = \cos(\theta)\mathbf{1} - \sin(\theta)\mathbf{k}$.

5. APPLICATION TO THE REPRESENTATION OF OPTICAL MEDIA

A. Superposition of Mueller–Jones States and Depolarization

As we have shown before [10], the Mueller–Jones state of a nondepolarizing optical medium can also be represented by a covariance vector $|h\rangle$ or by a matrix state $\mathbf{Z}$. Here we have shown that these are isomorphic to the same quaternion state h. Therefore, any coherent linear combination of quaternion states is also a quaternion state that corresponds to a new nondepolarizing optical medium state:

$$h = ah_1 + bh_2 + ch_3\ldots, \tag{44}$$

where the coefficients $a, b, c, \ldots$ are, in general, complex numbers.

In a coherent linear combination (superposition) process, the Stokes quaternion is simply subjected to a rotation by the combined quaternion state h. If the superposition process

is partially coherent or incoherent, we have to consider depolarization effects. In this case, the covariance matrix $\mathbf{H}$ associated with a depolarizing Mueller matrix will be of rank >1, and any depolarizing Mueller matrix can be written as a convex sum of at most four nondepolarizing Mueller matrices:

$$\mathbf{M} = w_1\mathbf{M_1} + w_2\mathbf{M_2} + w_3\mathbf{M_3} + w_4\mathbf{M_4}. \tag{45}$$

This is known as the arbitrary decomposition of a Mueller matrix [6,18,19]. $\mathbf{M_1}, \mathbf{M_2}, \mathbf{M_3}$, and $\mathbf{M_4}$ are nondepolarizing Mueller matrices; w_1, w_2, w_3, and w_4 are real and positive numbers with the condition

$$w_1 + w_2 + w_3 + w_4 = 1. \tag{46}$$

Decomposition of a depolarizing Mueller matrix into its nondepolarizing components is not unique. In the spectral (Cloude) decomposition [20], weights w_i are the eigenvalues of the covariance matrix, $\mathbf{H}$, and the component matrices $\mathbf{M}_i$ are the nondepolarizing Mueller matrices corresponding to the associated eigenvectors of $\mathbf{H}$.

For an incoherent combination, from the linearity of the convex summation of Eq. (45), we can immediately write a transformation formula for the Stokes quaternion:

$$s' = \sum_{i=1}^{4} w_i h_i s h_i^{\dagger}. \tag{47}$$

The same depolarization scheme given in [10] applies to the quaternion formulation as well.

B. Nondepolarizing Mueller Matrix

The nondepolarizing Mueller matrix can be recovered by shifting from the triple quaternion multiplication of Eq. (34) to a matrix–matrix–vector multiplication. Consider the second product ($sh^{\dagger}$) of the quaternion rotation in Eq. (34); it maps to the following matrix–vector product:

$$sh^{\dagger} \mapsto \mathbf{S}|h^*\rangle = \begin{pmatrix} s_0 & s_1 & s_2 & s_3 \\ s_1 & s_0 & -is_3 & is_2 \\ s_2 & is_3 & s_0 & -is_1 \\ s_3 & -is_2 & is_1 & s_0 \end{pmatrix} \begin{pmatrix} \tau^* \\ \alpha^* \\ \beta^* \\ \gamma^* \end{pmatrix}, \tag{48}$$

where $\mathbf{S}$ is the matrix associated with the Stokes quaternion s.

It can be shown that the order of multiplication can be reversed by means of the $\mathbf{Z}^*$ matrix:

$$\mathbf{S}|h^*\rangle = \mathbf{Z}^*|s\rangle, \tag{49}$$

where $|s\rangle$ is the Stokes vector ($|s\rangle = (s_0, s_1, s_2, s_3)^T$).

Since quaternion h is associated with the $\mathbf{Z}$ matrix, the triple quaternion product maps to the following matrix–matrix–vector product:

$$s' = hsh^{\dagger} \mapsto |s'\rangle = \mathbf{Z}\mathbf{Z}^*|s\rangle = (\mathbf{Z}\mathbf{Z}^*)|s\rangle = \mathbf{M}|s\rangle, \tag{50}$$

where $\mathbf{M}$ is the Mueller matrix. An explicit form of the Mueller matrix in terms of the parameters τ, α, β, and γ can be found in [9].

C. Exponential and Differential Forms of the Quaternion State

Any quaternion, $q = w\mathbf{1} + x\mathbf{i} + y\mathbf{j} + z\mathbf{k}$, can be expressed in an exponential form:

$$q = |q|(\cos\theta + \hat{u}\sin\theta) = |q|e^{\hat{u}\theta}, \qquad \text{(51)}$$

where $|q| = \sqrt{q\bar{q}}$, $\cos\theta = w/|q|$, $\hat{u} = (x\boldsymbol{i} + y\boldsymbol{j} + z\boldsymbol{k})/\sqrt{x^2 + y^2 + z^2}$, and $\sin\theta = \sqrt{x^2 + y^2 + z^2}/|q|$.

Similarly, the quaternion $\boldsymbol{h} = \tau\mathbf{1} + i\alpha\boldsymbol{i} + i\beta\boldsymbol{j} + i\gamma\boldsymbol{k}$ can be written in polar form using the expressions for τ, α, β, and γ in terms of the spectroscopic parameters [9,21]: η (isotropic phase retardation), κ (isotropic amplitude absorption), CD (circular dichroism), CB (circular birefringence), LD (horizontal linear dichroism), LB (horizontal linear birefringence), LD′ (45° linear dichroism), and LB′ (45° linear birefringence):

$$\tau = e^{-\frac{i\chi}{2}}\cos\left(\frac{T}{2}\right) \qquad \alpha = -e^{-\frac{i\chi}{2}}\frac{iL}{T}\sin\left(\frac{T}{2}\right), \qquad \text{(52)}$$

$$\beta = -e^{-\frac{i\chi}{2}}\frac{iL'}{T}\sin\left(\frac{T}{2}\right) \qquad \gamma = e^{-\frac{i\chi}{2}}\frac{iC}{T}\sin\left(\frac{T}{2}\right), \qquad \text{(53)}$$

where $\chi = \eta - i\kappa$, $L = \text{LB} - i\text{LD}$, $L' = \text{LB}' - i\text{LD}'$, $C = \text{CB} - i\text{CD}$, and $T = \sqrt{L^2 + L'^2 + C^2}$.

If we choose $\theta = T/2$, then the quaternion $\boldsymbol{h}$ can be written as

$$\boldsymbol{h} = e^{\hbar}, \qquad \text{(54)}$$

where $\hbar$ is another quaternion that can be written as

$$\hbar = \frac{-i}{2}(\chi\mathbf{1} + iL\boldsymbol{i} + iL'\boldsymbol{j} - iC\boldsymbol{k}). \qquad \text{(55)}$$

The quaternion $\hbar$ corresponds to the differential $\mathbf{z}$ matrix [9]:

$$\mathbf{z} = \frac{-i}{2}\begin{pmatrix} \chi & L & L' & -C \\ L & \chi & iC & iL' \\ L' & -iC & \chi & -iL \\ -C & -iL' & iL & \chi \end{pmatrix}. \qquad \text{(56)}$$

Now we can differentiate $\boldsymbol{h}$ with respect to l (distance along the direction of propagation of light):

$$\frac{d\boldsymbol{h}}{dl} = \frac{d\hbar}{dl}\boldsymbol{h} = \frac{\hbar}{l}\boldsymbol{h}, \qquad \text{(57)}$$

where we have taken into account that all the parameters in $\hbar$ (χ, L, L', and C) are proportional to l for a nondepolarizing medium [21]. This equation is a reformulation of the Stokes–Mueller differential formalism [22], and it can be compared with the well-known quaternion differentiation formula:

$$\dot{q} = \frac{1}{2}\omega q, \qquad \text{(58)}$$

where ω is the angular velocity. Hence, $2\hbar/l$ can be interpreted as the angular velocity of rotation by an angle $\theta (= T/2)$ of the quaternion state through the medium. Therefore, $\hbar$ describes the changing rate of $\boldsymbol{h}$ along the pathlength.

6. CONCLUSION

The Stokes–Mueller formalism can be reformulated in terms of quaternions. The vector state $|h\rangle$, the matrix state $\mathbf{Z}$, and the Jones matrix $\mathbf{J}$ are isomorphic to the same quaternion state $\boldsymbol{h}$. We have shown how quaternion algebra can be used to replace, or computationally simplify, the representation of optical media states and their mathematical operations.

The transformation of a Stokes vector given by a nondepolarizing Mueller matrix can be expressed by quaternion rotation that can be formally presented as the multiplication of three quaternions. Particularly, if $\mathbf{M}$ is a unitary matrix, then α, β, and γ are pure imaginary numbers, and the quaternion state, $\boldsymbol{h}$, becomes a real quaternion. In this case, the quaternion rotation of the Stokes quaternion can be conceived as a three-dimensional rotation on the Poincaré sphere.

In summary, quaternion algebra can embrace all aspects of the Stokes–Mueller formalism, allowing for a synthetic representation of the matrix algebra used for the description and transformation of polarized light. This compact notation offers practical advantages in computer calculations of polarization effects, and it shows the straightforward connections between different Mueller–Jones operators ($|h\rangle$, $\mathbf{Z}$, and $\mathbf{J}$).

APPENDIX A: OTHER PROPERTIES OF THE h QUATERNION AND SPECIAL CASES

1. The norm of the covariance vector is given by

$$\langle h|h\rangle = \tau\tau^* + \alpha\alpha^* + \beta\beta^* + \gamma\gamma^* = M_{00}. \qquad \text{(A1)}$$

In the quaternion language, this norm corresponds to the real part of the quaternion $\boldsymbol{h}$, multiplied by its Hermitian conjugate:

$$\mathbb{R}(\boldsymbol{h}\boldsymbol{h}^\dagger) = \tau\tau^* + \alpha\alpha^* + \beta\beta^* + \gamma\gamma^* = M_{00}. \qquad \text{(A2)}$$

2. The following property can be used to define successive rotations:

$$(\boldsymbol{h}_i\boldsymbol{h}_j)^\dagger = \boldsymbol{h}_j^\dagger\boldsymbol{h}_i^\dagger. \qquad \text{(A3)}$$

For example, if $\boldsymbol{h}_1$ and $\boldsymbol{h}_2$ are two quaternions corresponding to two rotations, the transformed Stokes quaternion can be written as

$$\boldsymbol{h}_2(\boldsymbol{h}_1 s\boldsymbol{h}_1^\dagger)\boldsymbol{h}_2^\dagger = (\boldsymbol{h}_2\boldsymbol{h}_1)s(\boldsymbol{h}_1^\dagger\boldsymbol{h}_2^\dagger) = (\boldsymbol{h}_2\boldsymbol{h}_1)s(\boldsymbol{h}_2\boldsymbol{h}_1)^\dagger, \qquad \text{(A4)}$$

which means that $\boldsymbol{h}_2\boldsymbol{h}_1$ is the combined rotator.

3. If τ is real, and α, β, and γ are pure imaginary, then

$$\boldsymbol{h}\boldsymbol{h}^\dagger = \boldsymbol{h}^\dagger\boldsymbol{h} = \tau\tau^* + \alpha\alpha^* + \beta\beta^* + \gamma\gamma^* = \langle h|h\rangle = M_{00}, \qquad \text{(A5)}$$

and if $|h\rangle$ is normalized to unity, then

$$\boldsymbol{h}\boldsymbol{h}^\dagger = \boldsymbol{h}^\dagger\boldsymbol{h} = 1. \qquad \text{(A6)}$$

In this case, $\boldsymbol{h}^\dagger$ is the inverse of $\boldsymbol{h}$, and the inverse rotation for Stokes quaternion can be written as

$$s = \boldsymbol{h}^\dagger s'\boldsymbol{h}. \qquad \text{(A7)}$$

This case corresponds to unitary $\mathbf{Z}$ and unitary $\mathbf{M}$ [9].

4. In general, inverse rotation is related to the Hamilton conjugate of the quaternion $\boldsymbol{h}$, which is defined as

$$\bar{\boldsymbol{h}} = \tau\mathbf{1} - i\alpha\boldsymbol{i} - i\beta\boldsymbol{j} - i\gamma\boldsymbol{k}. \qquad \text{(A8)}$$

Since

$$\boldsymbol{h}\bar{\boldsymbol{h}} = \tau^2 - \alpha^2 - \beta^2 - \gamma^2, \qquad \text{(A9)}$$

if $(\tau^2 - \alpha^2 - \beta^2 - \gamma^2) > 0$, the inverse of $\boldsymbol{h}$ can be defined as

$$\boldsymbol{h}^{-1} = \frac{\bar{\boldsymbol{h}}}{\tau^2 - \alpha^2 - \beta^2 - \gamma^2}. \qquad \text{(A10)}$$

Similarly, the inverse of the Hermitian conjugate of $\boldsymbol{h}$ is

$$(\boldsymbol{b}^\dagger)^{-1} = \frac{(\overline{\boldsymbol{b}^\dagger})}{(\tau^*)^2 - (\alpha^*)^2 - (\beta^*)^2 - (\gamma^*)^2}, \tag{A11}$$

where $(\overline{\boldsymbol{b}^\dagger}) = \boldsymbol{b}^* = \tau^*\mathbf{1} - i\alpha^*\boldsymbol{i} - i\beta^*\boldsymbol{j} - i\gamma^*\boldsymbol{k}$.

    5. If τ, α, β, and γ are real,

$$\boldsymbol{b} = \boldsymbol{b}^\dagger. \tag{A12}$$

In this case, transformation of the Stokes quaternion becomes

$$\boldsymbol{s}' = \boldsymbol{b}\boldsymbol{s}\boldsymbol{b}. \tag{A13}$$

This case corresponds to Hermitian $\mathbf{Z}$ and Hermitian $\mathbf{M}$ [9].

REFERENCES

1. P. Pellat-Finet, "Représentation des états et des opérateurs de polarisation de la lumière par des quaternions," Opt. Acta **31**, 415–434 (1984).
2. P. Pellat-Finet and Y. Souche, "Représentation de l'effet d'une réflexion et d'une réfraction sur la lumiére polarisée par le formalisme des quaternions," Opt. Acta **32**, 1317–1322 (1985).
3. L. Liu, C. Wu, C. Shang, Z. Li, and J. Wang, "Quaternion approach to the measurement of the local birefringence distribution in optical fibers," IEEE Photon. J. **7**, 6901014 (2015).
4. M. Karlsson and M. Petersson, "Quaternion approach to PMD and PDL phenomena in optical fiber systems," J. Lightwave Technol. **22**, 1137–1146 (2004).
5. J. J. Gil Pérez and R. Ossikovski, *Polarized Light and the Mueller Matrix Approach* (CRC Press, 2016).
6. J. J. Gil, "Polarimetric characterization of light and media," Eur. Phys. J. Appl. Phys. **40**, 1–47 (2007).
7. J. J. Gil, "Review on Mueller matrix algebra for the analysis of polarimetric measurements," J. Appl. Rem. Sens. **8**, 081599 (2014).
8. A. Aiello and J. P. Woerdman, "Linear algebra for Mueller calculus," arXiv:math-ph/0412061 (2006).
9. E. Kuntman, M. A. Kuntman, and O. Arteaga, "Vector and matrix states for Mueller matrices of nondepolarizing optical media," J. Opt. Soc. Am. A **34**, 80–86 (2017).
10. E. Kuntman, M. A. Kuntman, J. Sancho-Parramon, and O. Arteaga, "Formalism of optical coherence and polarization based on material media states," Phys. Rev. A **95**, 063819 (2017).
11. O. Arteaga, R. Ossikovski, E. Kuntman, M. A. Kuntman, A. Canillas, and E. Garcia-Caurel, "Mueller matrix polarimetry on a Young's double-slit experiment analog," Opt. Lett. **42**, 3900–3903 (2017).
12. M. A. Kuntman, E. Kuntman, J. Sancho-Parramon, and O. Arteaga, "Light scattering by coupled oriented dipoles: decomposition of the scattering matrix," Phys. Rev. B **98**, 045410 (2018).
13. J. J. Gil, "Characteristic properties of Mueller matrices," J. Opt. Soc. Am. A **17**, 328–334 (2000).
14. C. Whitney, "Pauli-algebraic operators in polarization optics," J. Opt. Soc. Am. **61**, 1207–1213 (1971).
15. W. R. Hamilton, "On a new species of imaginary quantities, connected with the theory of quaternions," Proc. R. Irish Acad. (1836-1869) **2**, 424–434 (1840).
16. T. Tudor, "Interaction of light with the polarization devices: a vectorial Pauli algebraic approach," J. Phys. A Math. Theor. **41**, 415303 (2008).
17. R. A. Chipman, "Polarization aberrations," Ph.D. thesis (University of Arizona, 1987).
18. J. J. Gil, I. San José, and R. Ossikovski, "Serial-parallel decompositions of Mueller matrices," J. Opt. Soc. Am. A **30**, 32–50 (2013).
19. J. J. Gil and I. San José, "Polarimetric subtraction of Mueller matrices," J. Opt. Soc. Am. A **30**, 1078–1088 (2013).
20. S. R. Cloude, "Group theory and polarization algebra," Optik **75**, 26–36 (1986).
21. O. Arteaga and A. Canillas, "Analytic inversion of the Mueller-Jones polarization matrices for homogeneous media," Opt. Lett. **35**, 559–561 (2010).
22. O. Arteaga, "Historical revision of the differential Stokes-Mueller formalism: discussion," J. Opt. Soc. Am. A **34**, 410–414 (2017).

A typo has been noted in the paper reproduced above. Below Eq. (31) it should say "where $|h\rangle$, $\mathbf{Z_2}$, $|h\rangle_2$" instead of "where $|h\rangle$, $\mathbf{Z_2}$, $|h\rangle_1$".

Other publications out of topic

The author contributed to these other publications during the doctoral period, but they do not constitute the core of this thesis:

- **Beyond polarization microscopy: Mueller matrix microscopy with frequency demodulation**

  O. Arteaga, E. Kuntman "Beyond polarization microscopy: Mueller matrix microscopy with frequency demodulation," SPIE Proceedings Vol. 9099 (2014).

- **Conversion of a polarization microscope into a Mueller matrix microscope. Application to the measurement of textile fibers**

  E. Kuntman, O. Arteaga, J. Antó, D. Cayuela, E.c Bertran, "Conversion of a polarization microscope into a Mueller matrix microscope. Application to the measurement of textile fibers," Óptica Pura y Aplicada 10.7149/OPA.48.4.309 (2015).

- **Mueller matrix microscopy on a Morpho butterfly**

  O. Arteaga, E. Kuntman, J. Antó, E. Pascual, A. Canillas and E. Bertran, "Mueller matrix microscopy on a Morpho butterfly," J. Phys.: Conf. Ser. 605 012008 (2015).

- **Retrieval of the non-depolarizing components of depolarizing Mueller matrices by using symmetry conditions and least squares minimization**

  E. Kuntman, A. Canillas, O. Arteaga, "Retrieval of the non-depolarizing components of depolarizing Mueller matrices by using symmetry conditions and least squares minimization," Applied Surface Science 421, 607-731 (2017).

Chapter 4

Discussion and Conclusions

In classical mechanics the state of the system is represented by a point in the phase space. In quantum mechanics state of the particle is a vector in the Hilbert space. In this thesis we introduce a vector state $|h\rangle$ that represents the state of the optical medium. $|h\rangle$ is a four component complex vector:

$$|h\rangle = \begin{pmatrix} \tau \\ \alpha \\ \beta \\ \gamma, \end{pmatrix} \tag{4.1}$$

Components of $|h\rangle$ can be defined in terms of basic spectroscopic parameters, isotropic phase retardation (η), isotropic amplitude absorption (κ), circular dichroism (CD), circular birefringence (CB), horizontal and 45° linear dichorism (LD and LD'), horizontal and 45° linear birefringence (LB and LB'):

$$\tau = e^{-\frac{i\chi}{2}} \cos\left(\frac{T}{2}\right),$$

$$\alpha = -e^{-\frac{i\chi}{2}} \frac{iL}{T} \sin\left(\frac{T}{2}\right),$$

$$\beta = -e^{-\frac{i\chi}{2}} \frac{iL'}{T} \sin\left(\frac{T}{2}\right),$$

$$\gamma = e^{-\frac{i\chi}{2}} \frac{iC}{T} \sin\left(\frac{T}{2}\right) \tag{4.2}$$

where $\chi = \eta - i\kappa$, $L = LB - iLD$, $L' = LB' - iLD'$, $C = CB - iCD$, $T = \sqrt{L^2 + L'^2 + C^2}$.

The vector state is closely related with the matrix state $\mathbf{Z}$. The matrix state, $\mathbf{Z}$, is a 4×4 complex matrix which is isomorphic to the 2×2 Jones matrix. In this thesis we have shown that there also exists a quaternion state representation of the optical medium. The Jones

matrix and $\mathbf{Z}$ matrix are isomorphic matrix representations of the quaternion state $\boldsymbol{h}$. It is also worth to emphasize that the quaternion state has a similar structure with the $|h\rangle$ vector, but, the quaternion state has one more property. Multiplication of $|h\rangle$ vectors as $|h_1\rangle|h_2\rangle\cdots|h_N\rangle$ is not feasible, but, quaternion multiplication of quaternion states is feasible and yields another quaternion state:

$$\boldsymbol{h} = \boldsymbol{h_1}\boldsymbol{h_2}\cdots\boldsymbol{h_N} \tag{4.3}$$

Jones matrices and $\mathbf{Z}$ have the same property:

$$\mathbf{J} = \mathbf{J_1}\mathbf{J_2}\cdots\mathbf{J_N}$$

$$\mathbf{Z} = \mathbf{Z_1}\mathbf{Z_2}\cdots\mathbf{Z_N} \tag{4.4}$$

But these state representations do not form a group under multiplication because multiplicative inverse elements do not exist, in general.

$|h\rangle$ vector, Jones matrix, $\mathbf{Z}$ matrix and $\boldsymbol{h}$ quaternion can be added by themselves to yield states of the same kind:

$$|h\rangle = c_1|h_1\rangle + c_2|h_2\rangle + \cdots c_N|h_N\rangle, \tag{4.5}$$

$$\mathbf{J} = c_1\mathbf{J_1} + c_2\mathbf{J_2} + \cdots c_N\mathbf{J_N}, \tag{4.6}$$

$$\mathbf{Z} = c_1\mathbf{Z_1} + c_2\mathbf{Z_2} + \cdots c_N\mathbf{Z_N}, \tag{4.7}$$

$$\boldsymbol{h} = c_1\boldsymbol{h_1} + c_2\boldsymbol{h_2} + \cdots c_N\boldsymbol{h_N}. \tag{4.8}$$

In order to make use of the usual vector and matrix manipulations, vector state, $|h\rangle$, may have several advantages over the other state representations. For example, it is possible to define a scalar product, $\langle h_i|h_j\rangle$, and an outer product, $|h_i\rangle\langle h_j|$, of $|h\rangle$ vectors. Scalar product of vector states is especially useful to implement the usual vector algebra for decomposition of media states into more basic states that serve as basis states. Outer product of $|h\rangle$ vectors allows to define another matrix state, $\mathbf{H}$:

$$\mathbf{H} = |h\rangle\langle h|. \tag{4.9}$$

The matrix state $\mathbf{H}$ can be interpreted as a density matrix with an analogy with the quantum mechanical density matrix. Density matrix interpretation becomes more significant when we study depolarization. In case of depolarization, $\mathbf{H}$ matrix represents the mixed state of the mixture.

2×2 complex Jones matrices are basic elements of the theory of deterministic optical systems. Addition and multiplication of two or more Jones matrices yields another Jones matrix,

therefore, Jones matrices are suitable to represent coherent parallel and series combinations of deterministic optical systems. For example, let $\mathbf{J_1}$ and $\mathbf{J_2}$ represent two deterministic optical systems, and let $\mathbf{J}$ be the Jones matrix of the coherent parallel combination of two systems:

$$\mathbf{J} = c_1\mathbf{J_1} + c_2\mathbf{J_2}. \tag{4.10}$$

The associated nondepolarizing Mueller matrix of the combined system can be obtained from the Jones matrices by the transformation, $\mathbf{M}_i = \mathbf{A}(\mathbf{J}_i \otimes \mathbf{J}_i^*)\mathbf{A}^\dagger$, where $\mathbf{A}$ is the unitary matrix defined in Eq. (1.13):

$$\mathbf{M} = \mathbf{A}[(c_1\mathbf{J_1} + c_2\mathbf{J_2}) \otimes (c_1\mathbf{J_1} + c_2\mathbf{J_2})^*]\mathbf{A}^\dagger, \tag{4.11}$$

where c_1 and c_2 are generally complex coefficients. 4×4 complex $\mathbf{Z}$ matrices have very similar properties with Jones matrices. They can be added, they can be multiplied, hence they are suitable for representing parallel and serial processes. $\mathbf{Z}$ matrices have a very simple relation with nondepolarizing Mueller matrices, $\mathbf{M} = \mathbf{Z}\mathbf{Z}^* = \mathbf{Z}^*\mathbf{Z}$. This relation considerably simplifies the algebra of Eq.(4.11). Let us consider a coherent combination of two deterministic optical systems represented by $\mathbf{Z}$ matrices:

$$\mathbf{Z} = c_1\mathbf{Z_1} + c_2\mathbf{Z_2}, \tag{4.12}$$

where $\mathbf{Z_1}$ and $\mathbf{Z_2}$ are the matrix states corresponding to component systems and $\mathbf{Z}$ is the matrix state of the combined system. The associated nondepolarizing Mueller matrix can be found without applying tedious steps of Kronecker matrix product and unitary transformations performed by multiplying from left and right with $\mathbf{A}$ and $\mathbf{A}^\dagger$ matrices:

$$\mathbf{M} = (c_1\mathbf{Z_1} + c_2\mathbf{Z_2})(c_1\mathbf{Z_1} + c_2\mathbf{Z_2})^*. \tag{4.13}$$

As it was shown in [22], $\mathbf{Z}$ matrix formalism is also very useful for formulating partial coherence. It is possible to study interference effects in a complete polarimetric version of Young's double slit experiment with gradually diminishing coherence. As the pinhole size increases, the phase variations are averaged over the measurement area leading to partially coherent or incoherent results that exhibit depolarization effects. These effects can be clearly observed in the elements of the Mueller matrix of the combined system.

A covariance matrix (density matrix), $\mathbf{H}$, can be defined as an outer product of $|h\rangle$ vectors: $\mathbf{H} = |h\rangle\langle h|$. Here, we have a strong analogy with the state description of quantum mechanics in terms of density operators (matrices). $\mathbf{H}$ matrix can be considered as a density matrix. If rank of $\mathbf{H}$ matrix is one, i.e., $\mathbf{H}$ matrix has only one nonzero eigenvalue, $\mathbf{H}$ is a density matrix

(density operator) representing a pure state (deterministic optical system). Analogy with quantum mechanical density operator formalism can be made for mixed states also. If two or more optical systems are incoherently combined Mueller matrix of the system becomes a depolarizing Mueller matrix which can be written as a convex sum of its components:

$$\mathbf{M} = w_1\mathbf{M_1} + w_2\mathbf{M_2} + w_3\mathbf{M_3} + \cdots \tag{4.14}$$

Rank of the $\mathbf{H}$ matrix associated with the depolarizing Mueller matrix, $\mathbf{M}$, is greater than one and, in general, it can be at most four. In other words, in case of depolarization, the matrix $\mathbf{H}$ has two, three or four nonzero eigenvalues, and it represents a mixed state of a mixture:

$$\mathbf{H} = w_1\mathbf{H_1} + w_2\mathbf{H_2} + w_3\mathbf{H_3} + \cdots \tag{4.15}$$

It is worth noting that, in quantum mechanics, a mixture does not have a vector state, $|\Psi\rangle$, it can only be represented by a density matrix, ρ. Similarly, in polarization algebra, a depolarizing Mueller matrix cannot be associated with a vector state, $|h\rangle$, i.e., a mixture does not have a vector state.

$\mathbf{H}$ matrix formalism is especially useful in the decomposition procedure of depolarizing Mueller matrices into their nondepolarizing components. It can be shown that, under certain symmetry conditions, two-term combinations of nondepolarizing Mueller matrices can be resolved, and the original component Mueller matrices can be retrieved uniquely by means of the rank considerations of $\mathbf{H}$ matrices.

In this thesis it is shown that Jones matrices, $\mathbf{Z}$ matrices and $|h\rangle$ vectors are just different forms of the quaternion state, $\boldsymbol{h}$. Quaternion states can be added, can be multiplied and they transform (rotate) the associated Stokes quaternion, $\boldsymbol{s}$ into $\boldsymbol{s'}$ by means of the triple quaternion multiplication, $\boldsymbol{s'} = \boldsymbol{h}\boldsymbol{s}\boldsymbol{h}^\dagger$, where $\boldsymbol{s}$ is the quaternion form of Stokes vector ($\boldsymbol{s} = s_0\mathbf{1} + is_1\mathbf{i} + is_2\mathbf{j} + is_3\mathbf{k}$), $\boldsymbol{h}^\dagger$ is the Hermitian conjugate of $\boldsymbol{h}$ and $\boldsymbol{s'}$ is the transformed (rotated) Stokes quaternion that corresponds to the output Stokes vector $|s'\rangle$ of Stokes-Mueller formalism,

$$|s'\rangle = \mathbf{M}|s\rangle, \tag{4.16}$$

where $|s\rangle$ is the usual Stokes vector.

The vector state $|h\rangle$ does not have an exponential form, but the quaternion state $\boldsymbol{h}$ (and $\mathbf{Z}$ matrix) can be written in an exponential form:

$$\boldsymbol{h} = e^{\hbar},$$

$$\hbar = -\frac{i}{2}(\chi\mathbf{1} + iL\mathbf{i} + iL'\mathbf{j} - iC\mathbf{k}). \tag{4.17}$$

When we differentiate $\boldsymbol{h}$ with respect to ℓ (distance along the direction of propagation of light) we get

$$\frac{d\boldsymbol{h}}{d\ell} = \frac{d\hbar}{d\ell}\boldsymbol{h} = \frac{\hbar}{\ell}\boldsymbol{h}. \tag{4.18}$$

This equation is a reformulation of the Stokes–Mueller differential formalism, and it can be compared with the well-known quaternion differentiation formula:

$$\dot{\boldsymbol{q}} = \frac{1}{2}\omega\boldsymbol{q}, \tag{4.19}$$

where ω is the angular velocity. Hence, $2\hbar/\ell$ can be interpreted as the angular velocity of rotation by an angle $\theta(= T/2)$ of the quaternion state through the medium, where $\hbar$ describes the changing rate of $\boldsymbol{h}$ along the pathlength. Since, the vector state $|h\rangle$ and matrix state concepts (Jones and $\mathbf{Z}$ matrices) are different forms of the same quaternion state, $\boldsymbol{h}$, quaternion state may serve as a key element for the unification of all formalisms developed thus far at different stages by many contributors.

The vector state approach is especially useful for the analysis of interacting systems. The state of an interacting system can be resolved into its basic constituents and interaction states:

$$|h\rangle = g_1|h\rangle_1 + g_2|h\rangle_2 + \cdots g_{int}|h\rangle_{int}. \tag{4.20}$$

In general, there may be more than one interaction state depending on the geometry and the number of particles.

As an implementation of vector state formalism we study the scattering matrix of a coupled dipole dimer and show that it can be written as a linear combination of three states which have clear physical (and geometrical) meanings. The study of the interaction term permits a clear understanding of several phenomena occurring in particle dimers, such as the emergence of optical activity in certain achiral and chiral configurations, hybridization effects and Fano resonances. As an example, we study the dipolar resonance of coupled plasmonic nanoantennas which are simulated by elaborated numerical methods.

Given these results, the main conclusions of this work are:

- The coherent (constant phase) parallel combination of deterministic systems can be written as a linear combination of $\mathbf{Z}$ matrices with complex coefficients. In practice this means that we can synthesize any nondepolarizing optical system as a coherent linear combination of a complete set of nondepolarizing basis systems. This leads to the concept of "linear combination of states" of optical media, and allows us to make

an analogy between the quantum mechanical wave function Ψ and $\mathbf{Z}$ matrix by means of the relation, $\mathbf{ZZ}^* = \mathbf{M}$.

- The analogy with quantum mechanics allows us to directly formulate the optical combinations of optical media without need of an explicit consideration of the superposition of electromagnetic fields, which is the starting point of other formulations of optical coherence. We think that our formalism introduces a unified theory of coherence and polarization that can be especially useful for experimental techniques that explore polarized light and material media interactions such as polarimetry or ellipsometry.

- As an application of the formalism we study interacting dipole systems and we obtain an analytic expression that provides the frequencies of the hybrid modes for any geometric arrangement of dipoles in a plane. Fano-like resonances can be also explained from the interference between the matrix states of our decomposition.

- The Stokes–Mueller formalism can be reformulated in terms of quaternions. The vector state $|h\rangle$, the matrix state $\mathbf{Z}$, and the Jones matrix $\mathbf{J}$ are isomorphic to the same quaternion state $\boldsymbol{h}$. We have shown how quaternion algebra can be used to replace, or computationally simplify, the representation of optical media states and their mathematical operations.

- The hybridization-induced spectral splitting in coupled oriented dimers can be well explained by our decomposition method. The hybrid basis that we have defined allows to quantitatively distinguish the contribution of in-phase and out-of-phase modes to the overall scattering intensity in particles with anisotropic polarizability, something that, to our knowledge, has never been achieved with prior descriptions of plasmonic hybridization processes. This is possible even for weakly coupled particles, where no evident peak splitting is observed in the scattering cross-sections. Our analytical model provides a simple framework to understand and quantify the relative contribution of coupled modes in complex nanostructures. We think that this analytic method can be particularly useful in nanophotonic applications that make use of small antenna-like elements for controlling electromagnetic waves such as optical trapping, single-molecule localization and recognition or surface-enhanced spectroscopy.

- Near-field scattering fingerprint for an achiral dipole dimer can be drastically modified by only adjusting the handedness of the incoming polarization, but this will not substantially alter far-field response for small scattering angles.

- For depolarizing polarimetric experiments,which are a combination of two nondepolarizing states, it is possible to analytically retrieve the individual polarimetric response of each component.

The nano scale, being an intermediate scale between the macroscopic and microscopic systems, is an area of optical effects peculiar of its own. But, these effects still can be described classically without making any reference to genuine quantum concepts such as quantization. However, when we go to more smaller dimensions, nanoparticles will inevitably begin to display quantum effects. In that limit we may expect that the analogy between the vector/matrix states and the quantum state vectors may offer a starting point for foundation of a new formalism that deals with quantized properties of nanoparticles.

Appendix: list of vectors and matrix states

This appendix contains a tabulated list of $|h\rangle$ vector states, $\mathbf{Z}$ matrix states and their corresponding Mueller matrix $\mathbf{M}$.

Optical element	$\lvert h\rangle$	$\mathbf{Z}$	$\mathbf{M}$
Free space	$\begin{pmatrix} 1 \\ 0 \\ 0 \\ 0 \end{pmatrix}$	$\begin{pmatrix} 1 & 0 & 0 & 0 \\ 0 & 1 & 0 & 0 \\ 0 & 0 & 1 & 0 \\ 0 & 0 & 0 & 1 \end{pmatrix}$	$\begin{pmatrix} 1 & 0 & 0 & 0 \\ 0 & 1 & 0 & 0 \\ 0 & 0 & 1 & 0 \\ 0 & 0 & 0 & 1 \end{pmatrix}$
Half-wave plate (Ideal mirror)	$\begin{pmatrix} 0 \\ 1 \\ 0 \\ 0 \end{pmatrix}$	$\begin{pmatrix} 0 & 1 & 0 & 0 \\ 1 & 0 & 0 & 0 \\ 0 & 0 & 0 & -i \\ 0 & 0 & i & 0 \end{pmatrix}$	$\begin{pmatrix} 1 & 0 & 0 & 0 \\ 0 & 1 & 0 & 0 \\ 0 & 0 & -1 & 0 \\ 0 & 0 & 0 & -1 \end{pmatrix}$
Half-wave plate 45º fast axis	$\begin{pmatrix} 0 \\ 0 \\ 1 \\ 0 \end{pmatrix}$	$\begin{pmatrix} 0 & 0 & 1 & 0 \\ 0 & 0 & 0 & i \\ 1 & 0 & 0 & 0 \\ 0 & -i & 0 & 0 \end{pmatrix}$	$\begin{pmatrix} 1 & 0 & 0 & 0 \\ 0 & -1 & 0 & 0 \\ 0 & 0 & 1 & 0 \\ 0 & 0 & 0 & -1 \end{pmatrix}$
Circular retarder ($\delta = \pi$)	$\begin{pmatrix} 0 \\ 0 \\ 0 \\ 1 \end{pmatrix}$	$\begin{pmatrix} 0 & 0 & 0 & 1 \\ 0 & 0 & -i & 0 \\ 0 & i & 0 & 0 \\ 1 & 0 & 0 & 0 \end{pmatrix}$	$\begin{pmatrix} 1 & 0 & 0 & 0 \\ 0 & -1 & 0 & 0 \\ 0 & 0 & -1 & 0 \\ 0 & 0 & 0 & 1 \end{pmatrix}$
Horizontal Linear Polarizer	$\begin{pmatrix} \frac{1}{\sqrt{2}} \\ \frac{1}{\sqrt{2}} \\ 0 \\ 0 \end{pmatrix}$	$\begin{pmatrix} \frac{1}{\sqrt{2}} & \frac{1}{\sqrt{2}} & 0 & 0 \\ \frac{1}{\sqrt{2}} & \frac{1}{\sqrt{2}} & 0 & 0 \\ 0 & 0 & \frac{1}{\sqrt{2}} & \frac{-i}{\sqrt{2}} \\ 0 & 0 & \frac{i}{\sqrt{2}} & \frac{1}{\sqrt{2}} \end{pmatrix}$	$\begin{pmatrix} 1 & 1 & 0 & 0 \\ 1 & 1 & 0 & 0 \\ 0 & 0 & 0 & 0 \\ 0 & 0 & 0 & 0 \end{pmatrix}$
Vertical Linear Polarizer	$\begin{pmatrix} \frac{1}{\sqrt{2}} \\ \frac{-1}{\sqrt{2}} \\ 0 \\ 0 \end{pmatrix}$	$\begin{pmatrix} \frac{1}{\sqrt{2}} & \frac{-1}{\sqrt{2}} & 0 & 0 \\ \frac{-1}{\sqrt{2}} & \frac{1}{\sqrt{2}} & 0 & 0 \\ 0 & 0 & \frac{1}{\sqrt{2}} & \frac{i}{\sqrt{2}} \\ 0 & 0 & \frac{-i}{\sqrt{2}} & \frac{1}{\sqrt{2}} \end{pmatrix}$	$\begin{pmatrix} 1 & -1 & 0 & 0 \\ -1 & 1 & 0 & 0 \\ 0 & 0 & 0 & 0 \\ 0 & 0 & 0 & 0 \end{pmatrix}$

Optical element	$\lvert h\rangle$	$\mathbf{Z}$	$\mathbf{M}$
Linear Polarizer at 45°	$\begin{pmatrix} \frac{1}{\sqrt{2}} \\ 0 \\ \frac{1}{\sqrt{2}} \\ 0 \end{pmatrix}$	$\begin{pmatrix} \frac{1}{\sqrt{2}} & 0 & \frac{1}{\sqrt{2}} & 0 \\ 0 & \frac{1}{\sqrt{2}} & 0 & \frac{i}{\sqrt{2}} \\ \frac{1}{\sqrt{2}} & 0 & \frac{1}{\sqrt{2}} & 0 \\ 0 & \frac{-i}{\sqrt{2}} & 0 & \frac{1}{\sqrt{2}} \end{pmatrix}$	$\begin{pmatrix} 1 & 0 & 1 & 0 \\ 0 & 0 & 0 & 0 \\ 1 & 0 & 1 & 0 \\ 0 & 0 & 0 & 0 \end{pmatrix}$
Linear Polarizer at 135°	$\begin{pmatrix} \frac{1}{\sqrt{2}} \\ 0 \\ \frac{-1}{\sqrt{2}} \\ 0 \end{pmatrix}$	$\begin{pmatrix} \frac{1}{\sqrt{2}} & 0 & \frac{-1}{\sqrt{2}} & 0 \\ 0 & \frac{1}{\sqrt{2}} & 0 & \frac{-i}{\sqrt{2}} \\ \frac{-1}{\sqrt{2}} & 0 & \frac{1}{\sqrt{2}} & 0 \\ 0 & \frac{i}{\sqrt{2}} & 0 & \frac{1}{\sqrt{2}} \end{pmatrix}$	$\begin{pmatrix} 1 & 0 & -1 & 0 \\ 0 & 0 & 0 & 0 \\ -1 & 0 & 1 & 0 \\ 0 & 0 & 0 & 0 \end{pmatrix}$
Circular Polarizer (right handed)	$\begin{pmatrix} \frac{1}{\sqrt{2}} \\ 0 \\ 0 \\ \frac{1}{\sqrt{2}} \end{pmatrix}$	$\begin{pmatrix} \frac{1}{\sqrt{2}} & 0 & 0 & \frac{1}{\sqrt{2}} \\ 0 & \frac{1}{\sqrt{2}} & \frac{-i}{\sqrt{2}} & 0 \\ 0 & \frac{i}{\sqrt{2}} & \frac{1}{\sqrt{2}} & 0 \\ \frac{1}{\sqrt{2}} & 0 & 0 & \frac{1}{\sqrt{2}} \end{pmatrix}$	$\begin{pmatrix} 1 & 0 & 0 & 1 \\ 0 & 0 & 0 & 0 \\ 0 & 0 & 0 & 0 \\ 1 & 0 & 0 & 1 \end{pmatrix}$
Circular Polarizer (left handed)	$\begin{pmatrix} \frac{1}{\sqrt{2}} \\ 0 \\ 0 \\ \frac{-1}{\sqrt{2}} \end{pmatrix}$	$\begin{pmatrix} \frac{1}{\sqrt{2}} & 0 & 0 & \frac{-1}{\sqrt{2}} \\ 0 & \frac{1}{\sqrt{2}} & \frac{i}{\sqrt{2}} & 0 \\ 0 & \frac{-i}{\sqrt{2}} & \frac{1}{\sqrt{2}} & 0 \\ \frac{-1}{\sqrt{2}} & 0 & 0 & \frac{1}{\sqrt{2}} \end{pmatrix}$	$\begin{pmatrix} 1 & 0 & 0 & -1 \\ 0 & 0 & 0 & 0 \\ 0 & 0 & 0 & 0 \\ -1 & 0 & 0 & 1 \end{pmatrix}$
QWP horizontal fast axis	$\begin{pmatrix} \frac{1}{\sqrt{2}} \\ \frac{i}{\sqrt{2}} \\ 0 \\ 0 \end{pmatrix}$	$\begin{pmatrix} \frac{1}{\sqrt{2}} & \frac{i}{\sqrt{2}} & 0 & 0 \\ \frac{i}{\sqrt{2}} & \frac{1}{\sqrt{2}} & 0 & 0 \\ 0 & 0 & \frac{1}{\sqrt{2}} & \frac{1}{\sqrt{2}} \\ 0 & 0 & \frac{-1}{\sqrt{2}} & \frac{1}{\sqrt{2}} \end{pmatrix}$	$\begin{pmatrix} 1 & 0 & 0 & 0 \\ 0 & 1 & 0 & 0 \\ 0 & 0 & 0 & 1 \\ 0 & 0 & -1 & 0 \end{pmatrix}$
QWP vertical fast axis	$\begin{pmatrix} \frac{1}{\sqrt{2}} \\ \frac{-i}{\sqrt{2}} \\ 0 \\ 0 \end{pmatrix}$	$\begin{pmatrix} \frac{1}{\sqrt{2}} & \frac{-i}{\sqrt{2}} & 0 & 0 \\ \frac{-i}{\sqrt{2}} & \frac{1}{\sqrt{2}} & 0 & 0 \\ 0 & 0 & \frac{1}{\sqrt{2}} & \frac{-1}{\sqrt{2}} \\ 0 & 0 & \frac{1}{\sqrt{2}} & \frac{1}{\sqrt{2}} \end{pmatrix}$	$\begin{pmatrix} 1 & 0 & 0 & 0 \\ 0 & 1 & 0 & 0 \\ 0 & 0 & 0 & -1 \\ 0 & 0 & 1 & 0 \end{pmatrix}$

Optical element	$|h\rangle$	$\mathbf{Z}$	$\mathbf{M}$
QWP fast axis 135º	$\begin{pmatrix} \frac{1}{\sqrt{2}} \\ 0 \\ \frac{i}{\sqrt{2}} \\ 0 \end{pmatrix}$	$\begin{pmatrix} \frac{1}{\sqrt{2}} & 0 & \frac{i}{\sqrt{2}} & 0 \\ 0 & \frac{1}{\sqrt{2}} & 0 & \frac{-1}{\sqrt{2}} \\ \frac{i}{\sqrt{2}} & 0 & \frac{1}{\sqrt{2}} & 0 \\ 0 & \frac{1}{\sqrt{2}} & 0 & \frac{1}{\sqrt{2}} \end{pmatrix}$	$\begin{pmatrix} 1 & 0 & 0 & 0 \\ 0 & 0 & 0 & -1 \\ 0 & 0 & 1 & 0 \\ 0 & 1 & 0 & 0 \end{pmatrix}$
QWP fast axis 45º	$\begin{pmatrix} \frac{1}{\sqrt{2}} \\ 0 \\ \frac{-i}{\sqrt{2}} \\ 0 \end{pmatrix}$	$\begin{pmatrix} \frac{1}{\sqrt{2}} & 0 & \frac{-i}{\sqrt{2}} & 0 \\ 0 & \frac{1}{\sqrt{2}} & 0 & \frac{1}{\sqrt{2}} \\ \frac{-i}{\sqrt{2}} & 0 & \frac{1}{\sqrt{2}} & 0 \\ 0 & \frac{-1}{\sqrt{2}} & 0 & \frac{1}{\sqrt{2}} \end{pmatrix}$	$\begin{pmatrix} 1 & 0 & 0 & 0 \\ 0 & 0 & 0 & 1 \\ 0 & 0 & 1 & 0 \\ 0 & -1 & 0 & 0 \end{pmatrix}$
Circular retarder ($\delta = \frac{\pi}{2}$)	$\begin{pmatrix} \frac{1}{\sqrt{2}} \\ 0 \\ 0 \\ \frac{i}{\sqrt{2}} \end{pmatrix}$	$\begin{pmatrix} \frac{1}{\sqrt{2}} & 0 & 0 & \frac{i}{\sqrt{2}} \\ 0 & \frac{1}{\sqrt{2}} & \frac{1}{\sqrt{2}} & 0 \\ 0 & \frac{-1}{\sqrt{2}} & \frac{1}{\sqrt{2}} & 0 \\ \frac{i}{\sqrt{2}} & 0 & 0 & \frac{1}{\sqrt{2}} \end{pmatrix}$	$\begin{pmatrix} 1 & 0 & 0 & 0 \\ 0 & 0 & 1 & 0 \\ 0 & -1 & 0 & 0 \\ 0 & 0 & 0 & 1 \end{pmatrix}$
Circular retarder ($\delta = -\frac{\pi}{2}$)	$\begin{pmatrix} \frac{1}{\sqrt{2}} \\ 0 \\ 0 \\ \frac{-i}{\sqrt{2}} \end{pmatrix}$	$\begin{pmatrix} \frac{1}{\sqrt{2}} & 0 & 0 & \frac{-i}{\sqrt{2}} \\ 0 & \frac{1}{\sqrt{2}} & \frac{-1}{\sqrt{2}} & 0 \\ 0 & \frac{1}{\sqrt{2}} & \frac{1}{\sqrt{2}} & 0 \\ \frac{-i}{\sqrt{2}} & 0 & 0 & \frac{1}{\sqrt{2}} \end{pmatrix}$	$\begin{pmatrix} 1 & 0 & 0 & 0 \\ 0 & 0 & -1 & 0 \\ 0 & 1 & 0 & 0 \\ 0 & 0 & 0 & 1 \end{pmatrix}$

QWP stands for Quarter Wave Plate.

Bibliography

[1] D. H. Goldstein and E. Collett. *Polarized Light*. New York: Marcel Dekker, (2003).

[2] J. Tinbergen, *Astronomical polarimetry*. Cambridge University Press, New York, N.Y (1996).

[3] R. A. Chipman, Polarimetry, chapter 22 in *Handbook of Optics* II, 2nd Ed, McGraw-Hill, (1995).

[4] J. J. Gil and R. Ossikovski, *Polarized Light and the Mueller Matrix Approach* (CRC Press, 2016).

[5] J. C. Maxwell, "A dynamical theory of the electromagnetic field," Philosophical Transactions of the Royal Society of London, 155, 459-513. (1865).

[6] P. A. M. Dirac, "A new notation for quantum mechanics," Math. Proc. Cambridge Phil. Soc. 35 (3): 416–418 (1939).

[7] N. G. Parke, "Optical Algebra," J. Math. Phys. 28, 131 (1949).

[8] C. R. Jones, "A New Calculus for the Treatment of Optical Systems I. Description and Discussion of the Calculus," J. Opt. Soc. Am. 31, 488-493 (1941).

[9] C. R. Jones, "New calculus for the treatment of optical systems. VII. Properties of the N-matrices," J. Opt. Soc. Am. 38, 671–685 (1948).

[10] G. G. Stokes, "On the composition and resolution of streams of polarized light from different sources," Trans. Cambridge Phil. Soc. 9, 399–416 (1852).

[11] H. Mueller, "The foundations of optics", Journal of the Optical Society of America 38, 661–662 (1948).

[12] M. P. Soleillet, "Sur les paramètres caractérisant la polarisation partielle de la lumière dans les phénomènes de fluorescence", Annales de Physique 12, 23 (1929).

[13] F. Perrin, "Polarization of light scattered by isotropic opalescent media," J. Chem. Phys. 10, 415-427 (1942).

[14] O. Arteaga, "Historical revision of the differential Stokes-Mueller formalism: Discussion," J. Opt. Soc. Am. A 34, 410-414 (2017).

[15] J. J. Gil, E. Bernabeu, "A depolarization criterion in Mueller matrices," Journal of Modern Optics pp. 259–261 (1985).

[16] J. J. Gil, E. Bernabeu, "Depolarization and polarization indices of an optical system," Journal of Modern Optics 33, 185–189 (1986).

[17] A. Aiello, J. P. Woerdman, "Linear algebra for Mueller calculus," arXiv:math-ph/0412061 (2006).

[18] S. R. Cloude, "Group theory and polarization algebra," Optik 75, 26-36 (1986).

[19] S. R. Cloude, "Conditions for the physical realizability of matrix operators in polarimetry." In Polarization Considerations for Optical Systems II, vol. 1166, pp. 177–185. Bellingham (1989).

[20] E. Kuntman, M. A. Kuntman, and O. Arteaga, "Vector and matrix states for Mueller matrices of nondepolarizing optical media," J. Opt. Soc. Am. A 34, 80 (2017).

[21] E. Kuntman, M. A. Kuntman, J. Sancho-Parramon, and O. Arteaga, "Formalism of optical coherence and polarization based on material media states," Phys. Rev. A 95, 063819 (2017).

[22] O. Arteaga, R. Ossikovski, E. Kuntman, M. A. Kuntman, A. Canillas and E. Garcia-Caurel, "Mueller matrix polarimetry on a Young's double-slit experiment analog," Opt. Lett. 42, 3900–3903 (2017).

[23] C. J. R. Sheppard, A. Le Gratiet and A. Diaspro, "Factorization of the coherency matrix of polarization optics," J. Opt. Soc. Am. A 35, 586-590 (2018).

[24] C. J. R. Sheppard, A. Bendandi, A. Le Gratiet and A. Diaspro, "Coherency and differential Mueller matrices for polarizing media," J. Opt. Soc. Am. A 35,2058-2069 (2018).

[25] O. Arteaga, Z. El-Hachemi, and R. Ossikovski, "Snapshot circular dichroism measurements," Opt. Express 27, 6746-6756 (2019).

[26] R. Chipman "Polarization Aberrations," Ph.D. thesis (University of Arizona, 1987).

[27] U. Fano, "Remarks on the Classical and Quantum-Mechanical Treatment of Partial Polarization," J. Opt. Soc. Am. 39, 859-863 (1949).

[28] U. Fano, "A Stokes-Parameter Technique for the Treatment of Polarization in Quantum Mechanics." Phys. Rev., 93, p. 121 (1954)

[29] L. Mandel, E. Wolf, *Optical Coherence and Quantum Optics*, Cambridge:Cambridge University Press (1995).

[30] O. Arteaga, E. Garcia-Caurel, and R. Ossikovski, "Anisotropy coefficients of a Mueller matrix," J. Opt. Soc. Am. A 28, 548–553 (2011).

[31] J. Schellman, H. P. Jensen, "Optical spectroscopy of oriented molecules," Chemical Reviews 87, 1359–1399 (1987).

[32] O. Arteaga, "Mueller matrix polarimetry of anisotropic chiral media," Ph.D. thesis (University of Barcelona, 2010).

[33] O. Arteaga, A. Canillas, "Analytic inversion of the Mueller–Jones polarization matrices for homogeneous media," Opt. Lett. 35, 559-561 (2010).

[34] J. J. Gil, "Polarimetric characterization of light and media," Eur. Phys. J. Appl. Phys. 40, 1 (2007).

[35] D. Griffiths, D. Schroeter, *Introduction to Quantum Mechanics*. Cambridge: Cambridge University Press (2018).

[36] S. Pancharatnam, "Generalized theory of interference, and its applications," Proc. Indian Acad. Sci. 44: 247 (1956).

[37] R. Ossikovski, O. Arteaga, J. Vizet, and E. Garcia-Caurel, "On the equivalence between Young's double-slit and crystal double-refraction interference experiments," J. Opt. Soc. Am. A 34, 1309-1314 (2017).

[38] D. F. J. Arago, A. J. Fresnel, "On the action of rays of polarized light upon each other," Ann. Chim. Phys. 2, 288–304 (1819).

[39] E. Kuntman, M. A. Kuntman, A. Canillas, O. Arteaga, "Quaternion algebra for Stokes-Mueller formalizm," J. Opt. Soc. Am. A 36, 492-497 (2019).

[40] W. R. Hamilton. "On a new species of imaginary quantities connected with the theory of quaternions," Proceedings of the Royal Irish Academy, 2:424–434, (1844).

[41] C. Whitney, "Pauli-algebric operations in polarization optics," J. Opt. Soc. Am. 61, 1207-1213 (1971).

[42] P. Pellat-Finet, "Représentation des états et des opérateurs de polarisation de la lumière par des quaternions," Opt. Acta 31, 415-434 (1984).

[43] P. Pellat-Finet, "Représentation de l'effect d'une réflexion et dune réfraction sur la lumiére polarisée par le formalisme des quaternions," Opt. Acta 32, 1317-1322 (1984).

[44] R. Barakat, "Exponential versions of the Jones and Mueller-Jones polarization matrices," J. Opt. Soc. Am. A 13, 158-163 (1996).

[45] M. A. Kuntman, E. Kuntman, J. Sancho-Parramon, and O. Arteaga, "Light scattering by coupled oriented dipoles: decomposition of the scattering matrix," Phys. Rev. B 98, 045410 (2018).

[46] J. J. Gil, "Review on Mueller matrix algebra for the analysis of polarimetric measurements," Journal of Applied Remote Sensing 8, 081599 (2014).

[47] S. B. Singham, C. F. Bohren, "Light scattering by an arbitrary particle: the scattering-order formulation of the coupled-dipole method," J. Opt. Soc. Am. A 5, 1867-1872 (1988).

[48] M. Schäferling, *Chiral Nanophotonics: Chiral Optical Properties of Plasmonic Systems*, Springer (2017).

[49] P. Nordlander, C. Oubre, E. Prodan, K. Li and M. I. Stockman "Plasmon Hybridization in Nanoparticle Dimers," Nano Letters 4 (5), 899-903 (2004).

[50] B. T. Draine, P. J. Flatau, "Discrete-Dipole Approximation For Scattering Calculations," J. Opt. Soc. Am. A 11, 1491-1499 (1994).

[51] J. Sancho-Parramon, S. Bosch, "Dark Modes and Fano Resonances in Plasmonic Clusters Excited by Cylindrical Vector Beams," ACS Nano 6 (9), 8415-8423 (2012).

[52] U. Fano, "Effects of configuration interaction on intensities and phase shifts," Phys. Rev. 124 1866–78 (1961).

[53] B. Auguié, J. L. Alonso-Gómez, A. Guerrero-Martínez, and L. M. Liz-Marzán "Fingers Crossed: Optical Activity of a Chiral Dimer of Plasmonic Nanorods," The Journal of Physical Chemistry Letters 2 (8), 846-851 (2011).

[54] M.Kuntman, E Kuntman, T. Çakir, J. Sancho-Parramon and O. Arteaga, "A dipolar model for the chiroptical responces of optical media," unpublished.

[55] R. Ossikovski, E. Garcia-Caurel, M. Foldyna, and J. J. Gil, "Application of the arbitrary decomposition to finite spot size Mueller matrix measurements," Appl. Opt. 53, 6030-6036 (2014).

[56] E. Kuntman, O. Arteaga, "Decomposition of a depolarizing Mueller matrix into its nondepolarizing components by using symmetry conditions," Appl. Opt., Vol. 55, No. 10, 2543-2550 (2016).

[57] E. Kuntman, A. Canillas and O. Arteaga, "Retrieval of the non-depolarizing componentsof depolarizing Mueller matrices by using symmetry conditions and least squares minimization," Appl. Surf. Sc. 421, 607-731 (2017).